Thin Glass

as Cold Bent Laminated Panels
in Architectural Applications

by N.I. Schlösser

TU Delft

Thin Glass

as

Cold Bent Laminated Panels in Architectural Applications

in partial fulfilment of the requirements for the degree of
Master of Science
in Building Engineering
at Delft University of Technology
to be defended publicly on Friday the 27th of July 2018

by Naomi Schlösser
4154266

TU Delft

Preface

Before you lies the final report of my graduation research, written to meet the requirements for a Master of Science degree in Building Engineering with a specialization in Structural Design at Delft University of Technology. The topic of this research concerns thin glass in architectural applications, focussing on cold bent laminated panels. By choosing this field of expertise, I had the opportunity to combine my love for architecture and engineering. I was able to expand my theoretical knowledge by conducting real life experiments. An opportunity I'm very grateful for with many people supporting me. I therefore would like to acknowledge those who have helped me complete this research.

First of all, I would like to thank my graduation committee and all the people involved from Delft University of Technology. Rob Nijsse, the chairman of the committee, who always had the patience to share his broad knowledge on structural glass and inspired me to push the boundaries. Telesilla Bristogianni, who introduced me to the field of glass, continuously remained positive and guided me throughout my entire research. Christian Louter, who shared his knowledge on thin glass and introduced me to everyone needed to complete this thesis. Special thanks to Gertjan Mulder and Johan Boender at Aerospace Engineering for providing equipment to manufacture the panels and helping me to obtain the necessary data during different stages of the analyses. I would also like to thank Kees Baardolf and Fred Schilperoort at Civil Engineering for preparing and supporting the experiments.

Secondly, I would like to express my gratitude to all the companies who have assisted me during my research. Special thanks to Eckersley O'Callaghan, and in particular James O'Callaghan, for giving me the opportunity to study glass as a structural material in the first two months of my graduation at their office in London. By introducing me to their expertise, I could gather crucial information I wouldn't be able to get by carrying out a regular desk study. I would also like to thank AGC and Anton Peters for providing Leoflex sheets and sharing their knowledge. Many thanks to Qdel and Trosifol for providing Saflex DG41 and SentryGlas respectively.

Finally, I would like to thank my family and friends for their unconditional support and patience. Especially my housemates and dear friends Silke and Suman, who had to listen to my endless stories on thin glass. Robbie, who was willing to help me with great patience to understand the quirky features of Strand7. Michiel, who was always there when I needed him. My parents and sister, for their love and support, and who even helped me manufacture the supports needed to conduct experiments. Thanks to everyone who made my masters an unforgettable journey!

N.I. Schlösser
Delft, July 2018

Abstract

Glass has been used for centuries. Originally to create weapons, jewellery and decorative ceramics. Nowadays as windows, reagent bottles and electronic devices. The Egyptians seem to have been the first to realise what could be done with glass by trailing molten glass around a shaped core. The idea of inserting glass in windows was conceived by the Romans, which laid the foundation fundamental to today's processes. By innovating its production process the market could be extended to larger window panes and eventually structural glass. It's only in the last two centuries that there has been substantial development of flat glass. A breakthrough came when the development of float glass was announced in 1959 by sir Alastair Pilkington. A continuous pane of glass moves out of the melting furnace and floats along the surface of an enclosed bath of molten tin, allowing excellent surface quality. A process that is still widely used today due to its high productivity and quality without the need for expensive machinery. The resulting products provide comfort, protection, energy reduction, security and transparency (Nascimento, 2014). It is for this reason that glass in modern architecture grew very rapidly in the past decade. Glass panels increased in size to push the boundaries for engineers and for architects to show what they are capable of and create even greater transparency. With that growth, the thickness of glass panels has increased from a modest 8 mm to a currently more regular thickness of 32 mm. On top of this, the required insulation values of glass constructions also increased. Future glass panels can include triple or more layers to provide for the required insulation, creating even heavier panels. According to Hundevad (2014), at a time where we strive to make ever larger and heavier glass panels, shouldn't we investigate new ways of pushing technological boundaries in order to save material rather than using more of it?

Where regular float glass is a rather thick, hard and brittle substance that can break easily when subjected to large stresses, thin glass can be found on the other side of the spectrum with its flexibility, clarity and higher strength. Thin glass has rarely been used for architectural applications, mainly because technologies for manufacturing thin glass in construction element sizes were not available or were often too expensive (Spitzhüttl, Nehring, & Maniatis, 2014). This product however shows large potential provided sufficient interest is shown from different sectors to lower the price and stimulate innovation. This research will therefore focus on how to implement thin glass on a larger architectural scale and embrace its features to create thinner and stronger load-bearing glazing elements in areas where regular float glass doesn't work. The main drawbacks of float glass are that it is hard to curve and tension, it doesn't allow for flexibility and it is becoming a rather heavy building material due to the build-up. Thin aluminosilicate glass is lightweight, flexible, able to curve and a more promising material to tension due to its higher tensile bending stress. However, limited geometrical bending stiffness in its flat form prevents thin glass to be used for structural purposes. Therefore, three main approaches can be distinguished to stiffen a thin glass panel. Firstly, to laminate the glass to a substrate providing increased out-of-plane stiffness. Secondly, to embrace its flexibility by cold forming the glass into curved developable surfaces. Thirdly, to treat the material as a fabric glass and design it for tensile membrane structures (Lambert & O'Callaghan, 2013). From these approaches, several design configurations are introduced.

A rating system has been introduced to give an indication of the potential of every design configuration. Boundaries and demands from different industries (e.g. building and marine industry) are translated into requirements concerning optical quality, geometry, mechanical properties, sustainability and economical properties. According to the system, a composite panel combining float glass with thin glass, a composite panel combining polymers with thin glass, a curved panel with only thin glass and a curved panel combining polymers with thin glass are still in the running to become the chosen concept. It must be noted that this list is not binding and every principle could benefit from further research. The most important demands concern larger transparent panels, minimal weight, more free formed architecture and high thermal insulation. Cold bent laminated thin glass panels tick most of these boxes, since they encourages transparency, lightweight structures and free formed architecture. Furthermore, the flexible nature of thin glass is an important and promising characteristic and shouldn't be compromised by introducing stiffening techniques. However, applying thin glass as load-bearing structures, deflections become governing and should be minimised to prevent causing alarm to users. Cold bent laminated thin glass panels use this flexibility to create a stiffer structure and therefore seems to be the perfect configuration to further explore.

Subsequently, the main goal of this research is to gain insight in the structural and post-breakage behaviour of cold bent laminated thin glass panels. To obtain a curvature, glass panes have to be cold bent into a certain shape. Although introducing higher bending stresses at the top, the curvature is chosen to be sinusoidal, because it provides the smoothest distribution of shear and the lowest risk of delamination. Four two layered thin glass panels with the same curvature and different interlayers are produced. These panels consist of Leoflex glass provided by AGC, where two panels include an interlayer of Saflex DG41 (SAF) provided by Qdel and two panels include an interlayer of SentryGlas (SG) provided by Trosifol. The panels are cold bent to a value well below the recommended tensile bending strength of 260 MPa to allow for an increase in stress at spring back and loading. From the moment the panels are released from their mould, a certain spring back can be observed causing higher stresses at the top of the lower ply. Afterwards the relaxation phase is initiated. During this stage, the panels are under a constant load due to thin glass wanting to go back to its original flat shape. From the experiments, it can be concluded that the panels with a SAF interlayer relax significantly, but

seem to come to a standstill after a certain period. The panels with a SG interlayer do not seem to relax after spring back. The measured geometries of this series are more or less the same at spring back and after two weeks of relaxation. It must be noted that, due to differences in the numerical and experimental results, it is important to further investigate the viscosity and properties of the interlayer during relaxation.

Additionally, experiments are performed on a smaller scale panel for a point load applied in the middle of the upper bent surface. The curved edges are simply supported, while the straight edges are able to move freely. Panels with a SAF interlayer seem to behave less stiff compared to panels with a SG interlayer. However, due to a higher curvature of panels with a SG interlayer at loading, the stiffness of the panel is also higher and may have influenced the stiffness as well. Particularly interesting is the shift in governing stresses, both shown in numerical and experimental models. The position of governing principal stresses in panels with a SAF interlayer change at a certain load. The highest stress goes from the bottom node at the top of the lower ply to an area in between the top and unsupported edge at the upper ply. Experimentally, one of the panels failed exactly at this position at a higher load than a panel with a similar geometry and build-up. This failure resulted in spalling of the top layer and is concerning in terms of safety and, in combination with a high fragmentation observed in all the panels, must be extensively investigated. The other panel fabricated with SAF and the panels fabricated with SG failed in a similar matter at the bottom node at the top of the lower ply. Only one sheet broke for every panel, allowing the panel to remain its shape after failure due to lamination.

The numerical models during loading could not be validated as cold bent laminated panels generally deflect more and failing at far lower loads if a tensile bending stress of 260 MPa is assumed. It seems that the assumptions made concerning the material properties of the interlayer and tensile bending strength of thin glass are conservative and should be further investigated. The model does however provide a better insight in the structural behaviour of cold bent laminated panels. Therefore, an additional analysis is performed into the effect of distributed loads representing wind loads on larger panels with an SG interlayer. From the results, it can be seen that the highest stress accumulates at the supported edge. This stress is well below the maximum stress, even with stresses added from production. A distributed wind load causes the top of the panel to move upwards, while the unsupported edges go down. The latter is governing with a deflection of 34.41 mm. Although EN16612 doesn't give specific requirement to limit the deflection of glass under load, this value is still in line within the recommended maximum allowed deformations.

This thesis first introduces a *research definition* by exploring the history of glass and its future developments. Hereafter, a *research framework* is set up to extensively investigate float and thin glass. This is done to determine the different *conceptual designs*, which are presented in the following chapters. Boundaries and demands from the marine and building industry determine the course of the subsequent research into cold bent laminated thin glass panels. The next block, *structural design*, first introduces a preliminary design based on literature studies. After investigating the structural behaviour of cold bent laminated thin glass panels, a final design is made based on the experimental results. The production process of these panels is also briefly discussed. Lastly, *final remarks* include the conclusions and recommendations obtained during this research.

Nomenclature

Symbols

A	Area or sinusoidal amplitude
a	Parabolic curvature variable
B	Sinusoidal span
C	Catenary curvature variable
DY	Displacement in y-direction
E	Young's modulus
G	Shear modulus
I	Moment of inertia
LT	Light transmission
r	Radius
t	Thickness
TA	Total area
t_{eff}	Effective thickness
$t_{eff,\sigma}$	Effective stress thickness
T_g	Transition temperature
t_p	Thickness of a glass ply
t_{pt}	Thickness of a glass ply on the tension side
t_{total}	Total thickness
v	Poisson ratio
α	Thermal expansion
λ	Thermal conductivity
ρ	Density
σ_{11}	Principal stresses
σ_b	Tensile bending strength

Abbreviations

AGC	Asahi Glass Co.
ANG	Annealed glass
CS	Compressive stresses
DIC	Digital Image Correlation
DOL	Depth of layer
EPDM	Ethylene Propylene Diene Monomer
ETFE	Ethylene tetrafluoroethylene
EVA	Ethyl vinyl acetate
FE	Finite element
FG	Falcon glass
FTG	Fully-tempered glass
GFRP	Glass fibre reinforced polymer
GG	Gorilla glass
HSG	Heat strengthened glass
ICLL	International Convention of Load Lines
IGU	Insulating glass unit
LED	Light-emitted diodes
LG	Leoflex glass
PC	Polycarbonate
PET	Polyester
PMMA	Polymethylmethacrylate
PVB	Polyvinyl butyral
ROR	Ring on ring
SAF	Saflex DG41
SG	SentryGlas
SLS	Soda lime silica
TPU	Thermoplastic polyurethane
TPU	Thermoplastic polyurethane
TSSA or TSSL	Transparent structural silicone adhesive or laminate
UV	Ultraviolet
VGU	Vacuum glazing unit

Contents

RESEARCH DEFINITION

1. Timeline

Glass was originally used to create weapons, jewellery and decorative ceramics. By innovating its production process the market could be extended to window panes and eventually structural glass. Refinement of the production process was done, but stayed more or less the same over the past century. Thin glass was discovered by accident and is nowadays used in gadgets, windshields and medical devices. This chapter will serve as a guide to explain the changes within the glass industry from the very first application to what it exhibits now and could be in the future.

1.1. History of glass

The first application of glass can be traced back thousands of years ago. Natural glass, like the volcanic obsidian glass, was used for carving arrowheads, knives, and other items needed for daily survival. These artefacts date back to about 7000 BC and were found in Egypt and Mesopotamia (Nascimento, 2014). The Egyptians seem to have been the first to realise what could be done with glass by trailing molten glass around a shaped core. By Roman times glass was being blown and moulded, cut, engraved, painted and gilded. The idea of inserting glass in windows was conceived by the Romans, thereby admitting light while, to a certain extent, keeping the ambient conditions in and the elements out (Whitehouse & Corning Museum Of Glass, 2004). They laid a foundation fundamental to today's processes, while in the Middle Ages, glass makers' main achievements were coloured glass windows. However, the decorative application of glass progressed rapidly under the Venetians, causing the need to develop better and bigger panes of flat glass (Pilkington, 1969).

Artificial fabrication of glass has been a slow and difficult process due to limited sizes of glass melting furnaces and the inability to produce high temperatures. For this reason, glass remained an exclusive and expensive product for many centuries. First, only three techniques were employed to make windowpanes. The first technique was rolling molten glass onto a smooth metal surface and manipulating the glass into the form of a thin sheet, called the plate glass process. Grinding involved several stages using different degrees of sand, after which polishing was done with rouge. Other ways to produce glass were blowing cylinders or crowns. These processes had other disadvantages such as the severe imperfections and wastage due to cutting rectangular plates (Figure 1.1). Crown or cylinder glass could be set up fairly cheaply, but more financial requirements were necessary for plate manufacture. It needed a big melting pot furnace, a casting table, cuvettes or cisterns, cranes, grinding and polishing machinery, and extensive warehousing facilities (Pilkington, 1969). Developments were aimed at reducing imperfections to produce clearer and less distorted glass in increasing sizes.

It's only in the last two centuries that there has been substantial development of flat glass. The very first flat glass process was patented in 1848 by English engineer Henry Bessemer. He was the first to attempt a continuous pane of flat glass by forming a glass string between rollers, but didn't succeed commercially. Emile Fourcault then invented the technique of producing a continuous glass plate by vertically drawing glass from a molten glass bath. However, distortions, irregularities and inhomogeneities still would appear, mainly as the result of small differences in viscosity due to chemical or thermal variations (Nascimento, 2014). A breakthrough came when the development of float glass was announced in 1959 by sir Alastair Pilkington. A continuous pane of glass moves out of the melting furnace and floats along the surface of an enclosed bath of molten tin, allowing excellent surface quality. The atmosphere is chemically controlled at a high enough temperature in order to melt irregularities out of the surfaces to become flat (Pilkington, 1969). This process is still widely used today due to its high productivity and quality without the need for expensive machinery.

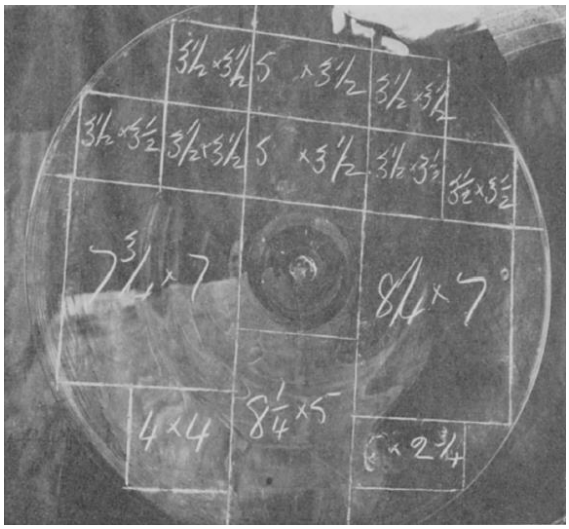

Figure 1.1: Panes cut from crown glass in inches (Pilkington, 1969)

1.2. Thin glass

Thin glass was discovered by accident in 1952. A chemist at Corning Glass Works heated a glass sample to 900 °C instead of 600 °C due to a faulty thermostat. Against all expectations, the glass sample had not melted. The chemist then, also accidental, dropped the glass while taking the sample out of the furnace. Surprisingly, instead of breaking, the sample bounced back. An important breakthrough, considering glass is a brittle material. Following, the Corning Glass Works Company decided to undertake a large research project to find ways to make ordinary transparent glass stronger (Rohrig, 2015). Altering existing production and strengthening processes allowed the developers to form very thin sheets of glass and significantly reduce surface flaws. With the so called fusion glass process, molten glass flows evenly over the top edges of a molten glass bath, forming two thin streams along the outer surfaces. The two sheets meet at the bottom and merge into a single sheet, cooled down by air on either side of the pane. By 1962, Corning had developed a very strong type of chemically tempered glass with significant different characteristics compared to ordinary glass. A few of those characteristics are high strength, scratch resistance, minimal thickness resulting in minimal weight, optimal optical properties and flexibility.

The automobile windshield industry was the initial incentive for the commercial application of chemically tempered thin glass where weight savings play a crucial role (Gomez, Dejneka, Ellison, & Rossington, 2011). Thin glass offers lightweight windows by replacing one of the window panes for a sheet of thin glass. Reduction of more than 30% can be achieved in comparison to conventional designs. Its superior optical quality and richer look also made this type of glass highly desirable in consumer electronic applications. Therefore, it didn't take long for this type of glass to make its way to nearly every smartphone screen. Now produced by several manufacturers, e.g. Corning, AGC and Schott, the application of thin glass stretches to other industries as well. Examples are cover plates for cellular phones, notebooks, medical devices, optics and cameras, where high strength and scratch resistance are essential due to every day's exposure.

1.3. Future developments

In general, existing solutions from one industry can be creatively imitated and translated to meet the needs of another market or product (Enkel & Gassmann, 2010). This phenomenon, called cross-industry innovation, can already be found in the thin glass market due to the promising characteristics of the material. While ordinary glass still exhibits the ancient characteristics of form and function, thin glass can carry us into the future as a performance platform for both practical and exotic technologies, such as flat panel displays, liquid crystal, super thin flat glass substrates, self-cleaning glass, mirrors, solar energy and electronic information (Nascimento, 2014). As for any industry, deeper understanding of borderline science and technology will ultimately allow great progress and innovation (LeBourhis, 2014). Other industries that can benefit severely from this innovation is the building and marine industry. Both are shifting towards more ambitious and demanding projects. These demands arise from improved physics, structural properties, transparency, aesthetics, safety, sustainability and economics. Applying thin glass could be a solution for these increasing demands. Although the building industry displays little innovation compared with other sectors due to its market structure, innovation in building and construction still pays off (Bruijn & Maas, 2005). For example, from the 21st century, Apple started to use glass in many of their buildings and making it their identity, pushing the industry to provide larger and larger panels (Figure 1.2). Also pushing architectural and engineering offices to design minimal connections and creating even more transparent structures.

Figure 1.2: 5th Avenue Apple store in New York built in 2006 (left) and 2011 (right)

2. Research

After a short introduction on the history of glass, recent changes and possible future developments, the problem statement and corresponding research questions are addressed to clearly identify the purpose of this thesis. Ultimately, the approach of this research is defined.

2.1. Problem statement

Glass in modern life can be coated, bent, shaped, laminated, and tempered. The resulting products provide comfort, protection, energy reduction, security and transparency (Nascimento, 2014). The latter is glass's prime attribute. The less you are conscious of the glass itself, the more valuable it is. The float process ensures a valuable, cheap and invisible product. Glass has to be flawless to achieve this invisibility, meaning that is has to be perfectly flat, totally uniform, and free from any distortion or contamination (Bricknell, 2009). It is for this reason that glass in modern architecture grew very rapidly in the past decade. Glass panels also grew in size to push the boundaries for engineers and for architects to show what they are capable of and create even greater transparency. These larger panels increased in thickness from a modest 8 mm to a currently more regular thickness of 32 mm. On top of this, the required insulation values of glass constructions also increased. The use of glass went from single to insulated glass and from clear glass to coated glass (Eekhout, 2016). Future glass panels can include triple or more layers to provide for the required insulation, creating even heavier panels. Another trend is to create more free form architecture, pushing glass panes to their maximum curvature limits.

In terms of the marine industry, glass panels are getting up to 3 meters wide and 10 meters long resulting in enormous windows. Yachts rely on their glazing elements to maintain their weather and water tightness. If the glazing fails, the vessel will be directly open to water and at great risk of sinking or capsizing. Due to the waves, general marine design guidance gives design loads on yachts to be 100 times more than the design loads for buildings. Therefore, glass elements in marine applications require high load-bearing capacity and post failure robustness (Kozlowski & Bao, 2016). In order to meet these standards, very thick laminated float glass is applied. Implementing these large thicknesses causes the glass panels to be extremely heavy. Unlike building, yachts cannot be supported by a foundation and therefore have to minimise their weight to stay afloat. According to Hundevad (2014), at a time where we strive to make ever larger and heavier glass panels, shouldn't we investigate new ways of pushing technological boundaries in order to save material rather than using more of it?

2.2. Research questions

Glass is among the most ancient materials in human history and it seems almost paradoxically that our knowledge of their structure and possible applications in industries is far from complete. Where regular float glass is a rather thick, hard and brittle substance that can break easily when subjected to large stresses, thin glass can be found on the other side of the spectrum with its flexibility, clarity and higher strength. Thin glass has rarely been used for architectural applications, mainly because technologies for manufacturing thin glass in construction element sizes were not available or were often too expensive (Spitzhüttl et al., 2014). This product however shows a large potential provided sufficient interest is shown from different sectors to lower the price and stimulate innovation. This research will focus on how to implement thin glass on a larger architectural scale and embracing its features to create thinner and stronger load-bearing glazing elements in areas where regular float glass will not work. The main research question therefore reads:

To what extend can thin chemically tempered aluminosilicate glass panes be applied on an architectural scale as a load-bearing element to create a structurally safe and transparent panel?

With this main question, the following sub questions arise:

- What kind of stiffening material and/or geometry can be used to create a load-bearing structure out of thin chemically tempered aluminosilicate glass panes?
- What are the physical and structural properties of thin chemically tempered aluminosilicate glass and the chosen stiffening material and/or geometry?
- What is the structural behaviour of thin chemically tempered aluminosilicate glass panels for the chosen principle when subjected to a point load or a static distributed load?
- How can safety be guaranteed when designing with thin chemically tempered aluminosilicate glass?

2.3. Methodology

The methodology used to conduct this research starts with an investigation into the production and properties of float glass and thin glass. Conclusions can be drawn based on these findings, where after several conceptual designs are proposed. Subsequently, boundaries and demands from the marine and building industry are discussed. The presented design configurations should be able to meet most of these boundaries and demands to be successfully implemented as a structural element. The chosen design principle is further explored in terms of its composition, curvature and structural behaviour. Based on these findings, a final design is presented. Hereafter, conclusions are drawn and recommendations for further research are made. A schematisation of the investigated principles is shown below.

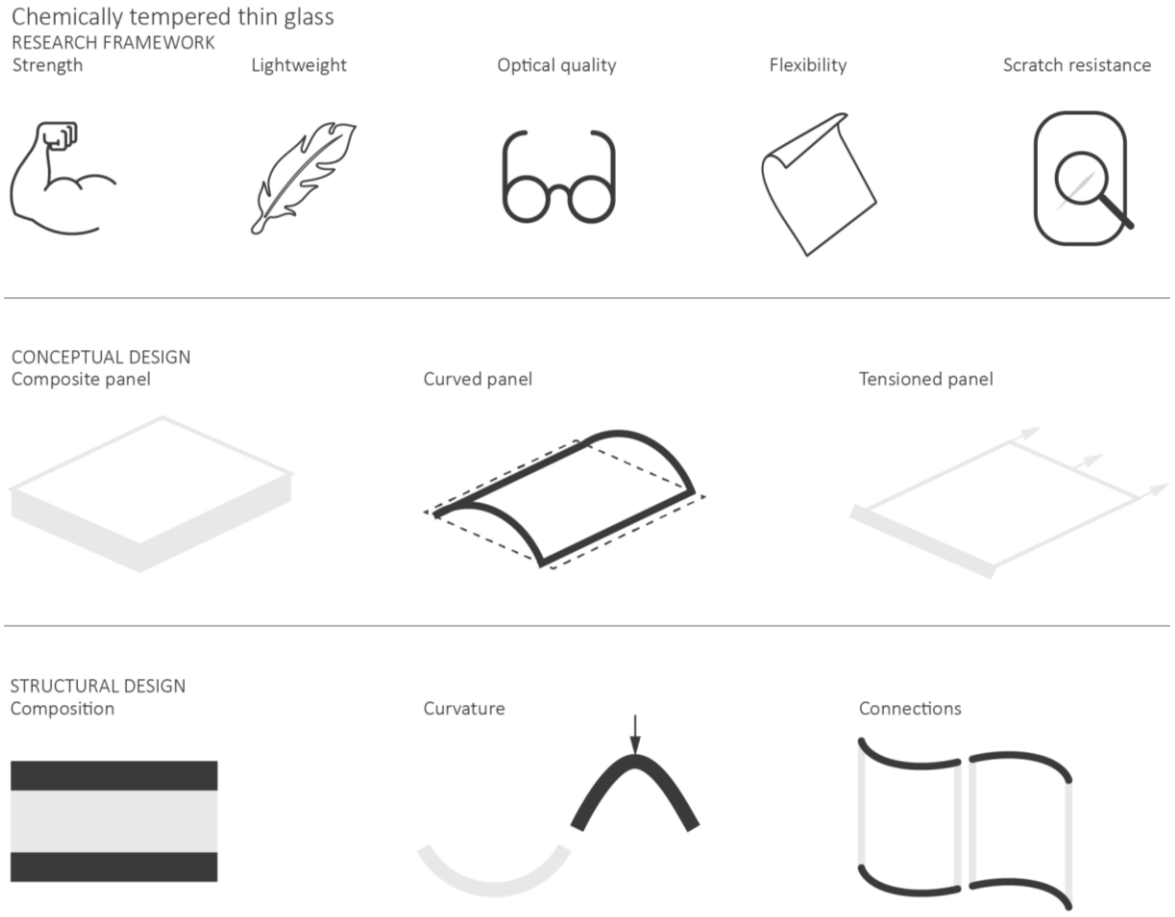

Figure 2.1: Schematisation of the investigated principles

RESEARCH FRAMEWORK

3. Float glass

A hard, brittle substance, typically transparent or translucent, made by fusing sand with soda and lime and cooling rapidly. It is used to make windows, drinking containers, and other articles. - Oxford Dictionary

Above is a fair definition for glass produced these days. While plate and sheet glass comprised 99% and float glass 1% of all flat glass in 1961, the situation completely reversed by the 1990s (Hynd, 1984). Due to the optical quality, low cost, speed of production and large sizes, float glass is now the most widely used manufacturing process. This chapter will focus on float glass, with special attention to the (post) production process, physical and structural properties, advantages and disadvantages.

3.1. Production

To meet demand, modern float glass lines produce several hundred tons each day, operating 24 hours a day all year round. The production of float glass consists of eight basic steps; mixing, melting, floating, coating, annealing, inspecting, cutting and storing. First, glass is weighed and mixed with the same raw materials composition from many years ago. The mixture consists of silica sand (SiO_2), soda (Na_2O), lime (CaO), magnesia (MgO) and other minor ingredients. A considerable amount of crushed recycled glass is also added to reduce waste. Due to the composition of the material, this type of glass also goes by the name soda lime silica float glass.

After mixing, the compound is melted in a furnace at a temperature of around 1550 °C. Molten glass enters the tin bath via a small tunnel to float on top of a more dense molten tin, forming a smooth flat surface at a thickness of 6 to 7 mm. Tin is used because of the large temperature range of its liquid physical state (232-227 °C) and its high specific weight in comparison to glass (Haldimann, Luible, & Overend, 2008). At this stage, the enclosed system contains a mixture of nitrogen and hydrogen gases to prevent oxidation of the molten tin. The glass is cooled while it passes down the bath to exit at a temperature of 600 °C, in order for the surface to harden before being carried on to conveyor rollers without suffering damage (Kumar & Buckett, 2002). Here, the glass thickness is controlled within a range of 2 to 25 mm by adjusting the speed of the rollers.

The manufacturer has the option to apply online coatings before entering the annealing lehr. In the annealing lehr, glass panes gradually cool down to room temperature to prevent residual stress being induced in the glass. At last, the glass is inspected for any visual defects and imperfections, cut in sizes, standard sizes being 3.21x6.00 m, and stored. Glass that didn't pass the inspection or is broken will be fed back into the furnace.

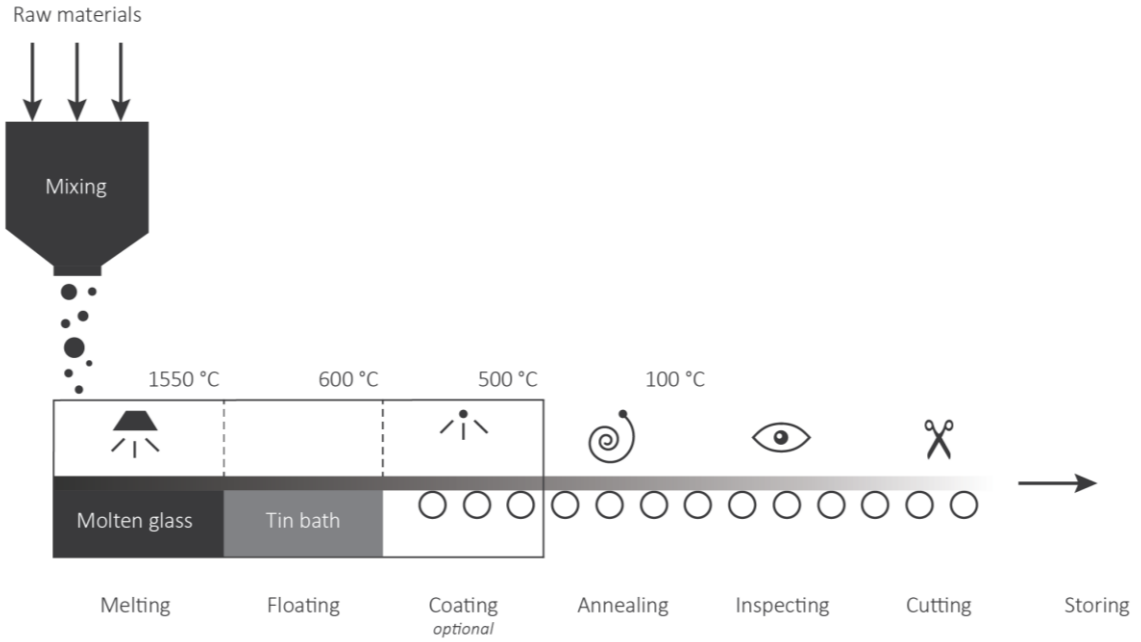

Figure 3.1: Float glass process

3.2. Physical properties

Glass is an inorganic solid material obtained in such a way that when passing the transition temperature during annealing, solidification occurs instead of crystallization. Consequently, the final temperature must be low enough for molecules or atoms to move too slowly to rearrange to a stable crystalline form (LeBourhis, 2014). During cooling, the viscosity of glass increases constantly until solidification, which happens at a temperature of around 530 °C. This transition does not take place at one precise temperature, but over a certain temperature range. And while most other materials have a geometrically regular structure (also referred to as crystalline structure), glass has an irregular network of mainly silicon and oxygen atoms with alkaline parts in between (also referred to as amorphous structure). The difference between a crystalline structure and an amorphous structure can be found in Figure 3.2. Despite this irregular structure, glass is considered to be a homogeneous material.

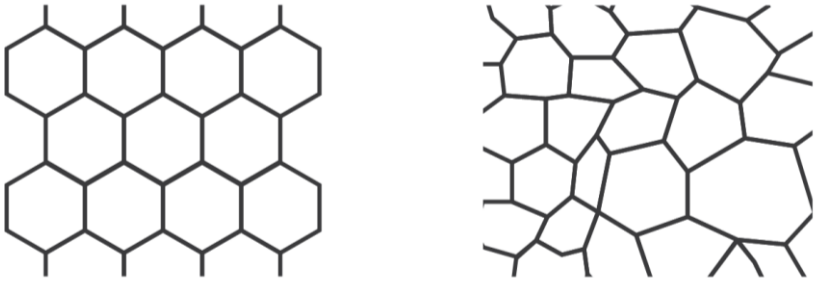

Figure 3.2: Crystalline structure (left) and amorphous structure (right)

At subatomic level, an atom consists of a nucleus in the centre with electrons orbiting around it. Mostly empty space consists in between the nucleus and electrons. Although electrons are initially designed to stay in the same orbit, it can transfer to another level if a passing light photon provides enough energy. Unlike other solids, the levels in glass molecules are so far apart that the electrons are strictly confined to particular energy levels. Meaning that the molecules cannot alternate between the different levels by absorbing light photons. Therefore, the energy passes straight through the molecule as if the electrons are not even there, enabling glass to be transparent (Haldimann et al., 2008). Even though glass is considered as solid, this phenomenon turns glass into a transparent material. Solar radiation reaching the earth consists of 3% short-wave ultraviolet (UV) radiation, 42% visible light and 55% long-wave infrared (IR) radiation. IR radiation heats the other side of the glass, whilst UV radiation is absorbed by electrons, making glass opaque. Another important property of glass is its excellent resistance against many aggressive chemical substances, making glass one of the most durable materials.

As mentioned, a glass mixture consists of silica sand, soda, lime, magnesia and other minor ingredients that influence the melting point during production or the mechanical and optic characteristics of the final product (Table 3.1). Silica sand forms the basic network of glass on a molecule level, lime and magnesia are added to provide a better durability and soda stimulates the melting process of glass. Adding small amounts of iron oxide to the mixture increases the melting rate and produces higher quality glass (Shute & Badger, 1942). However, iron oxide is also responsible for the greenish colour of normal iron float glass. Reducing the amount results in a reduction of this green colour, called low iron float glass.

Silica sand	SiO_2	70 - 74 %
Soda	Na_2O	10 - 16%
Lime	CaO	5 - 14%
Magnesia	MgO	0 - 5%
Alumina	Al_2O_3	0 - 3%

Table 3.1: Composition of soda lime float glass

During the floating stage, tin diffuses into the lower surface of the glass which shows significantly different optical properties and mechanical strength than the opposite air side. The optical properties also depend on the glass thickness, chemical composition and applied coatings. The mechanical strength of the tin side has been found to be marginally lower than that of the air side due to the conveyor rollers in the cooling area. These rollers cause surface flaws that reduce the strength (Haldimann et al., 2008). Furthermore, due to soda lime glass its high thermal expansion coefficient combined with a low tensile strength, annealed glass shatters relatively easily (O'Regan, 2014). Important physical properties are listed in Table 4.2.

3.3. Post processing products

After production, float glass is processed further to produce products of the shapes, performance and appearance that are required to meet particular needs (Haldimann et al., 2008). Desired pane shapes and sizes are produced by cutting the glass panels. Edges are altered into different shapes, surfaces are grinded and polished, holes are drilled into glass and coatings are applied. A few of the most significant post production processes are explained below.

3.3.1. Tempering

Four basic types of strengthened glass can be distinguished. These types are, in ascending order of strength, annealed glass (also referred to as float glass), heat strengthened glass (also referred to as semi-tempered or partly toughened glass), fully tempered glass (also referred to as toughened glass) and chemically tempered (also referred to as chemically toughened). All these processes result in pre-stressing of the glass.

As all structural glass, annealed glass behaves as an elastic and isotropic material until it breaks. No warning is given before failure. Whether or not fracture will occur depends on the presence of flaws, the stress level and the duration of the load. These flaws may arise from cutting, grinding or drilling of the glass, as well as from the environment the glass has been exposed to (O'Regan, 2014). As flaws do not grow or fail in compression, the compressive strength is much larger than the tensile strength (Haldimann et al., 2008). Therefore, exceeding the tensile strength of glass will cause the glass pane to break. Glass doesn't yield plastically, meaning that the stresses are not being reduced through stress redistribution, and exhibits brittle failure.

By thermally tempering the glass, a favourable residual stress field, featuring tensile stresses in the core of the glass and compressive stresses on and near the surface, is introduced (Figure 3.3). To keep this field intact, any cutting, grinding or drilling has to be carried out before tempering the glass. The core doesn't contain flaws and offers good resistance to tensile stresses, while the flaws on the glass surface can only grow if they are exposed to sufficient tensile stresses (Haldimann et al., 2008). To obtain thermally tempered glass, annealed glass is heated to approximately 620-675 °C in a furnace. This temperature range is approximately 100 °C above the glass transition temperature, causing the glass to be viscous. This viscous state combined with movement along the rollers introduces roller wave distortions, creating a severe optical defect when lightning is slightly polarized. After heating, the glass pane is quenched by jets of cold air, initially resulting in tensile stresses on the surface due to solidification and compressive stresses in the interior. But, as the interior cools down, the thermal shrinkage is resisted by the already solid surface, resulting in compressive residual stresses in the surface and tension in the interior. Both heat strengthened and fully tempered glass are produced following this strengthening process. The difference is that with heat strengthened glass, a lower cooling rate is used.

The fracture pattern varies due to a difference in residual stresses being released. Annealed glass breaks into large pieces of glass. Fully tempered glass breaks into small pieces of glass, with heat strengthened in the middle of the spectrum (Figure 3.4). Fully tempered glass has a small risk of breaking spontaneously due to nickel sulphide inclusions that arise from the production process. Under the influence of temperature, these particles can increase in size, and combined with high tensile stresses in the core, causing the glass to break. These inclusions can be reduced by a heat-soak test.

By chemically tempering the glass, annealed glass is immerged into molten alkali salt at a temperature around 500 °C. During the time of immersion, the alkali ions from the glass that are close enough to the surface are exchanged for those from the molten salt (Gy, 2008). The penetrating ions are 30% larger than that of the ions leaving the glass, resulting in compressive stresses at the surface. Increasing the compressive layer means increasing the strength. With chemical tempering, a higher surface compression and a larger strengthening level can be obtained compared to thermal tempering. Other advantages of this process are that no measurable optical distortion can be found, ultra-thin plates and irregular geometries can be strengthened, and cutting, grinding or drilling can be carried out afterwards. Disadvantages are a small compressive layer for soda lime glass that makes the glass susceptible to flaws, high costs, limited sizes due to extended bath immersion and limitations to alkali containing glass (Varshneya, 2001). Furthermore, to enhance diffusion in soda lime glass, elevated temperatures in a range of 400-500 °C are used for the treatment. These temperatures are high enough for stress relaxation to take place causing diffusion effects in the glass. Aluminosilicate glass is an alternative to soda lime glass that allows for a deeper compression layer depth and a better result in general. It is used to make thin glass and will be further discussed in chapter 4.

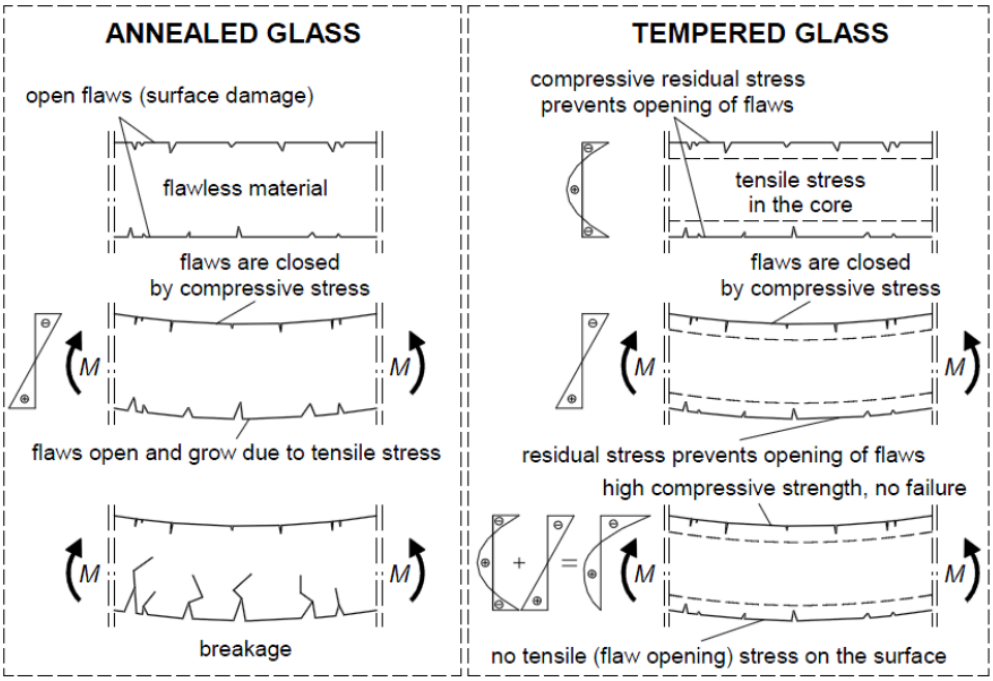

Figure 3.3: The principle of glass tempering (Haldimann et al., 2008)

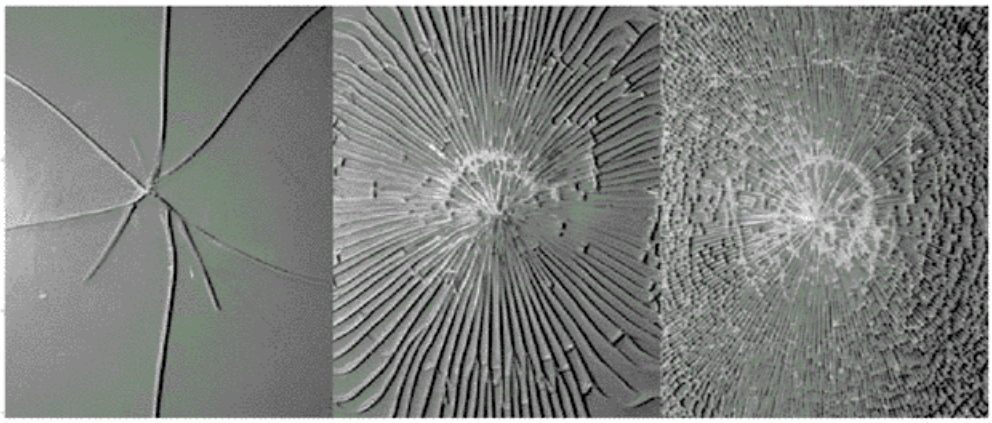

Figure 3.4: Comparison of fracture patterns: annealed glass (left), heat strengthened glass (middle) and fully tempered glass (right) (Haldimann et al., 2008)

3.3.2. Lamination

In 1910 the concept of laminated glass was introduced. The fundamentals were to create a multi-layered pane of glass bonded together through a transparent interlayer at a temperature of approximately 140°C. Interlayers can also be cured by using UV radiation with the objective that laminated materials shouldn't be UV sensitive. Initially, the technology was implemented by the automotive industry, until 1970, when the building industry adopted it to improve post-breakage behaviour. Although tempering improves the structural capacity, glass is still a brittle material. After breakage, lamination enables the glass panel to stick together and have a certain capacity depending on the fragmentation of the glass. Compared to fully tempered, annealed and heat strengthened fracture patterns results in a significant remaining load-bearing capacity after failure (Haldimann et al., 2008). Laminates can incorporate many thicknesses and combinations of glass types to give a range of products with the required range of mechanical and optical properties. For example, due to damping effect of the interlayer, laminated glass panes perform well when subjected to dynamic loads. It is common to use multiple layers to laminate the glass panes, because after failure the interlayer plays a significant role in the resistance of the structural element. In case of a fire, most interlayers in laminated glass lose most of their strength above 100°C.

Materials that are often used for the interlayer are poly vinyl butyral (PVB), thermoplastic polyurethane (TPU), ethyl vinyl acetate (EVA), polyester (PET), resins such as acrylic and ionoplast (O'Regan, 2014). The most common interlayer is PVB due to its low costs and ability to block UV radiation completely. PVB is also a viscoelastic material, meaning that its physical properties strongly depend on temperature and load duration. During short-term out-of-plane loading, the laminates act as a composite panel, while during long-term out-of-plane loading, the laminates act as a non-composite panel due to creep (Figure 3.5). Thermoplastic polyurethanes have very high tensile strength, toughness, scratch resistance and resistance to degradation (Teotia & Soni, 2014). However, the colour changes from colourless to yellow and eventually to brown during UV-aging. The most common ionoplast is SentryGlas (SG), developed to aim for a higher stiffness, temperature resistance, tensile strength or resistance to tearing (Haldimann et al., 2008). Even though SG is a structurally interesting interlayer, the optical quality is not as good as a PVB layer, which has been a reason for scientist to develop a structural PVB. PET interlayers allow for the installation of light-emitting diodes (LED) within the glass.

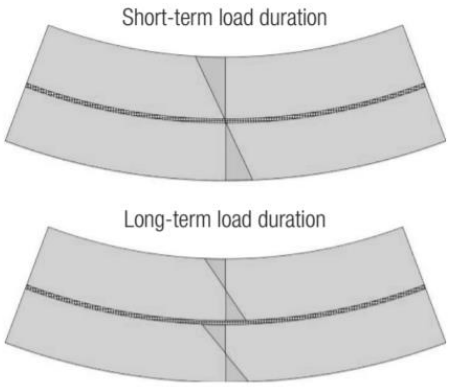

Figure 3.5: Section through PVB laminated glass indicating bending stress (O'Regan, 2014)

3.3.3. Bending

Curved glass can be produced by deforming glass panes, hot or cold, into a given shape. Hot bending can be done by means of gravity or by pushing the glass into a mould at a temperature of 600 °C. The latter process allows large curvature, but also enables large tolerances and reduced optical quality (Herwijnen, 2008). By means of gravity, glass panes sag into a mould and deform into their final shape. Due to the curved geometry acting as a shell, smaller bending stresses occur. This phenomenon allows the glass plates to become thinner or to span larger distances. However, this process has several drawbacks. These drawbacks are that rather high temperatures are necessary to produce hot bent curved glass, a steel mould has to be built for each different shape when free form architecture is desired. The glass is required to be annealed glass and therefore mechanically weaker. Thermally tempering is difficult during its production process, and most efficient thermal coating do not survive during production creating lesser thermally insulated panels (Raynaud, 2014). Also, the thickness varies along the curvature due to sagging of the glass pane, creating smaller thicknesses at the top and therefore a weaker spot. The Casa da Música in Porto (Figure 3.6) and the Museum aan de Stroom (MAS) in Antwerp are two well-known examples that incorporate hot bent corrugated glass in their facades. Within the curvature, a large difference is observed in the bending strength of convex (round) and concave (hollow) parts of an element (Figure 3.7). The convex shape is weaker and deforms easier than the concave shape, resulting in additional stresses in the element (Nijsse, 2008). Although corrugated glass represents a general resistance increase in the out-of-plane load-bearing capacity, it matters how and in which direction an element is loaded.

Figure 3.6: Casa da Música (Nijsse & Wenting, 2014)

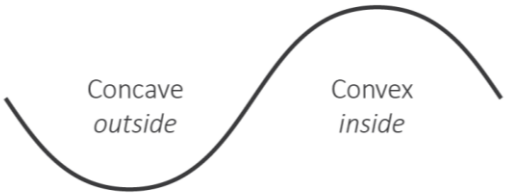

Figure 3.7: Concave vs convex shapes

Cold bending is done by means of assembly or lamination and allows for the construction of curved free-form glazed surfaces with no need of moulds. Cold bending by assembly requires constant fixation of the glass into a desired shape. In general, the cold bent surface is a single-curvature developable surface, because a double curved shape produces high membrane stresses. Compared to hot bending, cold bending is relatively cheap, has a better optical quality and by cold bending the glass pane, favourable tension and compression stresses occur that minimise the bending stresses when loaded from a certain out-of-plane direction (Herwijnen, 2008). However, induced stresses can also reduce the loading capacity causing the glass to break, a certain degree of optical distortion is still visible and the pane is limited to a maximum bending radii. Cold bending by lamination is a technique that constrains an unbonded glass interlayer package in the desired curved shape. The curvature is only partially maintained through the interlayer bond, varying in time due to the viscosity of the interlayer. After releasement from the mould an elastic spring back effect can be observed. This process produces high shear stress concentrations in the interlayer with consequential risks of delamination. The optimal configuration is sinusoidal, because it provides the smoothest distribution of shear stress (Galuppi & Royer-Carfagni, 2015).

3.3.4. Insulating Glass Unit (IGU)

Insulating glass units consist of at least two glass panes enclosing a sealed air space, separated by a metal spacer. The spacer is usually filled with desiccant to absorb moisture captured inside the cavity. The sealed air can be filled with ordinary air or molecular glass like Argon or Krypton, which have a lower thermal conductivity. The main function of an IGU is to reduce thermal losses. In combination with special coatings, modern IGU's can achieve heat transfer coefficients (U-values) of 1.1 W/m²K for double-glazed windows and 0.7 W/m²K for triple-glazed windows (Haldimann et al., 2008). IGU's also reduce condensation when the outside temperature is cold. In terms of structural performances, the sealed cavity ensures a certain degree of cooperation between the two outer panels assuming that the applied wind loads are uniformly distributed. The development of vacuum glazing units (VGU's) is significant in the area of low heat loss glazing systems with great potential to reduce building heating and cooling loads when combined with solar control glazing. Vacuum glazing uses a gas-filled space evacuated to low pressures in between the glass panes to minimise conductive and convective heat transfer. The remaining heat transfer is caused by radiation which can only be reduced by the use of coatings (Eames, 2008).

3.3.5. Coatings

Coatings are often used to change surface properties of a glass pane. The general wish is to combine optimal transparency with maximum solar reflection, making the selection challenging. Coatings can be applied during the production process, also referred to as online coatings, or after the glass is manufactured and cut, which are offline coatings. Common types of coatings are solar control coatings, designed to reflect as much IR radiation as possible, and low-emissivity coatings, developed to reflect thermal IR radiation for insulation purposes in IGU's.

Hard coatings, also known as pyrolytic coatings, are commonly applied using a chemical vapour deposition process by bringing a chemical mixture in contact with a glass pane at a temperature of 600-650 °C. A pyrolytic reaction will occur at the surface leading to the deposition of a coating bonding to the glass (Haldimann et al., 2008). Due to the temperature range, hard coatings are usually applied online, before entering the annealing lehr. The glass can still be tempered and bend afterwards, but is not as flexible as offline coatings. Also, a high scratch resistance can be achieved. An alternative of applying hard coatings is dip coating. During this process, the glass is dipped into a coating solution and heated up to 650 °C to let the coating bond with the glass pane. Soft coatings can be applied by using various techniques, but the most predominant process is Magnetron sputtering. Sputtering is performed in a vacuum environment so that ions composed of the desired coating material, strike a target to cause atoms from that target to be ejected with enough energy, to travel and bond with the glass surface. This allows for the production of flexible, high performance, multilayer coatings using different materials. The disadvantage of soft coatings is their susceptibility to aggressive environments and mechanical damage.

3.4. Structural properties

As mentioned, glass molecules do not consist of a crystalline structure, but of an irregular network of mainly silicon and oxygen atoms. This irregular network combined with the inability of atoms reforming when broken, does not allow for plastic behaviour before fracturing, making the glass perfectly elastic. Any local stresses around a defect that exceed the chemical bond strength will cause bond failure. This increases the local stresses, causing the glass to suddenly exhibit brittle failure (Veer, 2007). Glass is therefore unable to give any warning, making it hard to predict when failure will take place. Figure 3.8 shows a qualitative comparison of the stress strain diagram between glass, steel and wood.

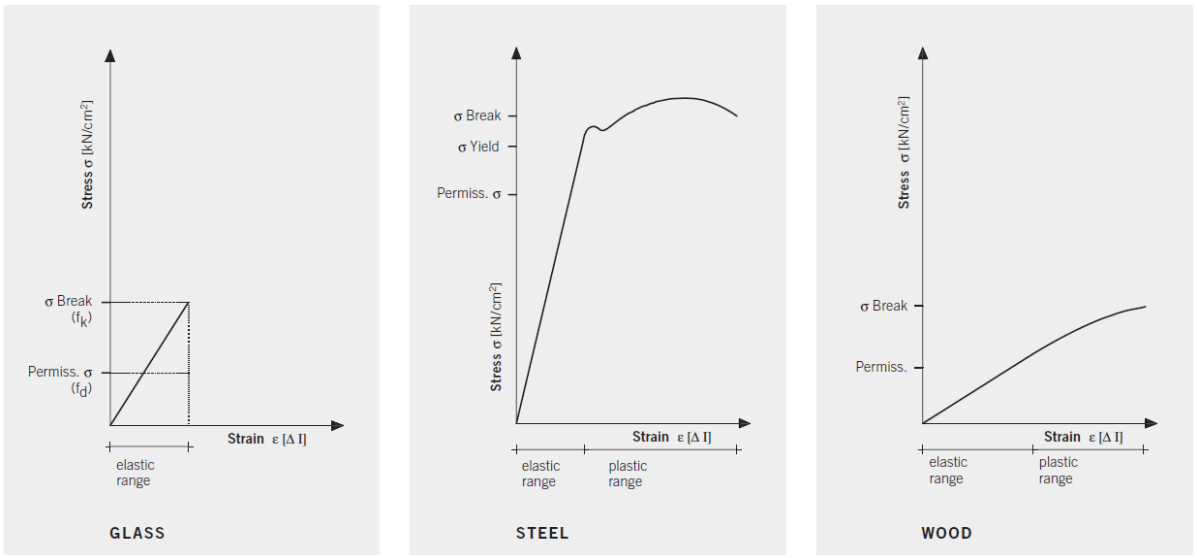

Figure 3.8: Qualitative comparison of the stress-strain diagram of glass, steel and wood (Wurm, 2007)

The theoretical strength of glass, due to its strong initial covalent molecular bonding, can be as high as 16000 MPa. However, flaws in glass cause stress concentrations. These flaws are the starting point for crack propagation. It is hard to predict whether an individual flaw is likely to develop into a crack. As stated in chapter 3.3.1, the core doesn't contain flaws, but the surface and edges of the glass do and may arise from the production, handling or environmental processes. During the production process, almost all float glass panels are cut. However, these cuts create severe flaws that make the edges of the panel even weaker than the surface. It's important to use the correct cutting wheel in terms of hardness and angle, recent equipment and the right pressure. Too much pressure can cause damage on the lower side of the glass. To transform the cutting edges into smoother surfaces with lesser stress concentrations, a grinding process is applied. Flaws originated from handling are local and often visible at the surface, while during production, flaws are widely distributed and hardly visible to the naked eye. To conclude, accurate characterization of the fracture strength of glass must incorporate the nature and behaviour of these flaws (Haldimann et al., 2008).

Pepi (2002) recorded three different failure modes, namely mode I, mode II and mode III, illustrated in Figure 3.9. The first is an opening mode, which is the most important and dominant. The other modes are shear modes, either sliding or tearing, and are quite rare. Furthermore, flaws fail at a critical opening depth and under external tensional loading, hence mode I being the opening mode. Flaws normally don't fail in compression. When loaded in compression, buckling failure will occur before compression failure due to the development of tensile stresses. An element's tensile strength is exceeded before it is loaded to its compressive strength (Haldimann et al., 2008).

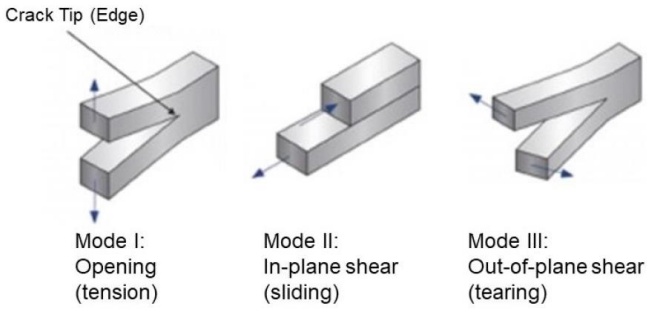

Figure 3.9: Failure modes (Pepi, 2002)

3.4.1. Strength

Although the theoretical strength of glass might be as high as 16000 MPa, the actual tensile strength is much lower due to flaws in the glass as explained in the previous chapter. Finding this strength, however, seems almost impossible due to a large number of factors affecting the strength. A few of these factors concern the load duration, load type, load velocity, humidity, condition of surfaces and edges, size of the panel, tempering type and glass age (Kruijs, 2009). Many attempts to measure and document the strength of glass have been made, but most of the information was scattered. Therefore, Veer (2007) conducted experiments using large series of specimens to determine the strength of glass. Tests on small specimens use three point bending and tests on large specimens use four point bending. According to the data, no specimen failed at stresses below 20 MPa (Figure 3.10). Although the results are widely dispersed, as a conservative design strength, it is assumed that all values greater than 20 MPa are a reasonable value. Implying that for larger pieces of glass or for a larger number of glass, somewhere, failure will start at a tensile stress of 20 MPa. Larger panels of glass just have an increased chance of containing flaws due to their size.

The European code EN16612: Glass in building - Determination of the load resistance of glass panes by calculation and testing, provides values for the characteristic strength for annealed, heat strengthened, fully tempered and chemically tempered glass. This strength is defined as that level of strength below which a specified proportion of all valid test results is expected to fall. However, no real agreement consisted on the validity of these values for design of glass beams or columns. Therefore, Veer, Louter and Bos (2009) researched the effect of tempering on the strength of glass in different positions to obtain an independent set of values. The positions included standing and lying of glass plates. It appeared that, for the specimens used, the strength for standing glass plates is about 67% of the strength for lying glass plates. To provide a more conservative strength, the lower boundary is again assumed to be the design strength of glass. According to Figure 3.11, annealed glass has a failure stress of 20 MPa, which indeed corresponds to the results from Figure 3.10. Heat strengthened glass has a failure stress of 40 MPa and fully tempered glass has a failure stress of 80 MPa. Table 3.2 shows the difference in characteristic strength obtained by EN16612 and Veer et al. (2009).

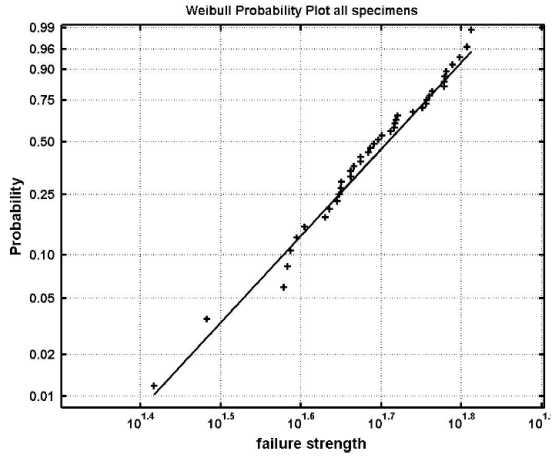

Figure 3.10: Weibull plot of combined data sets for the tensile bending strength of annealed glass (Veer, 2007)

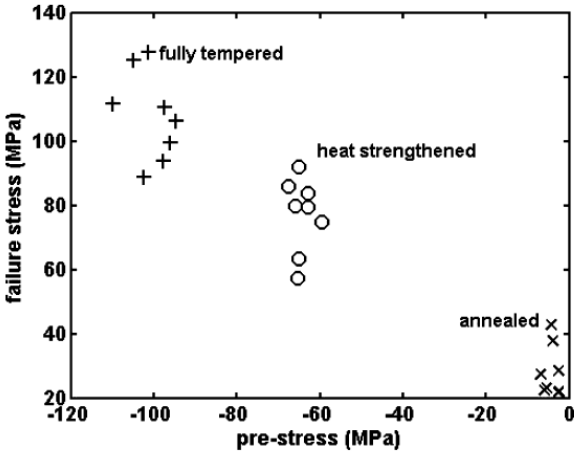

Figure 3.11: Relation between tempering and tensile bending strength of float glass (Veer et al., 2009)

A series of partial factors are applied to the characteristic glass strength to establish the design strength. These factors take into account the surface texture of the glass element, the nature of the load and its duration (O'Regan, 2014). Macrelli (2016) determined the characteristic bending strength of chemically tempered soda lime glass by conducting several four point bending tests and concluded it to be 227 MPa. However, inducing flaws in chemically tempered glass may result in sudden unexpected fatigue failures if those flaws exceed the compressive layer depth. The final strength depends on the original surface quality of the glass and the local strength depends on the damages induced during its lifetime. These flaws reduce the strength severely, and as a result, a rather low characteristic strength is given by the European codes as illustrated in Table 3.2.

	Characteristic strength EN16612	Characteristic strength (Veer et al., 2009)	
Annealed	45	20	MPa
Heat strengthened	70	40	MPa
Fully tempered	120	80	MPa
Chemically tempered	150	-	MPa

Table 3.2: Tensile bending stresses of float glass

Two design standards are preferred for yachts, namely the International Convention of Load Lines (ICLL) published by the International Marine Organization in 1966 and the standard ISO-11336-1:2012 Large yachts - Strength, weather and water tightness of glazed openings. The latter specifies that glazed openings are limited to above the highest waterline and stresses the importance of weather and water tightness. Design pressures are dependent on the location of the opening and the size of the vessel. The largest loads come from outside due to wind and water. Therefore, if the glass satisfies these loads, it also satisfied the suction loads from wind on the inside. Although the minimal design load is specified as 15 kN/m^2, in most cases, the design load can exceed 70 kN/m^2. Just as for buildings, partial factors are applied to the characteristic glass strength of glass to establish the design strength. However, the approach is very conservative, since the factors are only related to glass type, disregarding load duration and stress location. Meaning that the design value refers to the maximum allowable stress of the weakest part of the panel (Kozlowski & Bao, 2016). For example, the design value for thermally tempered glass can go down to 40 MPa which barely meets all the criteria of structure, aesthetics and comfort. Chemically tempered glass allows for a greater design value but limits the comfort criteria due to the fact that this type of glass cannot have coatings or frits on its surface.

3.4.2. Post-breakage behaviour

With thermal tempering, a compression layer depth of 20% of the glass pane thickness is achieved, while the compression layer depth for chemically tempered soda lime glass is limited to 9-15 µm. This compressive layer depth in combination with the surface compression and central tension determines the strength. As explained before, when failure occurs, the fracture pattern of thermal tempered glass varies due to a difference in residual stresses being released. Annealed glass breaks into large pieces of glass, fully tempered glass breaks into small pieces of glass, with heat strengthened being in the middle of the spectrum. Annealed glass has a low strength and breaks in dangerous large and sharp pieces of glass. This improves post-breakage behaviour when laminated. These large pieces of glass in combination with lamination enables the glass panel to have a certain load-bearing capacity. Heat strengthened glass is stronger than annealed glass, breaking into slightly smaller pieces of glass whilst remaining load-bearing capacities after failure. Fully tempered glass is even stronger than heat strengthened glass, but breaks into very small pieces of glass resulting in hardly any loading-bearing capacity after failure. This principle is shown in Figure 3.12 with heat strengthened being the best option when both the structural performances and remaining structural capacity are taken into account. As a result, heat strengthened glass is, due to its initial high strength, promising post-breakage behaviour and rather low costs, the most widely used glass type in the building industry these days.

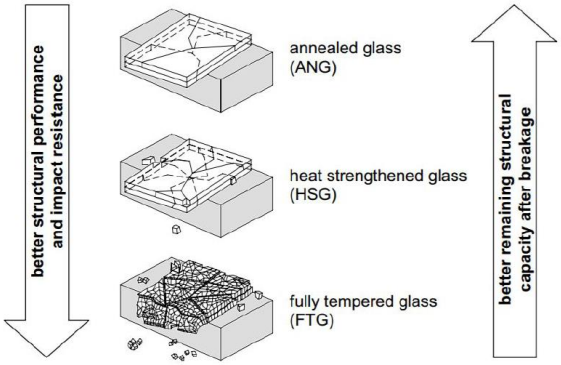

Figure 3.12: Structural performances vs remaining structural capacity for different glass types (Haldimann et al., 2008)

Chemically tempered float glass has a high strength and breaks into large pieces of glass, comparable to annealed glass. When laminated, this type of glass is a very promising post failure structural element. However, safety issues arise due to limited values of central tension levels in thicker glass as a consequence of ion exchange. Surface compression stresses are developed as a result of the larger volume of the ions invading the glass, which in return is balanced by internal tension. The depth of the compressive layer is however far smaller than the glass thickness, hence only a small central tension is generated (Macrelli, 2016). It's this weak central tension that is responsible for the large fragmentation. Thus, when the bond between compression and tension is broken, the pane behaves as annealed glass.

3.4.3. Failure patterns

Glass failures may generally be classified as an instability failure or a failure by overstressing of the glass in direct or indirect tension. An instability failure means that glass elements are susceptible to elastic buckling instability or lacks adequate lateral fixing. Overstressing of the glass means that failure may be caused by excessive uniform loads, uneven or inappropriate supports, blasts, impacts or thermal stresses (Haldimann, Berger, & Bern, 2007). However, flaws and inclusions in the glass will often cause premature failure. A few of these failures are schematized in Figure 3.13.

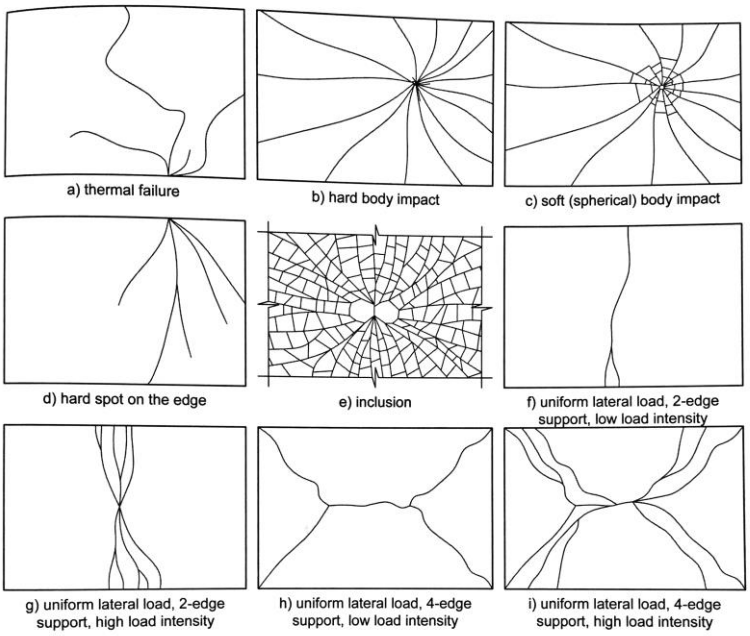

Figure 3.13: Schematic representation of typical glass failures (Haldimann et al., 2007)

3.5. Connections

In general, glass is limited by the length of vehicles used for transportation, forcing manufacturers to cut glass panes in standardised sizes of 3.21x6.00 m. Due to increasing demands, larger and larger glass panes are becoming more common, but require specialised transportation. Even though glass panels become larger, glass still needs to be connected. The basic principle of connections is that they need to redistribute applied forces evenly and limit localised stresses. Therefore, connections are designed to protect the glass from hard materials via the use of a softer material, like plastic, rubber and wood. Bearing or setting blocks are often used along the line of a glass panel to cushion and/or centre the glass in a typical installation. These blocks are not physically connected to the glass and thus only work in compression.

3.5.1. Continuous connections

Continuous linear supports, usually made from aluminium, steel, plastic or timber, are the simplest and most widespread method of supporting a glass pane. Support is given to the edges of the glass pane of which the frame is connected to another frame or surface. With the frame being slightly larger than the pane, materials like rubber or silicone are used to transmit lateral loads that are applied to the glass pane into its supporting frame. The out-of-plane loads are transmitted through a structural sealant, whereas the in-plane loads are transmitted through setting blocks (O'Regan, 2014). Although softer materials are used to transfer the loads evenly, it is still possible for the stress distribution to not be constant along the line of support. Furthermore, attention must be paid to the finishing of pane's edges, the corners of the pane and the effect of thermal movement.

3.5.2. Clamped connections

Instead of linearly supporting glass panes, one can also use clamped connections. These fixings consist of a small metal clamp with a softer layer in between the glass and the metal, and are fixed onto a sub-frame support structure. A setting block is installed to transfer in-plane loads and provide vertical support to the glass pane. Friction grip clamped connections have a bolt passing through the glass pane. The bolt hole is larger than the bolt and filled with a weaker, less rigid material. The latter is applied to develop the necessary friction, to prevent any contact between the bolt and the glass and to distribute the clamping force evenly (O'Regan, 2014).

3.5.3. Bolted connections

Bolted connections induce higher local stresses due to the smaller contact surface. As forces are applied to the glass pane, the stresses around the bolt fixing vary considerably, leading to localised stresses within bolted connections. This can be reduced by allowing the bolt to yield locally or by including softer materials between the glass and the bolt. Examples of these softer materials are soft aluminium, plastics and resins. Typical arrangement of bolted connections consists of two bolts being restrained in the vertical in-plane direction, only one bolt resists both vertical and horizontal in-plane loads and one bolt is free to move vertically and horizontally. This allows the pane to expand and contract as a result of temperature change or accommodate in-plane movement of the supports. Countersunk bolted connections can

also be designed, the disadvantages being significantly reduced tolerances, a greater complexity and therefore this solution is costlier. Common to all bolted connections is the risk of loosening due to vibration. Other aspects that must be considered are edge distances, thickness of the glass pane, the isolating material between bolt and glass, and the closeness of fit of the bolt itself (O'Regan, 2014).

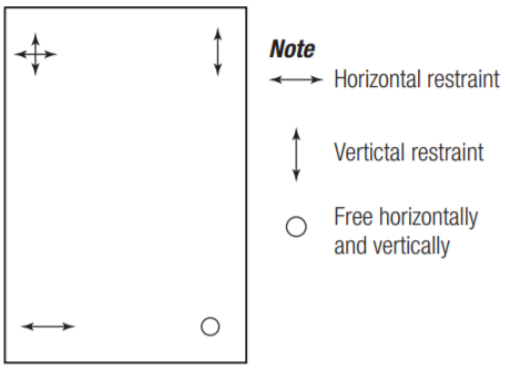

Figure 3.14: Typical arrangement of bolted connections (O'Regan, 2014)

3.5.4. Adhesive connections

Adhesive connections are used to connect glass panes by bonding them to supporting frames or to other pieces of glass, achieving an almost fully transparent structure. Two types can be distinguished, namely soft adhesives and stiff adhesives. The former can also be divided in weather and structural silicones. Weather silicones are used to connect glass panes together without the need of structural performances, for example in cable net glass facades. This type of silicone can shorten and elongate 50% of its original thickness, while structural silicones shorten and elongate 25% of its original thickness. Structural silicone comes in different types, colours and stiffness's. White, grey and black structural silicone adhesives are used, as well as a transparent structural silicone adhesive or laminate (TSSA or TSSL). The latter combines high transparency, strong adhesion performance, thermal stability, and excellent weatherability (Sitte et al., 2011). It also turns white when the stress level increases above the allowed design value and returns back to transparent when stresses are removed, allowing for a safety indicator of the bonding strength. These features make transparent structural silicone adhesives very expensive. The structural silicone can be cured by air, heating or as a result of a reaction between two components. When loaded, the connection ensures an evenly distributed force along the area or length of the glass panes. The distribution results in a reduction of local stresses, a great advantage compared to other connection methods. These adhesives also perform well under uniform tension. However, they have trouble resisting peeling or shear loads and are less resilient when loaded long-term. In yachts, using structural silicone on site effects the anti-fouling paint, used to slow the growth and facilitate detachment of organisms that attach to the hull. Therefore, this adhesive isn't allowed on site and can only be used to for glass to metal connections off site. Instead, polyurethane is used in yachts, with the great disadvantage of being UV unstable, turning transparent adhesives into yellow, forcing manufacturers to apply black adhesives.

Using stiff adhesives (epoxy adhesives and polyester resins) is a relatively unproven technology in the field of structural glass, but has already found its way into the automotive and aeronautical industries. A major advantage of stiff adhesives over soft adhesives is that it can achieve composite action, while the former has poor shear resistance (O'Regan, 2014). However, variations in thickness of stiff adhesive connections can generate localised stress concentrations and, due the bond being stronger than the base material, failure of stiff adhesives results in pulling of the glass surface. Furthermore, stiff adhesive connections restrain thermal movement and unlike structural silicone, a structure designed with stiff adhesives needs to be replaced in its entirety when damaged.

3.6. (Dis)Advantages

Over the years, processes are developed to steer towards a more efficient float glass production at lower costs, better quality and lower energy consumption. However, glass still consumes a large amount of energy as high temperatures are needed to mix the raw materials. Therefore, the glass industry is usually referred to as an energy intensive industry together with the production of steel, aluminium and cement (Schmitz, Kamiński, Maria Scalet, & Soria, 2011). Automated float glass lines produce several hundred tons each day, operating 24 hours a day all year round to meet demand. Oristep Consulting (2015) shows that the glass market was worth €38.85 billion in 2014 and is projected to reach €68.32 billion in 2020. In other words, with an increased and growing market, the glass industry needs to step up in terms of its production and environmental footprint. Standard sized annealed float glass of 4 mm thick costs around €10-12 per square meter, standard sized tempered float glass of 4 mm thick costs around €20 per square meter with the price linearly increasing up to 8 mm thickness. Larger panels are available, but at a higher price.

Due to its initial high strength, promising post-breakage behaviour and low costs, heat strengthened glass is the most widely used glass type in the building and automotive industry these days. While fully tempered glass is necessary for marine applications to meet regulations. Chemically tempering can be preferred over thermally tempering due to its ability to temper different geometries and better optical qualities. However, soda lime glass is difficult to chemically temper due to its composition. It is also limited to a certain size due to the dimensions of the chemical toughening bath. This only becomes a determining factor for larger panels. New chemical toughening baths need to be built to keep up with the ever increasing size of glass panels, hence the increase in price. Both tempering methods are subjected to failures due to flaws. In spite of all the post processing processes, the material remains a fragile and brittle material with a low scratch resistance and relatively low strength. With a density of 2500 kg/m^3, conventional glass can be assumed to be a heavy material. Additionally, coverings always demand coatings for thermal and optical reasons. Only indoor doors or balustrades will not require coatings.

The disadvantages and advantages of soda lime float glass are summarized in the table below.

Disadvantages	Advantages
Fragile and brittle material	Low costs
Heavyweight	Automated production
Optical distortions	Availability of large panels
Low scratch resistance	Easy to thermally temper
Relatively low strength	Large architectural market
Hard and expensive to chemically temper	
High energy consumption	
Limited curvature	

Table 3.3: (Dis)Advantages of soda lime float glass

4. Thin glass

Due to the disadvantages in soda lime float glass in certain applications, other types of glass needed be developed. In the beginning of the 20th century, scientists established that borosilicate glass had a superior resistance to chemical attacks and a better thermal shock resistance because of their lower thermal expansion (LeBourhis, 2014). Therefore, borosilicate glass became a success for ovenware and laboratory equipment. Borosilicate glass is however harder to temper thermally and chemically due to the lower thermal expansion and small amount of alkali ions. From 1960, the fusion draw process encouraged the development of very thin glass using aluminosilicate glass. This strong, scratch resistant, lightweight and clear material was initially applied in the automotive industry, but also made its way to other dedicated applications like highspeed train windshields and smart phones. To get a better understanding of thin aluminosilicate glass, this chapter focusses on its production, physical and structural properties, advantages and disadvantages.

4.1. Production

Thinner glass is more difficult to produce with respect to their flatness (Kloss, 1996). To produce glass which achieves smooth, flat surface characteristics in the required micron range, only three different processes are used. These are the micro float process, the overflow fusion process and the down draw process. Each process includes a glass sheet that needs to be cooled down sufficiently, where after they are inspected, cut and stored.

The micro float process is very similar to the floating process, producing thicknesses down to 0.55 mm. The only difference is that after the raw materials are combined and fed into the melting tank, the mixture is heated to temperatures higher than the floating process. The molten glass is then refined to remove bubbles, impurities and eventually cooled at an even more slow and controlled rate (Wegert, 2010). As with the float process, the micro float process produces glass with inequivalent sides, namely a tin side and an air side. The tin side shows substantial tin absorption, as deep as 2-10 µm, together with the conveyer rolls creating small optical distortions (Varshneya & Bihuniak, 2017). The micro float process has a smaller output compared to the float glass process, but the big advantage is that the process can generate sheets as big as 3 m wide.

With the overflow fusion process, the glass sheet is formed from a continuous glass flow from a bath. By using the principle of overflowing and gravity, glass flows out along the two sides of the bath and joins downwards to form a glass sheet (Figure 4.1). With this process, thicknesses down to 0.1 mm are achieved. The external faces of the sheet are not mechanically damaged and no polishing of the glass is necessary since the process delivers excellent glass surface quality (LeBourhis, 2014). Any damaged edges are removed later.

As mentioned, Emile Fourcault invented the technique of producing a continuous glass plate by vertically drawing glass from a molten glass bath, also referred to as the down drawn process (Figure 4.1). At the time of invention, the quality was not satisfactory and the market was too small for further innovation. Nowadays, this process can create ultra-thin sheets of glass ranging from a millimetre to several micrometres, eliminating the need for post-production processes to meet application requirements.

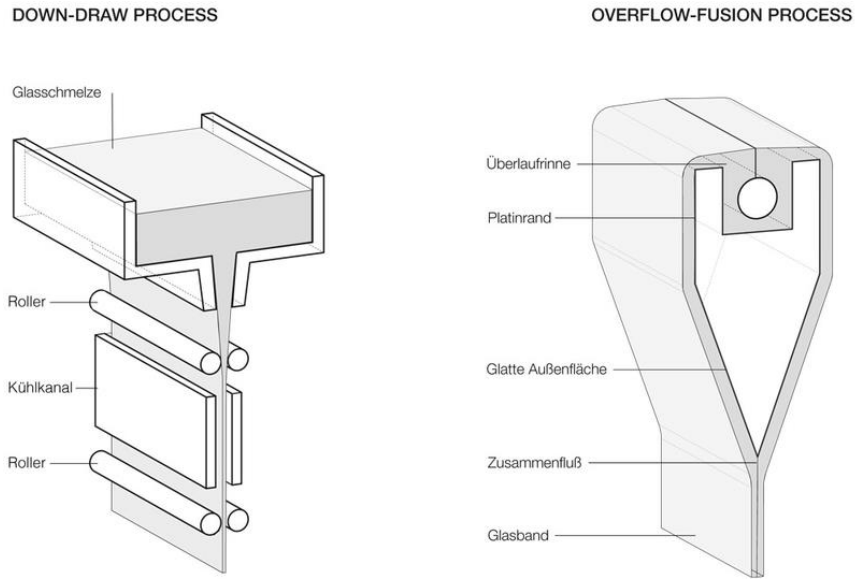

Figure 4.1: Down drawn and overflow fusion process (Albus & Robanus, 2014)

After production, thin aluminosilicate glass is strengthened by chemical tempering. Thermal tempering of thin glass is not feasible, because of the high thermal exchange coefficient that would be required to produce a large enough temperature difference between core and surface upon cooling (Gy, 2008). Also, conventional thermal tempering would mark the surface. By chemical tempering, the compressive stress is balanced by the tensile stress below, resulting in a tensile core stress level that may become comparable to the surface compression. As mentioned in chapter 3.3.1, this phenomenon arises because of larger volume ions replacing smaller volume ions in the glass. Time, temperature and salt bath composition are critical factors in obtaining appropriate depths of compression and stress levels. Compared to soda lime float type glasses, aluminosilicate glasses can be chemically tempered to larger depths of compression and higher surface compressive stresses in shorter amounts of time (Gomez et al., 2011). Moreover, the surface becomes shock and scratch resistances, as required for today's applications.

4.2. Physical properties

As mentioned, borosilicate glass is harder to temper thermally and chemically due to the lower thermal expansion and small amount of alkali ions. Therefore, an aluminosilicate glass mixture is used to produce thin glass. This mixture consists of silica sand (SiO_2), soda (Na_2O), lime (CaO), magnesia (MgO), alumina (Al_2O_3) and boron-oxide (B_2O_3) in the composition as illustrated in Table 4.1. The focus is specifically directed to alkali aluminosilicate glasses since the high alkali content prepares the glass better for ion exchange and thus improves the surface compressive strength significantly. Using chemically tempered alkali aluminosilicate glass gives the glass high transformation temperatures and outstanding mechanical properties, such as hardness and scratch behaviour (Schott, 2014). Alkali borosilicate is a type of borosilicate glass that can also be chemically tempered, but the surface compression generated by ion-exchange in alkali borosilicate glasses is not as strong as the surface compression in alkali aluminosilicate glasses (Talimian, 2016).

Silica sand	SiO_2	62 %
Soda	Na_2O	1%
Lime	CaO	8%
Magnesia	MgO	7%
Alumina	Al_2O_3	17%
Boron-oxide	B_2O_3	5%

Table 4.1: Composition of aluminosilicate glass

Glass thicknesses of 2 to 25 mm are considered to be float glass, glass thicknesses of 0.5 to 2 mm are considered to be thin glass and glass thicknesses below 0.5 mm are considered to be ultra-thin glass. An interesting example is Willow glass from Corning that can be produced in rolls of up to 1.3 m wide and 300 m long, with a thickness of only 100-200 µm. However, its minimal thickness combined with the way of production and a composition of alkali-free borosilicate glass makes it hard to strengthen the glass using thermal or chemical treatment. Therefore, this type of glass will never be as strong as thin aluminosilicate glass. This thesis will focus on thin aluminosilicate glass with a thickness ranging from 0.5 to 2 mm.

As mentioned in chapter 3.2, the optical properties depend on the glass thickness, chemical composition, applied coatings and the way the glass is fabricated. All these properties are outstanding for thin glass and give the material an advantage over float glass. Especially the minimal thickness causes thin glass to be clear, lightweight and in combination with chemical tempering, flexible but still very strong. The minimal thickness, however, also results in small values for heat transfer (U-value) and limited bending stiffness. In terms of fire resistance of thin aluminosilicate glass, no actual research has been done yet. Glass with a high thermal expansion coefficient combined with a low tensile strength shatters relatively easily. Aluminosilicate glass has a slightly higher thermal expansion coefficient, but better tensile strength properties compared to soda lime glass. Therefore, for now, it can be assumed that thin glass behaves in a similar way as float glass when exposed to fire.

4.3. Types of thin glass

Float glass is produced by many manufacturers all over the world, the production of thin glass and ultra-thin glass is limited to manufacturers like Asahi Glass Co. (AGC) from Japan, Corning from the United States and Schott from Germany. Only a few seem to have promising characteristics for structural use in terms of the composition, size, allowance for tempering and strength. This chapter provides an overview of the most promising types of thin aluminosilicate glass. Table 4.2 illustrates a few physical properties of the different types of thin glass that made the list.

4.3.1. Schott Xensation glass

Xensation glass is micro floated aluminosilicate glass produced by German company Schott, with cover glass protecting touch screen devices and robust lightweight glazing solutions as the main applications. Schott advertises Xensation glass as a material with extremely high impact and bending strength that enables thinner, sleeker and more sensitive devices without compromising the strength. It has a high scratch resistance, durability, clarity, visual quality and allows for tolerances. Moreover, it is rather easy to produce due to the use of the micro float process. Standard sizes are available in 475x575 mm and 950x1150 mm with a thickness range of 0.5-3.0 mm. No further information could be found on the applicability of coatings.

4.3.2. Corning Gorilla glass

Corning® Gorilla® Glass is produced by Corning located in New York as a thin alkali aluminosilicate glass mainly applied in the electronics or automotive industry. Gorilla glass is formed using the fusion process to create an accurate highly-automated process that produces glass with clean, smooth, flat surfaces and outstanding optical quality. Gorilla Glass allows for a deep layer of high compressive stress created through chemically tempering which makes the glass strong, damage resistant and helps to prevent deep flaws and scratches that degrade the appearance and can cause glass to break. Standard sizes are available in 2020x1365 mm and 2020x1200 mm with a thickness of 1 mm or 2 mm respectively. Other thicknesses are 2.0, 1.5, 1.0, 0.7 and 0.55 mm. No further information could be found on applicable coatings.

4.3.3. AGC Dragontrail glass

Asahi Glass Co. (AGC) produces Dragontrail glass using the micro float process. This glass is an alkali aluminoborosilicate composition with a fairly high glass transition temperature (Varshneya & Bihuniak, 2017). Dragontrail glass is brought to the market to provide an innovative glass that best suits new generation mobile devices due to its superior qualities in strength, scratch resistance and texture. Standard sheet sizes are 1219.2x736.6 mm and 1524x736.6 mm available in a thickness of 1.1 mm. Custom sizes may be available upon request. Dragontrail glass is produced in Japan and mainly available for displays. No further information could be found on applicable coatings.

4.3.4. AGC Leoflex glass

Leoflex glass is also produced by AGC as a very thin, chemically tempered, aluminosilicate glass type. It offers a great impact resistance, scratch resistance and weather resistance. Due to its lightweight, flexibility and optical clarity, AGC promotes the glass to be applied in the electronics, industrial and architectural environment. The glass is currently produced and processed in Japan. Sheet sizes up to 2070x1650 mm are available in thicknesses of 0.55, 0.85, 1.1, 1.3 and 2.0 mm. Cutting, grinding and drilling can be done before or after chemically tempering the glass. Laminating, painting, printing, coating or cold bending can only be done after the chemical treatment. The glass is bendable between a 100-300 mm bending radius.

4.3.5. AGC Falcon glass

Falcon glass is produced by AGC as a chemically tempered hybrid aluminosilicate glass and fabricated in Belgium. Falcon glass is created to bridge the gap between soda lime and aluminosilicate glasses in the most cost efficient way. This type of glass is applied in consumer electronics, transportation and buildings. It is suitable for architectural applications due to its cheaper production process and the possibility of producing smaller series. Sheet sizes from 1245x3120 mm up to 1600x3120 mm are available depending on the thicknesses from 0.5, 0.7, 1.1 to 2.1 mm. Post processing processes can be applied, such as cutting, grinding, drilling, painting, printing and wet coating. The graph from Appendix A.5 also shows that you can even cut the chemically hardened glass below a certain "depth of layer" without further fragmentation.

		Float glass	Xensation glass	Gorilla glass	Dragontrail glass	Leoflex glass	Falcon glass	
Density	ρ	2500	2477	2390	2480	2480	2480	kg/m^3
Young's modulus	E	70000	74000	68000	74000	74000	73000	MPa
Shear modulus	G	30000	30000	27900	30000	30000	30000	MPa
Poisson's ratio	v	0.22	0.215	0.22	0.23	0.23	0.22	-
Transition temperature	T_g	530	615	574	604	604	575	°C
Thermal expansion	α	85E-7	88E-7	76E-7	98E-7	98E-7	91E-7	$°C^{-1}$
Thermal conductivity	λ	0.96	0.96	-	-	-	0.95	W/m°C
Light transmission	LT	90	91	91	91	91	91	%
Maximum size	A	3.2x18	0.95x1.15	1.37x2.02	0.74x1.52	1.5x1.85	1.6x3.21	m
Thickness range	t	2-19	0.5-3	0.55-2	0.5-5	0.55-2	0.5-2.1	mm

Table 4.2: Physical properties of glass retrieved from EN16612 (float glass) and Appendix A (thin glass)

4.4. Structural properties

Although the characteristic value for the tensile bending strength of chemically tempered float glass is described in EN16612, the values for thin glass are not included and require a different approach to determine the strength. Firstly, because a different composition is used compared to float glass. Secondly, chemically tempered thin glass behaves differently than chemically tempered float glass due to its thickness and the resulting residual stress distribution within the glass panel. Thirdly, the flexibility of thin glass also causes the panel to behave differently compared to regular float glass. It is due to this flexibility that the standards are generally hard to use. A flexible structure doesn't necessarily mean that the structure is unsafe. However, according to these standards, deflections have to be limited in the service limit state in order to let people feel comfortable in their surroundings. In other words, the building industry regulations do not allow for the benefit of flexible thin glass. A different approach is taken when designing yachts. These structures have to resist the worst conditions. As long as the glass does not break, deflections are the least of their worries.

The difference in composition, thickness, residual stress distribution and flexibility compared to float glass prohibit the use of existing test scenarios as described in standards such as EN 1288 (four-point bending test or large ring on ring test). Furthermore, possible test scenarios for determination of the ultimate bending strength of thin glass are currently not distinctly regulated in standards and have to be investigated before the strength can be determined. Neugebauer (2017) investigated and analysed different test set-ups for their applicability for determination of the bending strength of thin glass. These different test set-ups are illustrated in Figure 4.2. The first two scenarios, ring on ring test and pressure pat on ring test, determine the ultimate bending strength without the influence of edge strength. The edge strength completely depends on the edge quality, which is determined by flaws introduced by cutting the glass. As mentioned in chapter 3.4, these flaws cause stress concentrations and are the starting point for crack propagation. Since the maximum stress arises in the middle of the pane, glass supported by continuous connections is a good example of an application where edge effects do not have to be taken into account. The other scenarios determine the strength with the influence of edge quality.

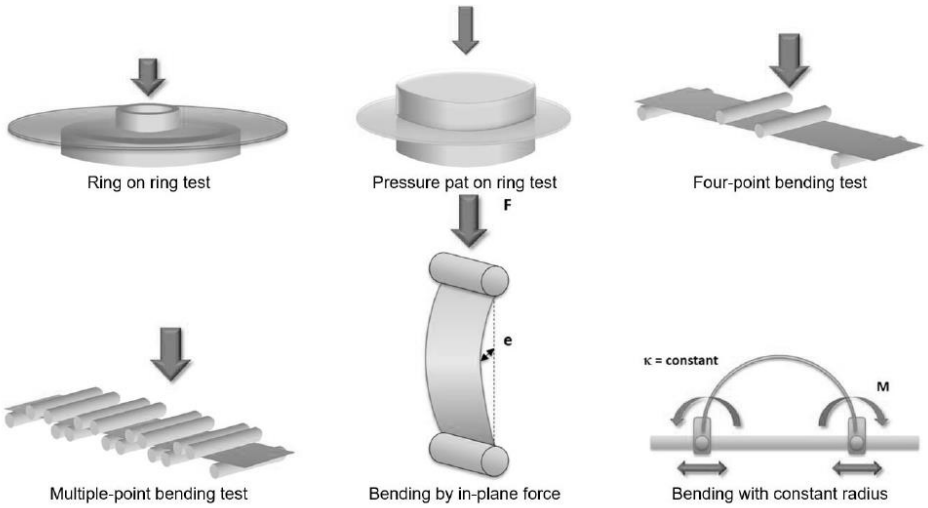

Figure 4.2: Different test set-ups for thin glass (Neugebauer, 2017)

Effects due to nonlinearity, sample size, imperfections and load duration have to be taken into account to find the correct test scenario and determine the ultimate bending strength of thin glass. Therefore, it is needed to find an accurate balance between size and effective area, in which the measured stress can be assumed homogeneous. As well as sensitivity related to imperfections and nonlinear effects (Neugebauer, 2017). Neugebauer concluded that the most promising test scenario is bending a thin sheet of glass with a constant radius. The advantage of this scenario is that the influence of the sample size can be minimized, meaning that the area is increased in which the maximum stress can be assumed as homogeneous. However, bending with a constant radius scenario must be investigated much more related to the applicability of thin glass. The ring on ring test set-up can also be applied, but has to be improved to minimize the probability of effects related to imperfections and stability effects.

4.4.1. Strength

Smaller ions diffuse faster than larger ions, resulting in larger depths of compression that protect the glass surface from flaws or damage. The depth of compression is also referred to as the depth of layer (DOL). On the other hand, larger ions can produce higher compressive stresses (CS) than smaller ions resulting in higher strength glass. Ultimately, a combination of the larger compression depth and larger diffusion particle size is ideal. Temperature and time allow controlling the rate and extent of ion diffusion, and as a consequence the magnitude of the stresses and compression depth (Gomez et al., 2011). Figure 4.3 shows the relationship between the depth of layer and compression stresses for

a set of soda lime silica (SLS) glasses compared to Gorilla glass (GG) and a series of alkali aluminosilicates. Gorilla glass is mainly used for smart phones, implying that they need a rather high scratch resistance to deal with everyday exposure. From Figure 4.3 it can indeed be concluded that this type of glass has a large depth of layer, protecting the glass surface from flaws and damage.

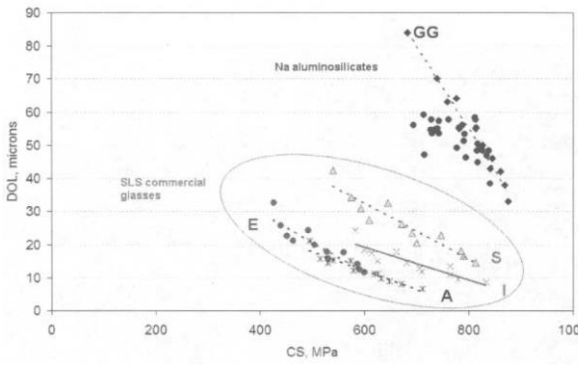

Figure 4.3: Depth of layer (DOL) versus compression stresses (CS) (Gomez et al., 2011)

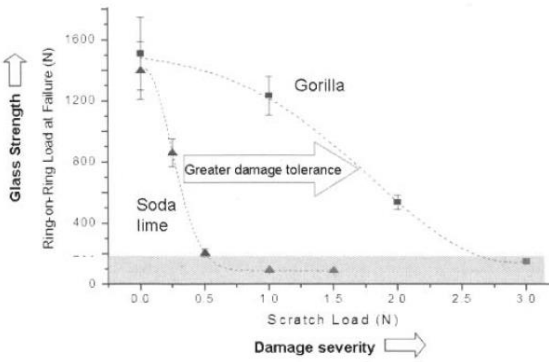

Figure 4.4: Damage severity versus glass strength (Gomez et al., 2011)

The greater damage tolerance between soda lime silica glass (SLS) and Gorilla glass (GG) is implied by comparing the retained strength via ring on ring (ROR) after scratching the surface at various loads (Figure 4.4). The slower drop in strength for Gorilla glass denotes this greater damage tolerance. Again, the depth of the compression layer plays an important role. While the DOL of soda lime glasses range between 9-15 µm, the DOL of thin aluminosilicate glass range between 25–60 µm (Varshneya & Bihuniak, 2017). The deeper DOL enables Gorilla glass to retain its strength after scratching, while soda lime glass lost its strength because the induced flaws penetrated its compressive layer (Gomez et al., 2011). Assumptions are made that the findings are also true, to a certain extent, for other types of thin glass.

Using thin glass as a structural material is a rather new development. It is for this reason that little research has been conducted and that the tensile bending strength of thin aluminosilicate glass is not included in the regulations. An example of a failure mode that needs further research is related to the frangibility of the material. Experiments have shown that the centre tension created by ion exchange results in spalling. While the recommended design strength used by suppliers is already about a third of the ultimate bending strength, the frangibility limit seems to be even lower. It is therefore recommended to extensively investigate the strength of thin aluminosilicate glass. This is beyond the scope of this research. For now, the tensile strength values are obtained from the different thin glass suppliers as shown in Table 4.3. The tensile strength for Xensation and Dragontrail glass is only expressed in the ultimate bending strength. The design strength for these types of thin glass is assumed to be a third of the ultimate bending strength.

	Ultimate bending strength	Design strength	
Xensation glass	800	±260	MPa
Gorilla glass	-	200	MPa
Dragontrail glass	600	±200	MPa
Leoflex glass	-	260	MPa
Falcon glass	-	200	MPa

Table 4.3: Tensile bending stresses of thin glass retrieved from Appendix A and Eckersley and O'Callaghan (2018)

4.4.2. Post-breakage behaviour

Higher compressive stresses result in higher strength glass. When glass breaks, the fragmentation pattern depends on these generated stresses. In general, a higher degree of prestressing results in finer dicing at failure. When laminated, small fracture patterns cause the glass pane to have almost no load-bearing capacity. To keep a decent amount of load-bearing capacity, a larger fracture pattern is preferred. As mentioned in chapter 3.4.2, chemically tempered float glass breaks into large pieces of glass due to limited values of central tension levels in thicker glass. In thin glass, the tensile core stress level may become comparable to the surface compression (Gy, 2008). Chemically tempered thin glass has a residual stress profile, whose case depth, although still shallow in terms of micrometres, is significant in terms of percentage of the overall glass thickness. The failure pattern then depends on the stresses introduced in thin glass sheets. Flat thin glass normally fails into large pieces, while bent thin glass fails into smaller pieces due to the introduced bending stresses. Ultimately a balance needs to be found between the introduced stresses and the post failure load-bearing capacity.

4.5. (Dis)Advantages

Thin aluminosilicate glass is a promising material with great advantages. The already mentioned high strength and thinness of the material result in a flexible and lightweight panel with high optical properties. A remarkable scratch resistance is obtained due to a combination of the used composition and chemically tempering process. The fabrication is however more difficult and expensive than that of soda lime silicate glass (LeBourhis, 2014). According to AGC, the price for chemically tempered thin glass is mainly determined by the display market and is set on €23-25 per square meter from the end of 2018. The price will decrease once a larger market for this type of glass is established. At this moment, thin glass is mainly used in smart phones, LCD screens and tablets. Implementation of thin glass in other industries demands a different way of thinking for the material to be successfully marketed. For example, thin glass will never be a substitution for float glass as conventional windows due to the properties that serve the purpose well and large scale production. In order for other glass innovations to work, one has to think of areas where float glass doesn't work. Spitzhüttl et al. (2014) describes thin glass as a promising material in multiple glazing units, as laminated safety glass with reduced weight or as photovoltaic elements. By using thin glass, structures made of cold bent glass can be realised more easily and at less cost. Other areas worth investigating are related to tensioned, lightweight, pneumatic and flexible structures.

The disadvantages and advantages of chemically tempered glass are summarized in the table below.

Disadvantages	Advantages
Expensive	Flexibility
Lack of stiffness	Lightweight
Small architectural market	High strength
High energy consumption	High optical properties
	Scratch resistant

Table 4.4: (Dis)Advantages of thin aluminosilicate glass

CONCEPTUAL DESIGN

5. Application of thin glass

As stated in the previous chapter, thin glass will not be a substitute for normal applications of float glass in terms of stiffness and costs. Only by finding the incapacities of float glass, it might be possible to implement thin glass on a larger architectural scale. Eventually, reducing the prices of thin glass sheets creates a bigger market. The main drawbacks of float glass are that it is hard to curve and tension. It doesn't allow for flexibility and it is becoming a rather heavy building material due to the build-up. While thin aluminosilicate glass is lightweight, flexible, able to curve and a more promising material to tension due to its higher tensile bending stress. However, limited geometrical bending stiffness in its flat form prevents thin glass to be used for structural purposes. According to Lambert and O'Callaghan (2013), three main approaches can be distinguished to stiffen a thin glass panel. Firstly, to laminate the glass to a substrate providing increased out-of-plane stiffness. Secondly, to embrace its flexibility by cold forming the glass into curved developable surfaces. Thirdly, to treat the material as a fabric glass and design it for tensile membrane structures.

5.1. Composite panel

Traditionally, laminated glass panels are used to reduce the risk of broken glass falling and to improve their post-breakage behaviour. Multi-layered panes of glass bonded together by a transparent interlayer gives the panel its redundancy and strength after failure. By laminating thin glass to similar or other materials, the product resembles common glazing products currently on the architectural market in terms of planar panels with sufficient out-of-plane stiffness to resist imposed loads by bending moment action. Compared to these products, a thin glass composite panel offers a reduction in panel thickness and consequently weight, an excellent visual quality depending on the materials used, an enhanced redundancy and a high impact and blast resistance (Lambert & O'Callaghan, 2013). Two types of thin glass composite panels can be distinguished, namely lamination with transparent materials and semi-transparent materials. Table 5.1 summarises the most important properties of the materials investigated in this chapter.

5.1.1. Transparent sandwich panel

Thin aluminosilicate glass was initially applied in the automotive industry by replacing the inner float glass of a windshield laminate with a thin glass sheet. The most common windshield damage comes from small, sharp stones. The experimental set-up thus includes ball drop, high speed ball bearing and hail impact testing. The results illustrated that higher robustness in all three experiments is achieved and glass spalling on the inside was avoided (Leonhard, Cleary, Moore, Seyler, & Fisher, 2015). Testing such a windshield doesn't fully align with load case scenarios for other industries, but it definitely shows promising results for application of thin glass combined with float glass as a composite panel. Furthermore, an overall reduction in windshield weight of more than 30% can be achieved with the proposed configuration in comparison to conventional designs.

Conventional architectural laminated glass has a relatively low post-fracture strength and stiffness, which imposes several constraints on the structural use of glass (Overend, Butchart, Lambert, & Prassas, 2014). With the aim to establish scenarios in which thin glass laminates offer advantages over these conventional laminated glass products, research and experiments have been carried out by Eckersley O'Callaghan in collaboration with Cambridge University. The main focus of the tests was to provide data on the bending stiffness and strength performance of the laminated panels through the sequence of breakage scenarios. The experimental set-ups included four point bending tests and coaxial double ring tests for different supporting conditions and load case scenarios. Three specimens of each sample type were tested to each of the test procedures. Several composite samples consisted of two outer surfaces made of Gorilla glass, sandwiching different types of float glass with different interlayers (Figure 5.1). The results of these composite panels are compared to a reference model of two equally laminated sheets of heat strengthened glass with twice the total thickness and weight.

Figure 5.1: Float glass with Gorilla glass (left) and polymer with Gorilla glass laminates adapted from Lambert & O'Callaghan (2013)

When the load is applied to the reference model, the stress limit is reached in the lower glass pane and cracks. Reloading shows that the panel has residual strength in the unbroken sheet, but with significantly reduced panel stiffness. The remaining sheet therefore breaks at a lower load than initially imposed. This mechanism of the ultimate panel strength being less than the initial panel strength can be described as brittle failure (Figure 5.2). In composite panels with annealed glass substrates, initial fracture occurs in the core sheet, but the panel stiffness is only slightly reduced due to the fragments of the core being restrained between the outer unbroken Gorilla glass sheets. Using SG gives an initial mean fracture load of approximately 1.5 kN. The lower sheet resists the tensile bending stresses, while the broken core and upper sheet resist the compressive bending stresses. Hence, the panel continues to resist an increasing applied load. Secondary fracture then occurs in the lower glass pane at a mean load of 5.0 kN which is a much greater load than that of the initial fracture. The load applied during secondary fracture varies significantly between the three tested specimens and is a combination of the glass and interlayer material properties as well as the adhesion between them, fragmentation pattern and the testing boundary conditions. Further investigation is required to identify the exact cause of the variation in the secondary fracture loads (Lambert & O'Callaghan, 2013). Although the remaining intact glass does provide some residual strength and integrity, the overall stiffness of the panel has severely decreased. A mechanism of which the ultimate panel strength being greater than the initial panel strength, can be described as ductile failure and suggests a potential for security and seismic applications (Figure 5.2). Although composite panels with heat strengthened and fully tempered glass behaved in a similar way, with the core breaking first followed by the lower sheet, the secondary failure was approximately equal to the load causing initial breakage. For composite panels with annealed glass, the load at initial fracture is still higher than the load at initial fracture. Choosing a configuration depends on what is preferred, a higher initial breakage load or better post-breakage behaviour.

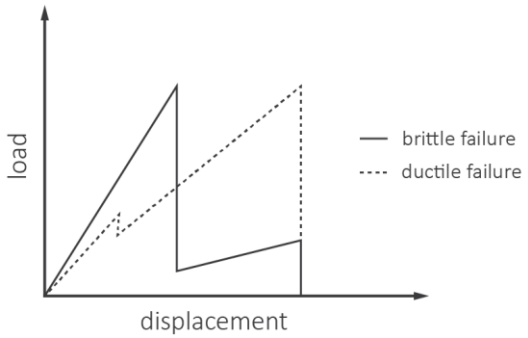

Figure 5.2: Brittle vs ductile failure mechanism adapted from Lambert & O'Callaghan (2013)

Another way of transparently laminating thin glass is using a polymer material. Polymer materials have high impact resistance due to their energy absorbing characteristics. They are commonly used for protection against vandalism, forced entry, bomb blast and other high impact scenarios. However, polymers have a low stiffness and a low surface scratch resistance. Two useful types of polymers can be distinguished, namely polycarbonate (PC) and polymethylmethacrylate (PMMA), also referred to as acrylic. Polycarbonate has a higher impact resistance, is easier to work with in terms of cutting, but is more likely to scratch, more expensive, has poorer clarity and tends to yellow over time due to UV radiation. Polymethylmethacrylate has less impact resistance than polycarbonate, but is more resistant against distributed loads, is less likely to scratch, has better clarity and does not yellow over time. An example of a structure entirely made out of acrylic is the Embassy Gardens Sky Pool engineered by Eckersley O'Callaghan, which ensures watertight connections without the use of non-transparent materials. Although glass still has a better clarity, small distortions in acrylic are hard to recognize while swimming in water. The wave like distortions arise from the production process at the surface and are expected to be reduced when laminated to thin glass. Furthermore, fracture turns both polymers white. The white area can be polished off, but it is recommended to stay into the elastic zone of the material, especially when laminated to thin glass. The great advantage is that these polymers can be poured into a mould enabling curvature and free from architecture. Additionally, colours can be applied which can have both architectural and solar gain control properties.

Weimar (2012) proposed laminating float glass with polycarbonate to combine a high resistance against attack with slender cross sections and reduced dead load, concluding that they have sufficient post-breakage behaviour and inherent redundancy. Float glass contributes to the stiffness of the composite panel, whereas the polycarbonate provides high impact strength in combination with low weight. To reduce the weight of the panel even more, a polymer material can be combined with sheets of thin glass improving the scratch resistance compared to a solid polymer. The compromise being the stiffness of the composite panel. Eckersley O'Callaghan did a small investigation into polymers combined with thin glass in collaboration with Cambridge University. The composite samples consist of a lower sheet made of Gorilla glass, bonded by thermoplastic polyurethane (TPU) with a polycarbonate or acrylic sheets on top (Figure 5.1). Polymers don't spall at failure and therefore don't need to be sandwiched into two layers of thin glass. Therefore, in this configuration, Gorilla glass is only attached at the bottom to function as some sort of reinforcement. Consequently, loads can only be applied in one direction. TPU is applied as an interlayer instead of PVB due to improvements in adhesion and

impact performance between polymers and glass (Teotia & Soni, 2014). This interlayer also has a very low transition temperature, as such that laminating thin glass to polycarbonate or acrylic doesn't result in the polymers becoming viscous. The experiments showed that initial fracture occurs in the thin glass sheet at lower loads than composite panels with thin and float glass. At this point, a severe reduction in panel stiffness can be observed and testing is terminated due to excessive deflections. Although its residual strength is significant, the panel is no longer effective in resisting loads due to this flexibility. Though, the change in stiffness demonstrates an effective composite action through the interlayer in unfractured state (Lambert & O'Callaghan, 2013).

		Float glass	Thin glass	PC	PMMA	Aluminium	
Density	ρ	2500	2480	1200	1170	2690	kg/m^3
Young's modulus	E	70000	74000	2300	3100	68300	MPa
Transition temperature	T_g	530	604	150	105	-	°C
Thermal expansion	α	85E-7	98E-7	65E-6	70E-6	24E-6	$°C^{-1}$
Thermal conductivity	λ	0.96	0.97	0.21	0.193	238.5	W/mK

Table 5.1: Physical properties of glass retrieved from EN16612, Appendix A, Martienssen & Warlimont (2005) and Aalco (2005)

5.1.2. Semi-transparent sandwich panel

The previous chapter explored transparent composite panels with a core that homogenously supports thin glass. Point, regional or line supports are used in semi-transparent composite panels to allow for solar control, privacy, energy savings and an increased stiffness without increasing its weight. Not all materials are suitable to use in a composite panel. Questions are raised on how to laminate different materials to glass in terms of manufacturing, bonding, thermal expansion and thermal insulation. Also, the structural performance of the composite elements is largely dependent on the stiffness of the glass and adhesive, the layer thickness of the adhesive and the distance between the core elements. For a given load, reducing the profile height, the shear modulus of the adhesive, the adhesive thickness or the number of core elements leads to higher stresses in the glass and hence to a higher probability of failure (Wurm, 2007).

Wurm (2007) presented a glazing prototype for composite insulating glass unit with integrated solar shading. Two glass panes of an insulating glass unit are structurally bonded to a core layer of different cross-sectional glass fibre reinforced plastic polymer (GFRP), which are arranged in parallel in the glazing cavity. The result is a uniaxial, composite slab component. Four point bending tests concluded that failure occurred in the area of maximum bending moment, hence in the centre. There was no evidence that the bond failed. The different composite cross-sections showed a similar moment of inertia and thus comparable stiffness. Due to the structural action of the GFRP profiles, the composite elements have a high residual load-bearing capacity. After breakage, the configuration was still capable of carrying a continually increasing load even with considerable deformations.

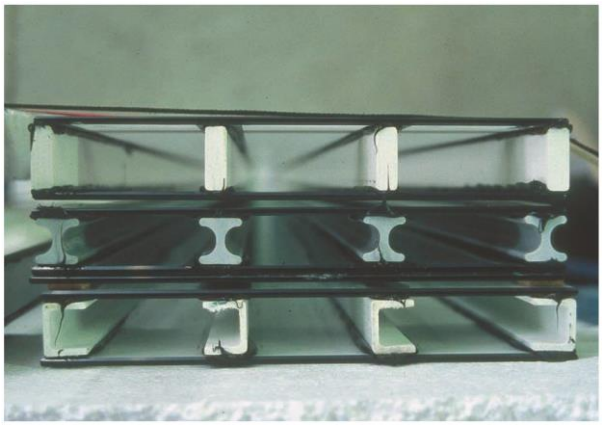

Figure 5.3: Prototypes with different profile geometries (Wurm, 2007)

Another interesting composite panel was designed by Bellapart for the Berkeley glass pavilion. Their sandwich panel consists of two glass sheets bonded to a microperforated aluminium honeycomb core by means of a continuous layer of UV-curing transparent acrylic (Figure 5.4). Fabricating glass-honeycomb panels requires special equipment, skilled personnel and a clean environment. Structural and visual properties, viscosity and vapour emissions during curing are important factors that must be taken into account when choosing an adhesive. During fabrication, the liquid adhesive climbs on the honeycomb by capillarity creating small distortions. Still, the light and solar transmission of the panels is high due to reflection between the used materials, thus, a protective solar coating is required. The thermal performance is lower than a similar conventional IGU due to the thermal bridge caused by the aluminium honeycomb. Therefore, triple glazing combined with an argon-filled air chamber is needed to neutralise the thermal bridge. The bending stiffness of the panel is however significantly increased due to the larger moment of inertia. Compared to a conventional IGU,

deflections at the centre of the panel and stresses around point fixings decrease. After breakage, the glass fragments remain attached to the honeycomb thanks to the used adhesive. Despite this excellent post-breakage behaviour, laminated glass was used in all lower glass plies of the Berkeley pavilion in order to satisfy the requirements set by the authorities (Teixidor, 2016). All these aspects combined create a rather complicated panel and actually increase the overall weight of the panel, especially when compared to a conventional IGU.

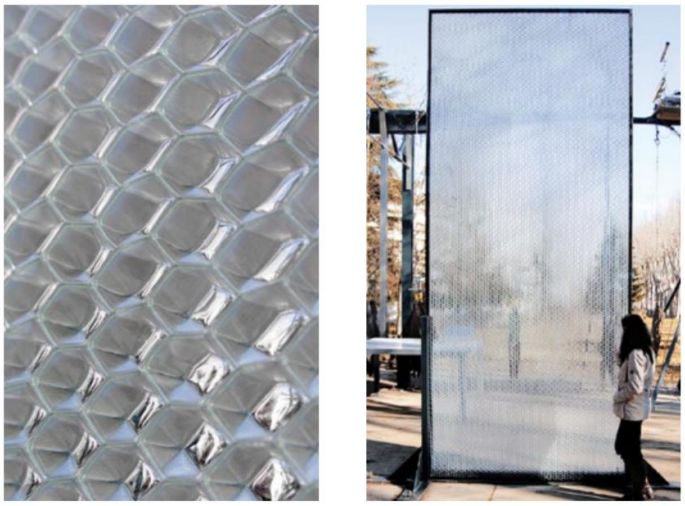

Figure 5.4: Triple Glass aluminium honeycomb composite panel (Teixidor, 2016)

Applying thin glass to semi-transparent materials can reduce the thickness and the weight of the panel even further. However, only a few students from Delft University of Technology investigated composite thin glass panels with semi-transparent materials. Van der Weijde (2016) researched composite façade panels as being part of a curtain wall. The composite panels consisted of an extremely lightweight, high strength, non-metallic aramid honeycomb pattern sandwiched in between two layers of thin glass. M. Akilo and T. Neeskens are studying the possibility of a 3D printed pattern as the core material between thin glass layers.

5.1.3. Conclusion

The automotive industry takes the lead in researching float glass combined with thin glass. It must be noted that only one sheet of thin glass is needed on the inside of the windshield due to the applied load cases, for other scenarios different build-ups can be required. While there may be enough knowledge to design transparent composite panels, no direct application has been found yet to incorporate these panels in another industry. This has to do with the fact that someone has to take the responsibility to make sure the structure is safe. For now, only a small investigation has been carried out by Eckersley O'Callaghan and Cambridge University. The main objective was to provide data on the bending stiffness and strength performance, not to obtain a certain norm. Only three specimens per configuration were tested with a large difference in results. A ductile behaviour mechanism was observed in all the composite specimens, meaning that the ultimate panel strength is greater than the initial panel strength. In terms of weight savings, the impact of halving the weight of the glazing on the main structure of an office building is limited. But the weight-saving offered by thin glass has a greater impact on industries which are more weight-sensitive, such as the automotive and marine industry. Furthermore, the disadvantages and limitations of float glass are still present.

Combining thin glass with a polymer further reduces the weight, but decreases the stiffness compared to combining thin glass with float glass. However, a significant advantage is that free formed curvatures can be produced. To laminate polymers with thin glass, the glass transition temperature of the polymers cannot be exceeded. Special adhesives must be used that allow for lower lamination temperatures. A stiffer interlayer generally results in a better composite action, but TPU had to be used as the most compatible interlayer in the experiments conducted by Eckersley O'Callaghan and Cambridge University. Though, the output showed that the change in stiffness demonstrates an effective composite action through the interlayer in unfractured state. An interesting alternative to research will be UV-radiation lamination which limits the panel to use PMMA, because of PC being UV unstable. Furthermore, both materials turn white when cracking and cannot be polished when laminated to thin glass. To retain an aesthetical value, the design must not exceed its fracture limit resulting in even more restrictions. Laminating thin glass to semi-transparent materials introduces another set of questions on how to laminate these materials to glass in terms of manufacturing, bonding, thermal expansion and thermal insulation. The structural performance of the composite elements is largely dependent on the stiffness of the glass and adhesive, the layer thickness of the adhesive and the distance between the core elements. The honeycomb panels for the Berkeley glass pavilion show that all these aspects combined create a rather complicated panel.

Composite thin glass panels can achieve controlled transparency, scratch resistance, stiffness without increasing self-weight and safety due to its high impact resistance and better post-breakage behaviour. Additionally, existing connections type can be used to connect the panels. They also can compete with current products on the market in terms of planar panels with sufficient out-of-plane stiffness to resist imposed loads by bending moment action. Depending on the incorporated core material, these panels can be applied in security windows, canopies and roof panels. An industry that could benefit from additional safety and weight savings is the automotive industry. The marine also requires high strength under infrequent loading conditions and high quality glazing with visual excellence. In all composite panel cases, further research is required to identify if the configurations can be applied as structural elements.

5.2. Curved glass

Curved glass structures offer the possibility of using a three dimensional shape of the panel to stiffen the glass by increasing the structural height and creating a global shape that allows activating membrane forces in the structure (Weber, 2009). As stated in chapter 3.3.3, float glass can be hot bent and cold bent. Hot bending allows the rigid glass pane to be formed in in a certain shape at a temperature of approximately 600 °C. This temperature is high enough to let the glass reach its viscous state. For thin glass, reaching this viscous state means that it also will be much affected by the mechanical machines, inducing distortions. It also doesn't make any sense to hot bent thin glass since it can already bend very easily at ambient temperatures. Compared to cold bending float glass, a better optical quality will be accomplished by cold bending thin glass. Due to the thickness of float glass, the compression side will show crumbling of the glass on a microscopic level. The compression side of thin glass will remain relatively flat and create a higher quality surface (Figure 5.5).

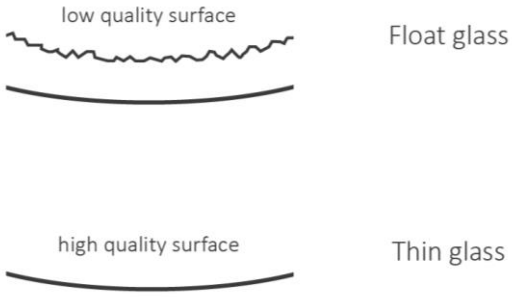

Figure 5.5: Surface quality bending float glass vs thin glass

Cold bending of float and thin glass can be done by assembling or laminating the panes into a fixed shape. Thin glass can be cold bent to a greater radius of curvature than float glass before a similar tensile stress is generated. Combined with the greater tensile stress capacity of the chemically tempering process, an even greater radius of curvature is achieved while leaving sufficient stress capacity within the glass for structural performance (Lambert & O'Callaghan, 2013). Table 5.2 compares constant minimum bending radiuses between annealed float and chemically tempered thin glass, depending on the thicknesses of a single glass pane. Note that the tensile bending strength for annealed glass includes partial factors derived from the European code EN16612. To calculate the bending radius the following formula is adapted from Feijen, Vrouwe and Thun (2012):

$$R = \frac{Et}{2\sigma_b} \qquad (5.1)$$

With R as the bending radius, E as the modulus of elasticity, t as the thickness and σ_b as the tensile bending stress.

		Annealed float glass			Chemically tempered thin glass (Leoflex)			
Young's modulus	E	70000			74000			MPa
Tensile bending strength	σ_b	25			260			MPa
Thickness	t	6	4	3	2	1.1	0.55	mm
Minimum bending radius	r	8400	5600	4200	285	157	79	mm

Table 5.2: Thickness vs minimum cold bending radius of a single glass pane

5.2.1. Bending by assembly

Bending by assembly can be done by single or double curving a thin sheet of glass of which the final form must come from an originally flat panel (Figure 5.6). A single curved panel follows a thrust line, enabling the structure to transfer long term loads purely by axial membrane forces and minimises constant bending moments in the glass. Asymmetric loads will still have to be taken via bending (Weber, 2009). Single curvature structures also tend to exhibit certain instabilities when under compression loads (Hundevad, 2014). Double curved glass panels have either synclastic, of which both curvatures are pointing in the same direction, or anticlastic curvature, of which both curvatures are pointing in another direction. Theoretically, these curvatures enable the structure to bare distributed loads purely by means of axial stress in compression and tension. As mentioned, glass is relatively weak in tension and therefore these stresses should be minimised. Double curved structures are also relatively weak against point loads as these cause localised bending (Weber, 2009). Connections for curved panel edges are more complex than straight panel edges and have to accommodate higher manufacturing tolerances. All these configurations have been experimented with in terms of thin glass by students from Delft University of Technology and Gent University, except for the paraboloid and saddle configurations.

Simoen (2016) explored the feasibility of applying thin glass sheets in a static second skin façade using transversal single bending, concluding that thin aluminosilicate glass still behaves flexible while being in a cold bended configuration. Applying pressure at one end deforms the other end. This effect gradually decreases with increased thickness. Another effect exposing itself is that the panel became convex near unsupported edges, resulting in optical distortions and disadvantages in terms of stiffness. As explained before, a convex shape is weaker and deforms easier than a concave shape. For this reason, Simoen (2016) chose to design a repetitive element which consisted of a concave thin glass pane fixed into a steel frame. Initially, the report stated that cold bending thin glass by assembly would allow for more design freedom in curved surfaces. However, relatively much steel was needed to stiffen and fix the glass which led to a decrease in the overall transparency and limits the industry to certain design options.

Silveira (2016) used the flexibility of thin glass to research the possibility of an adaptive second skin façade by single bending the sheets into the longitudinal direction. Research showed that cold bending a 0.55 mm glass pane resulted in minor bending stresses, but deformed quite a lot when applying a certain pressure. The pressure resistance is better with a thin glass pane of 2 mm, however, the stresses caused by cold bending the glass leave a small margin for additional stresses. A balance between the bending stresses and pressure resistance can be found by using a thin glass pane of 1.1 mm. Topçu (2017) also used the flexibility of thin glass as a kinetic second skin façade. Apparently, the radius-stress relationship of different sheet sizes is equal, meaning that two sheets of different sizes bent with the same radius are subjected to a similar stress. The maximum stresses are located at the point where the largest curvature occurs. This location forms the weakest spot of cold bent glass. The maximum stress under the same bending radius increases with a larger glass thickness, a larger interlayer thickness and a stiffer interlayer. Differences in the glass thickness also increase the maximum principal stress. Furthermore, the required force for bending a thin sheet of glass is proportional to the resulting stress values.

According to Galuppi, Massimiani and Royer-Carfagni (2014), an effective technique of cold bending rectangular glass plates is by constraining two or three points in the same plane and twisting the others out-of-plane. Hereby, a twisted curvature and a hyperbolic paraboloid are created. According to the linear Kirchhoff–Love theory, the edges of these configurations remain straight. The geometry is fixed by linearly supporting the edges or applying a force in the corners. However, experiments have proven that a particular form of instability occurs above a certain limit of twisting. One of the principal curvatures becomes dominant with respect to the other, the plate bulges into an asymmetric configuration and the edges do not remain straight anymore creating optical distortions and decreasing the overall stiffness. In other words, the glass plate buckles. Mainil (2015) investigated these geometries in combination with thin glass and determined that linearly supported edges allow for a greater corner displacement before buckling. Linearly supports combined with laminated panes enables the most promising result. This research concluded that using twisted thin glass with linearly supported edges can be an attractive alternative for warm bending float glass in the field of doubly curved architecture. Still, the panels can only be twisted to a certain degree and consists of relatively much steel, limiting the actual curvature of a surface and decreasing the overall transparency.

Curved glass panels have also been an interest of the marine industry where traditional glazed openings are typically restricted to fully supported framing and relatively small glass panels. By implementing double curved glass panels in the hull without splitting it into small pieces, and providing more transparency whilst offering a unique alluring appearance, a whole new dimension can be created. Cold bending float glass only allows for single curvature, but thin glass can play an important role in achieving double curved surfaces. As mentioned, manufacturing connections for curved panels edges is more complex, but since the shape of yachts already incorporated these curvatures, special connections need to be produced anyway. Drawbacks are that yachts are subjected to large loads and the marine industry is restricted to rather conservative codes restricting the design freedom. Besides, thin glass still comes in limited sizes.

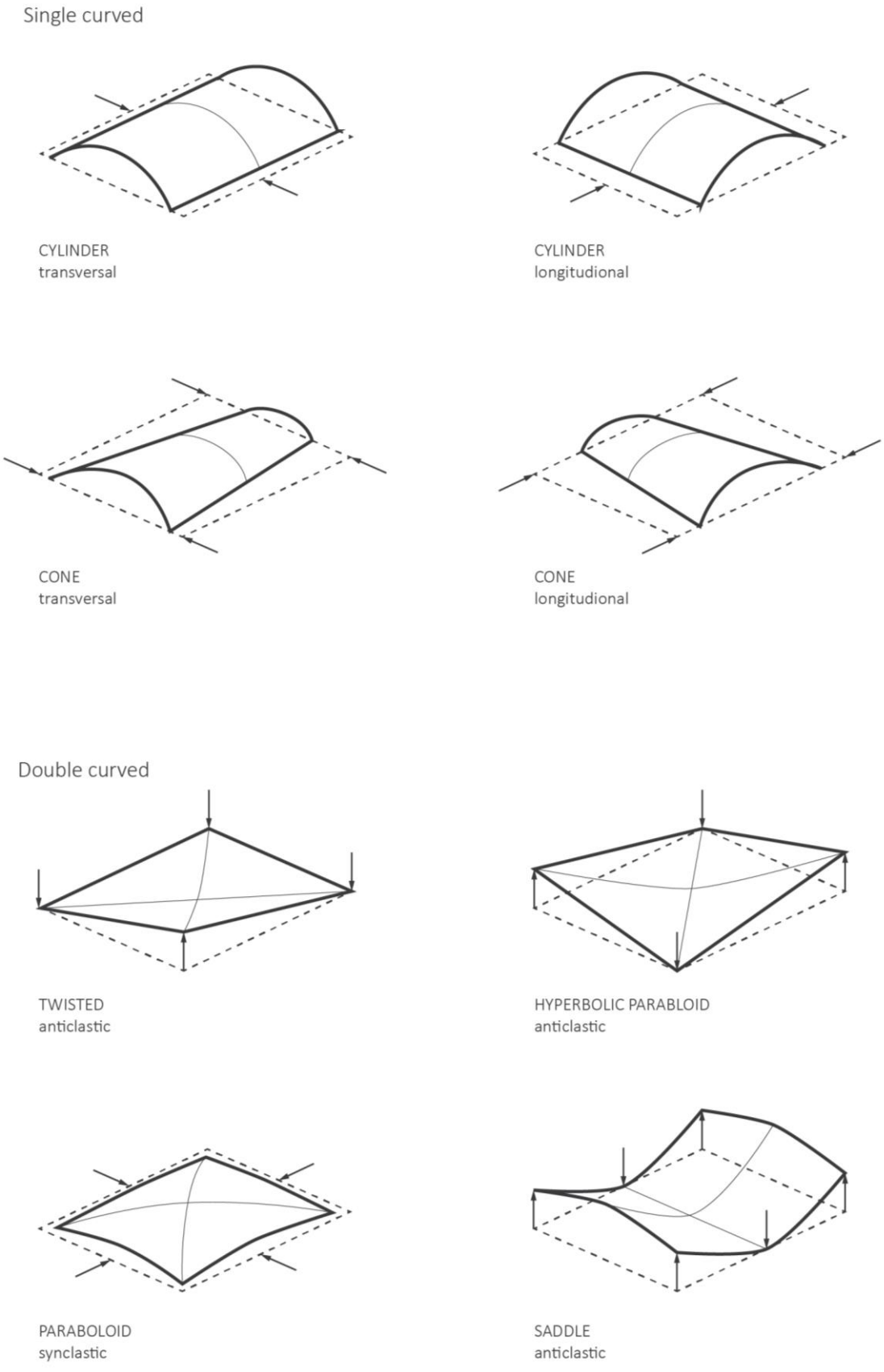

Figure 5.6: Single and double curved configurations

5.2.2. Bending by lamination

Three different configurations for curved glass panels that enhance the idea of architecture being more transparent and free formed can be distinguished (Figure 5.7). The first principle uses two flat sheets of thin glass which are cold bent and laminated together into a certain curvature. The second principle uses an already defined shape by pouring a polymer into a mould with a layer of thin glass attached to it. The third principle is an alternative of the former configurations by using prefabricated flat polymer sheets. Due to the energy absorbing characteristics of polymers, these panels could be used for high impact protection. They however lack stiffness. The thin glass attached could act as some kind of reinforcement as well as a protective layer to make up for the low scratch resistance. However, pouring the polymer into a mould requires a different mould for every curvature and thus increases the labour intensity. Together with the sensitivity of polymers during production, both processes are expensive. Polymer and thin glass lamination costs around €300-400 per panel, while laminating thin glass with a PVB costs around €10 per panel. The thickness of the latter two configurations allows for the use of existing connection types and a better workability. Due to the thinness of the first configuration, joints connecting the panels need special attention.

Moreover, for short term loads the interlayer provides enough stiffness to allow for reasonable bending moments in the panels. However, it is beneficial to create a geometry that minimises long term bending moments in the glass to avoid weakening effects due to creeping of the interlayer (Weber, 2009). Single curved panels with a constant curvature along its length enable the structure to transfer long term loads purely by axial membrane forces and minimises constant bending moments. Therefore, single curved surfaces are preferred. Galuppi and Royer-Carfagni (2015) concluded that cold bending with constant curvature theoretically leads to concentrated shear forces at the ends of the beam and risks of delamination. A sinusoidal geometry is therefore recommended to be the optimal configuration to provide the smoothest distribution of shear stress in the interlayer. The bending radius depends on the glass and interlayer thickness, stiffness and allowable stresses.

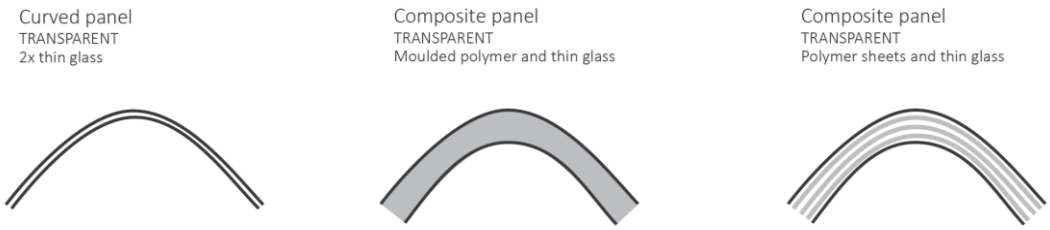

Figure 5.7: Different configurations for curved glass panels

An example of a first application of the first configuration is the Fluid Glass installation proposed for the London Design Festival, designed in collaboration with Eckersley O'Callaghan. The combination of cylindrically and conically shaped geometries captures the flexibility of the glass. The applied curvature is maintained through the interlayer bond by using a stiff interlayer, such as SG. Nevertheless, applying a stiff interlayer doesn't fully prevent the curvature to spring back to its original flat form. Therefore, by overbending the geometry of about 5% of its original curve, the exact shape is achieved. The fluid glass sculpture would consist of 22 identical conically shaped laminated panels. The radii differ at the top and bottom and depend upon its orientation. To maintain the required geometry, two Gorilla glass panes are cold bent and laminated together using a SG interlayer forming a very thin panel. The laminated thin glass panels are prefabricated offsite to ensure their quality. They are connected with a steel fitting at the top and are supported through a steel friction clamp at the bottom. Unfortunately, the structure was never built due to issues with the frangibility of the material.

Figure 5.8: Fluid Glass installation (Carpenter & Lowings, 2012)

5.2.3. Conclusion

Cold bent thin glass structures can indeed be used to stiffen the structure by increasing the moment of inertia and creating a shape that activates membrane forces. Although cold bending introduces bending stresses into the glass, it also allows for a greater curvature, more lightweight structures, better optical qualities and reduced thicknesses compared to float glass. Applications of this principle can be used in sculptures, aesthetic features and complex curved façades or cladding in both the building and marine industry.

Curved thin glass surfaces can be separated into single curved or double curved surfaces as illustrated in Figure 5.6. To maintain the curvature, the principals bending by assembly and bending by lamination have been introduced. The former has already been severely investigated by students from Delft University of Technology and Gent University. Single curved surfaces were mainly researched to be applied as a second façade without the need of weather and water tightness, while double curved surfaces were investigated to be used as the main façade. However, cold bending by assembly means that a substructure is always needed to keep the glass in place. Combining the need of a substructure with the manufacturers size limitations means that the eventual build-up includes a large amount of non-transparent materials, leading to lesser transparency. Although repetitive elements can be manufactured, it also limits the design freedom to a certain extend. Within the yacht industry, this seems to be less of a problem when applying glass to the hull. But, limited sizes of thin glass result in the same small windows as traditionally built. Bending by lamination does encourage the design freedom and transparency. Still, a lot of research needs to be done to implement this principle in any industry in terms of its limitations, connections and structural performances. Using a polymer complicates the manufacturing process and increases the costs significantly. Thus, bending by lamination using only thin glass seems to be the most attractive option to further investigate in terms of using curvature as the stiffening principle in its purest form.

5.3. Tensioned structures

The physical properties of thin glass concerning its strength and stiffness suggest that a pane can be used as a tensile membrane in a load-bearing structure. By considering thin glass as a stiff fabric, it can be placed between structural framing elements and tensioned by using a special device or pressure creating membrane structures or pneumatic structures. This results in a two or three dimensional form. Another way of using thin glass in a tensioned structure is by applying it into a cable net façade. The main advantage of tensile structures over compression structures is that they can be as thin and as light as their tensile strength allows (Berger, 1999).

5.3.1. Membrane structures

Fabric structures have been used in many permanent buildings. The reasons for selecting a fabric structure often include their speed of erection, use of daylight, reflection of heat from the sun, dispersal of interior sound, the beauty of the interior space, and the excitement of the exterior sculpture (Berger, 1999). Stiffness in membrane structures is created by double curving anticlastic shapes and as long as these surfaces are in tension the structure is stable. With the help of form finding, the double curved surfaces are obtained. The fabrics used are a woven material with the warp threads interlaced between the loom and the weft threads woven in between. The warp threads are tensioned during the weaving process, and the weft threads therefore pace up and down. When the weft direction is tensioned, it will strain much more than the warp direction. This results in a non-homogenous material which cannot resist shear force and special care needs to be taken when designing with such a fabric (Coenders, 2008). To translate the found shape into a realisable membrane structure, separate pieces of fabric are manufactured. The boundaries of these pieces are referred to as cutting patterns. The orientation of cutting patterns needs to be in the direction of the principle curvature to reduce shear. The separate pieces are sewn back together, creating seams. These seams have a double layer of fabric, thus twice as stiff and therefore attract stresses.

Although Lambert and O'Callaghan (2013) explain that thin glass has characteristics similar to fabrics, there are also a few aspects that are severely different. Thin glass is a homogenous material. Therefore, the orientation of the cutting patterns isn't an issue. However, fabricating large thin glass cloths from rather small flat panes seems almost impossible. Thin glass cannot be sewed together like fabric, so other connection types need to be introduced between glass panes. Additionally, the connection with the substructure must be thoroughly investigated. Due to the size of thin glass panels and unrealisable connection types, applying thin glass in traditional larger membrane structure doesn't seem feasible. Nevertheless, this principle of stiffening a thin glass panel can still be applied by clamping the pane on one side and tensioning on the other side. A small scale application can be found in the decorative second skin façade of the Corning Museum of Glass (Figure 5.9). Fins of laminated Gorilla glass are attached to a steel frame (Figure 5.10). A balance had to be found between the induced catenary forces, required to limit the horizontal deflections under wind loading, and the silicone bond area, required to transfer the catenary forces back to the main building structure. A concept involving springs within the connection was developed to further refine and reduce the required connection size (Eckersley & O'Callaghan, 2012). Unfortunately, the façade was never build due to its complexity.

Figure 5.9: Corning Museum of Glass

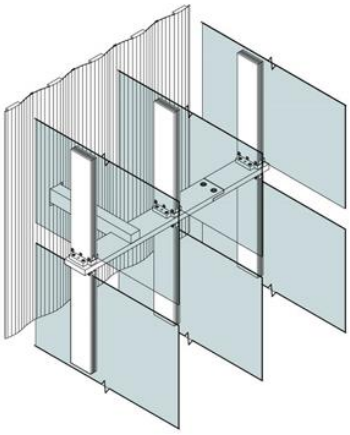

Figure 5.10: Gorilla glass fins detailing

Ottens (2018) researched thin glass as a stiff structural fabric at Delft University of Technology by tensioning thin glass into a anticlastic surface with a stretchable composite connection. These connections are likely to govern the design of tensile membrane structures. As mentioned and confirmed by Ottens (2018), these structures can be as thin and as light as their tensile strength allows. Chapter 4.4 explained that thin glass as a structural material is a rather new development and little research has been conducted in terms of its bending tensile strength. A tensioned façade depends severely on this tensile strength. With the lack of a consistent value, a rather conservative approach must be used to prevent the structure from failing completely at once. For this reason, a balance needs to be found that satisfies the required stiffness to minimise deflections and at the same time offers sufficient resistance to different applied loads. To calculate the structural behaviour, the tensioned thin glass panels can be assumed to behave as a catenary.

5.3.2. Pneumatic structures

Pneumatic structures are lightweight and use a constant air pressure to satisfy equilibrium, stiffen and stabilize the system. The pressure can create an inflated or deflated synclastic paraboloid shape as illustrated in Figure 5.11. Most larger structures use the inflated variant. The shape of these structures are difficult to stabilise due to excessive deformation (low E-modulus) or creep of the material. To create the desired stiffness and strength, weaves made of natural, nylon, polyester or glass fibres are often chosen. To protect the weave and to create weather and water tightness, the weave is covered with a plastic layer on both sides. An overpressure of 100-300 Pa is already sufficient to maintain the shape of the structure and is comparable to the change of air pressure that needs to be overcome when climbing to the 8th floor of a building. In order to maintain the overpressure in inflated systems, cold air ventilators are needed. These ventilators have to be controlled due to small air leaks at the seams and connections, but can also be used to adapt the pressure to the current windspeeds to prevent higher stresses in the skin than needed (Coenders, 2008).

Figure 5.11: Pneumatic structure configurations

The materials used for pneumatic structures are thin, flexible and isotropic foils. This description seems to match the description of thin glass and could be a proper substitution to create transparent pneumatic structures in order to add stiffness. Larger structures will not be possible due to the limitations in size of thin glass panes. The material is more likely to be used in smaller panels added together, similar to ETFE cushions. Traditional ETFE cushions consist of multiple layers of ETFE foils that are clamped and sealed into a lightweight frame. Air is pressured between the layers forming an inflated cushion with significant thermal properties. Due to small leaks, the pressure has to be constantly regulated. The materials physical characteristics enable it to be used in a variety of situations where a large expanse of glass is not suitable. ETFE cushions allow the weight of the structure to be greatly reduced whilst providing the same level of stability (Robinson-Gayle, Kolokotroni, Cripps, & Tanno, 2001). There is a good reason for choosing ETFE over other materials. In comparison to thin glass, EFTE as a material performs better in inflated elements. According to Table 5.3, ETFE has a lower weight, lower stiffness and better light transmittance than thin glass. These properties allow for more transparent and lightweight structures. The lower stiffness is convenient in terms of applying pressure to get a certain shape. A larger stiffness results in the need of larger pressure to get to the same shape. In return, applying larger pressure means that more stresses

develop in the surface of the material, especially when a sheet is double curved. Thin glass would only provide a better scratch resistance, durability and clarity compared to ETFE. In other words, there is already a large market for inflated transparent pneumatic structures and it doesn't seem that thin glass can compete with this market.

		Thin glass (Leoflex)	EFTE	
Density	ρ	2480	1700	kg/m^3
Young's modulus	E	74000	1000	MPa
Light transmission	LT	91	95	%

Table 5.3: Physical properties of glass and ETFE retrieved from (Martienssen & Warlimont, 2005)

Vacuum glazing has been briefly mentioned in chapter 3.3.4 and makes use of the deflated principle. These panels are built up of a gas-filled space evacuated to low pressures in between the glass panes to minimise conductive and convective heat transfer. Reducing the pressure in the space between the two glass sheets results in a certain stiffness as well as pushing the sheets together into a deflated configuration. The latter imposes the need for a support structure to hold the two glass sheets apart. Small pillars are sized and spaced so that the glass sheets do not touch in between the pillars and the glass structural integrity is not compromised. However, large pillars can represent cold bridges and may be visually disturbing. Using thin glass instead of regular glass can cause problems in terms of spacing due to its flexibility. Another important area of the panel is located at the edge seal, which must be substantial enough to maintain the vacuum within the glazing below 0.1 Pa for the duration of the glazing lifetime. It was found that the edge influenced the temperatures of the glazing surface for a distance of approximately 75 mm from the edge seal. The influence of the edge seal on the total glazing U-value thus depends on the glazing area and dimensions (Eames, 2008). This may be less important for larger panels, but dominant for smaller systems. Due to the limited size of thin glass, this can be a governing issue. Furthermore, structural safety challenges traditional vacuum glazing units due to the high residual stress arising during fabrication.

5.3.3. Cable systems

Cable net systems enable large coverings to be lightweight and transparent by using a network of tensioned cables to act as the backbone of a structure. The stiffness of a traditional cable net system is defined by the geometric nonlinearity, resulting in a rather large deflection of the structure. The theoretical deflection was often found to be greatly different to the practical one, because the effect of the glass panels was not taken into account. Feng, Wu and Shen (2007) researched the effect of the glass panel stiffness and concluded that the bending stiffness of the glass panel has little effect on the deflection of the structure, but the glass face membrane action does have a significant effect and depends on the deflections of the glass panel and cable net. While the glass stiffness contribution for two dimensional cable net systems is initially high and reduces when the load increases, the glass stiffness contribution for three dimensional cable net systems increases gradually as the load increases. If the glass stiffness is considered, the pretension in the cables can be reduced by approximately 50% of the initial prestressing force when statically loaded (Yussof, 2015). An interesting example of a cable net system is the façade of the Markthal in Rotterdam. Although pretension is applied to the cable net, a deflection of 700 mm both ways can still be seen during high wind loads. Elongation of the cables is introduced by the pretension force as well as by the wind loads. The glass panels are approximately 1.1x1.1 m in size, allowing for smaller sized panels compared to other glass façades.

As mentioned, the theoretical deflection was often found to be greatly different to the practical one because the stiffness of the glass panels was not taken into account. When replacing regular float glass for thin glass in cable net systems, the stiffness is very much reduced and therefore the structural performance of the overall system. At Delft University of Technology, Mureau (2017) investigated different configurations to stiffen a thin glass pane to be applied in green houses and concluded that the deflection of simply supported thin panes combined with a pretensioned cable still results in relatively large deflections due to the difficulty of maintaining sufficient pretension. During the experiments, the cable supported pane was initially curved upwards due to the pretension of the cable and buckled downwards when the pretension value was reached.

5.3.4. Conclusion

Using thin glass in tensioned membrane structures can result in stiff, lightweight, scratch resistant and highly transparent systems. This principle can be applied in façades, canopies, pavilions or other types of coverings. By considering thin glass as a stiff fabric, several configurations can be designed. Although replacing the fabric in large tensile membrane structures for thin glass may not be feasible due to the size of thin glass panels and unrealisable connection types, the principle remains interesting and could benefit from further research. With tensile membrane structure, the connection will be governing and with the lack of a consistent tensile bending value, a rather conservative approach must be used. Furthermore, a balance between the pretension and applied loads needs to be found.

Two types of pneumatic structures are distinguished, inflated and deflated panels. These structures would result in highly efficient insulated units with perfect clarity and as far as known, no extensive research is done on applying thin glass in pneumatic structures. Due to size limitations of thin glass, inflated panels are in close resemblance to ETFE cushions. However, thin glass will not be a great substation for ETFE due to its material properties. It therefore seems that thin glass cannot compete with this rather large market of inflated pneumatic structures. However, at a time where glass panels become heavier and heavier due to their increasing size and required insulation values resulting in double and triple glazing units, thin glass in vacuum glazing can be an interesting substitution for float glass. Special attention must be paid to the sealing edges, applied pressure, double curvature and cavity support structure. Manufacturers already apply a non-structural layer of thin glass to decrease the weight of double or triple glazing. Insulating or vacuum glazing units are therefore more of an interest in terms of building physics.

Applying thin glass in cable net façades probably results in relatively large deflections due to the difficulty of maintaining sufficient pretension. These deflections can cause visible distortions and maybe even a certain noise due to different panels bending in and outwards. However, cable net façades are especially designed to allow for flexibility and larger deflections. A thin glass cable net system can benefit from further research.

6. Boundaries

The previous chapters laid the groundwork for this chapter, which introduces a set of boundaries and demands obtained from different industries. The presented design configurations should be able to meet most of these boundaries to be successfully implemented as a structural element.

6.1. General demands

As in any industry, the production, transportation, construction and maintenance costs need to be as low as possible. Due to the thriving electronics market, the material costs for thin glass have already significantly decreased compared to a couple of years ago. Nevertheless, thin glass is still more expensive than regular float glass and only a few manufacturers are developing larger sized panels to be adopted in different markets. Once another large enough market is established, the costs of large thin glass panels will also decrease. This opens up the opportunity to keep extending to other industries with the condition being that there is a large enough interest and clear allocation of responsibilities when implemented for the first time. Relatively easy production is also necessary to minimise labour intensity, save time and consequently reduce cost.

With the globalization of supply chains, longer travel distances lead to increased vehicle emissions on the transportation routes. While the exact emission levels will depend on the engine type, terrain driven and the driver tendencies, the general relationship between vehicle weight and emissions will not change (Elhedhli & Merrick, 2012). In other words, reducing the weight of the cargo results in lesser emissions, thus, a deflated carbon footprint and a reduction in fuel cost. Thin glass will therefore be a great substitution for float glass in terms of its transportation cost and additional emissions. Sustainability can also be found in efficient use of the different materials, whether these materials can be separated and recycled or whether the complete panel build-up can be easily re-used. The durability of the materials and the constructed panel is an important factor to take into account as well.

6.2. Demands from the industry

Over the last few decades, developments regarding the structural application of glass were driven by a desire for more transparency. Developments in production and engineering allow for larger panels and minimal connections that enable these more transparent structures. This trend seems to continue and should be factored in when designing with upcoming new materials. Whereas regular float glass is produced in standard sizes of 3.21x6.00 m, thin glass goes up to 1.6x3.21 m. With the current developments, these panels could become even larger. In the building and marine industry, most structural elements span from top to bottom with an average floor height of around 3 m, enabling thin glass sheets to span these distances. Connections can be easily provided at both ends due to an already present secondary structure. Choosing existing connections for float glass as for thin glass would be convenient, however, they are not always applicable. Meaning that new connections may need to be designed when using thin glass as a structural element. All these connections need to be weather and watertight, which is more trivial in marine applications than in the building industry due to the great risk of sinking or capsizing at failure.

Although fully transparent structures are favoured, they are not always needed depending on the application. Applying colours or patterns by painting or printing the surface will generally satisfy the client needs. Optimal light transmittance is always a requirement, just like avoiding distortions or greenish tinted glass. Another important trend is to create more free from architecture, pushing glass panes to their maximum curvature limits. On top of this, the required insulation values of glass constructions are also increased. Future glass panels can include triple or more layers to provide for the required insulation. In terms of weight savings, the impact on a building is limited, but has a great impact on industries that are more weight-sensitive, such as the automotive and marine industry.

Structural elements need to have a certain strength and stiffness during their lifetime to comply with regulations. A structure fails the strength criterion when the stress induced by the loading is greater than the capacity of the structural material. In other words, the structure should be strong enough to resist the load without breaking, also referred to as the ultimate limit state. A structure fails the stiffness criterion when the deflection of a structure under loading is larger than the allowable deflection, also referred to as the serviceability limit state. When a structure fails, the post failure behaviour and redundancy are both of interest in terms of safety. A structural element can be considered load-bearing when it has to withstand environmental loads, is part of the overall integrity of a structure or both.

7. Conclusion

Chapter 5 introduced three different ways to stiffen thin glass of which an overview of the design configurations is shown in Figure 7.1. Laminating the glass to other materials is a means to add out-of-plane stiffness by adding material thickness, shaping a curved surface is a means to add global out-of-plane stiffness through geometrical form and treating the material as a fabric glass is a means to add out-of-plane stiffness through membrane action (Lambert & O'Callaghan, 2013). In order to get a clear overview of which design configurations has the most potential to be further explored, a rating system is developed (Appendix B.3). The boundaries and demands from the previous chapter are translated into requirements concerning optical quality, geometry, mechanical properties, sustainability and economical properties. Grades ranging from 1-3 are given of which 1 is not good and 3 is very good. The higher the total number, the better the design configuration will perform. This list is not binding, but gives a first indication on the performances of each design configuration. Note that every principle has its advantages and disadvantages and that the eventually chosen configuration will be the most promising one based on the completed literature studies. According to the rating system, a composite panel combining float glass with thin glass, a composite panel combining polymers with thin glass, a curved panel with only thin glass and a curved panel combining polymers with thin glass are still in the running to become the chosen concept.

The previous chapters explained that the most important demands concern larger transparent panels, minimal weight, more free formed architecture and high thermal insulation. The mentioned composite panels will have a large impact on the industries where weight savings are essential. The automotive industry takes the lead in researching the combination of float glass and thin glass and together with the combination of polymers and thin glass, a small investigation has been carried out by Eckersley O'Callaghan and Cambridge University to provide data on the bending stiffness and strength performance. The conclusion stated that enough knowledge was gathered to design structures consisting of these composite panels. Additionally, the initial purpose of this thesis was to implement thin glass as a product where float glass does not work and combining float glass with thin glass still contains the disadvantages and limitations of float glass. Adding a polymer to the thin glass in its flat or curved form, results in rather high production expenses. It also detracts the optical quality of thin glass due to the material properties and structural properties of turning white when fractured. These design configurations are therefore off the table.

Cold bending and laminating sheets of thin glass does encourage transparency, lightweight structures and free formed architecture. With float glass, curvatures can be applied by cold or hot bending the glass. As mentioned in chapter 3.3.3, hot bending introduces many disadvantages over cold bending, but enables to bend the glass at a smaller radius than cold bending. Although hot bending is in development, thin glass can be very well bend into a smaller radius with all the advantages of the cold bending process. Still, a lot of research needs to be done to implement this principle in any industry in terms of its limitations, connections and structural performances. Since this concept has never been studied, the main focus will be to show to what extend thin glass can be used and to demonstrate the public what this material is capable of. Therefore, the principle of creating stiffness by cold bent laminating thin sheets of glass for architectural applications will be further investigated. By choosing this concept, research on chemically tempered aluminosilicate thin glass will be done in its purest form.

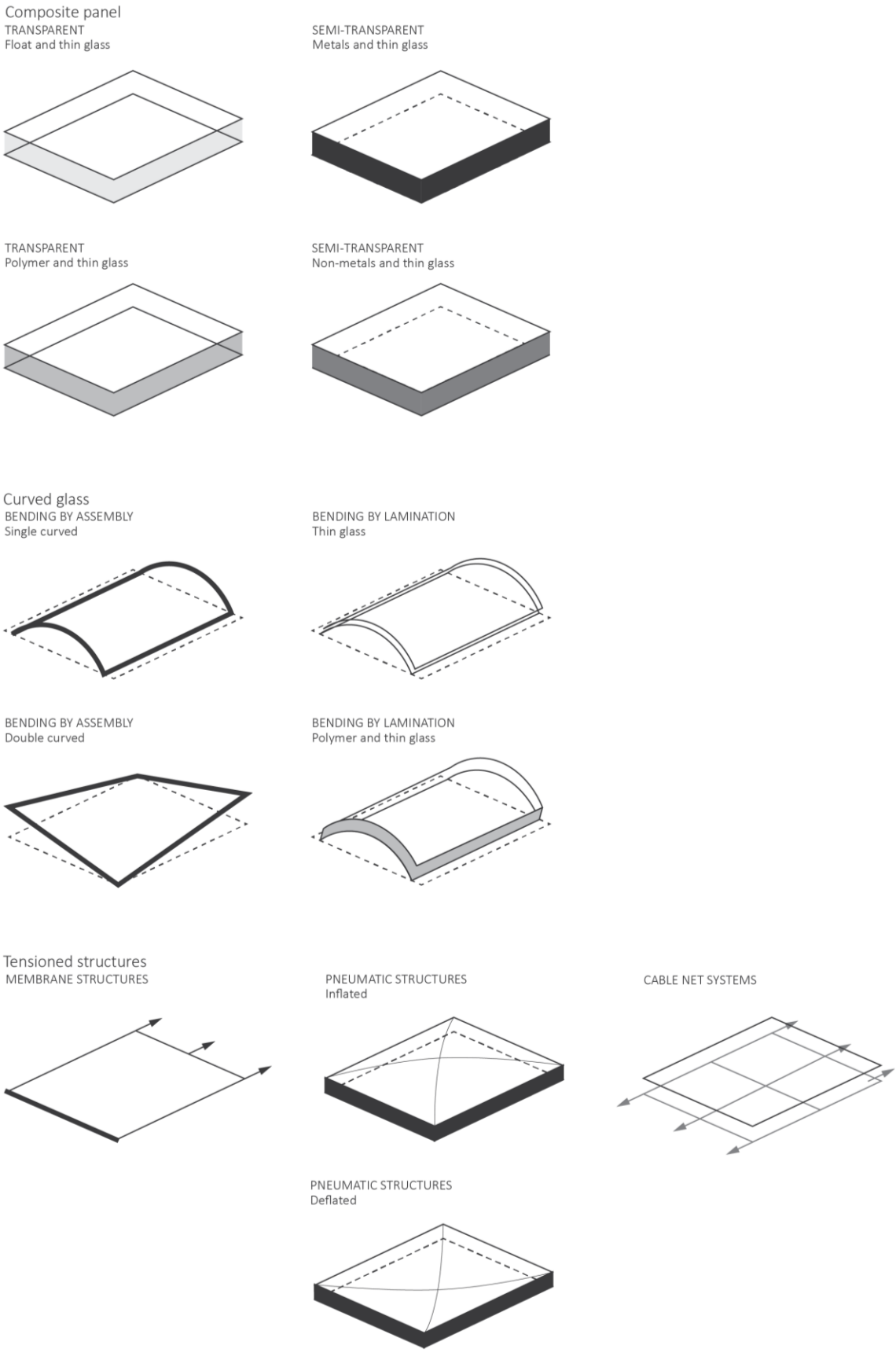

Figure 7.1: Investigated design configurations

STRUCTURAL DESIGN

8. Preliminary design

Before continuing the investigation of chemically tempered aluminosilicate thin glass as a free form load-bearing structural panel, the scope of the research needs to be defined to clearly control its direction. This chapter translates the proposed conceptual design of cold bent laminated thin glass panels into an architectural model. The composition of the laminated panels is defined and analytical calculations are made to determine the influence of different curvatures on the behaviour of a laminated single glass panel during the first steps of the production process. The derivation of the required formulas can be found in Appendix C. Furthermore, using curvature as the stiffening principle of thin glass sheets requires special attention towards its connection types.

8.1. Composition

Cold bending by lamination maintains its curvature through the interlayer bond, varying in time due to the viscosity of the interlayer. The most common interlayer is PVB due to its low costs and ability to block UV radiation completely. When in need of a larger stiffness, a SentryGlas interlayer is normally used. Several structural PVB's are also available to provide a stiffer interlayer with greater optical properties. In the case of cold bent laminated thin glass panels, an interlayer with a larger stiffness is necessary to keep the curved composition in place, hence Saflex DG41 (SAF) by Eastman or SentryGlas (SG) by Trosifol. Table 8.1 provides the Young's modulus, shear modulus and Poisson ratio for an applied load of 3 seconds at a temperature of 20 °C and other properties for thin glass, Saflex DG41 and SentryGlas. Although the Young's modulus and shear modulus for Saflex DG41 are initially significantly higher than for SentryGlas, it must be noted that the physical properties of Saflex DG41 strongly depend on temperature and load duration and almost decrease to zero at extreme conditions. These variables could change the geometry and structural behaviour noteworthy. Both interlayers will be used to further investigate the principle of cold bent laminated glass. Leoflex glass of 0.55 mm thick as the type of thin glass is made available by AGC.

		Leoflex glass (LG)	Saflex DG41 (SAF)	SentryGlas (SG)	
Density	ρ	2480	1080	950	kg/m^3
Young's modulus	E	74000	1007	612	MPa
Shear modulus	G	30000	341	211	MPa
Poisson's ratio	v	0.23	0.476	0.449	-
Tensile bending strength	σ_b	260	32.4	34.5	MPa
Maximum size	A	1.5x1.85	2.46x3.2	1.2-200	m
Thickness range	t	0.55-2	0.76	0.89	mm

Table 8.1: Physical properties of AGC Leoflex glass and interlayers retrieved from Appendix A

8.1.1. Effective thickness

The effective thickness needs to be calculated to determine the introduced stresses during the first steps of the production process. According to the European code EN16612, the following simplified and conservative method to calculate the effective thickness for bending deflection is:

$$t_{eff} = \sqrt[3]{\sum_k t_p^3 + 12\omega(\sum_i t_p t_{m,p}^2)} \quad (8.1)$$

With t_{eff} as the effective thickness, t_p as the thickness of a glass ply, ω as the coefficient between 0 and 1 representing no shear transfer (0) and full shear transfer (1) and $t_{m,p}$ as the distance of the mid-plane of the glass ply from the mid-plane of the laminated glass.

The effective thickness for calculating the stress of glass ply number j is:

$$t_{eff,\sigma} = \sqrt{\frac{t_{eff}^3}{t_{pt}+2\omega t_{m,p}}} \quad (8.2)$$

With $t_{eff,\sigma}$ as the effective stress thickness and t_{pt} as the thickness of a glass ply on the tension side.

The shear transfer coefficient is 0.7 assuming that the wind load in other areas than Mediterranean areas lasts for 3 seconds in a temperature range of 0-20 °C and that the interlayer stiffness family of Saflex DG41 and SentryGlas is family 3. The effective thicknesses of two plies of Leoflex glass, an interlayer of 0.76 mm thick Saflex DG41 and an interlayer of 0.89 mm thick SentryGlas are given in Table 8.2.

Leoflex glass 1 (mm)	SAF/SG (mm)	Leoflex glass 2 (mm)	t_{total} (mm)	t_{eff} (mm)	$t_{eff,\sigma}$ (mm)
0.55	0.76	0.55	1.86	1.63	1.71
0.55	0.89	0.55	1.99	1.72	1.81

Table 8.2: (Effective) thicknesses of different panel build-ups

8.2. Curvature

To obtain the curvature in a cold bent laminated panel, a single glass sheet is first cold bent into a certain curve. The derivation of the formula for the induced bending stresses starts with a general formula that is translated to parametric equations. Hereafter, the curvature can be found. The Kirchhoff Love plate theory is used to derive the cold bending moments that in return can be translated to the cold bending stresses of a single sheet of Leoflex glass. Note that the formulas derived in Appendix C are only valid for bending in one direction.

After lamination, the panel springs back slightly. This spring back effect redistributes the stresses and have to be added to the stresses for cold bending a single glass sheet. As shown in Figure 8.1, each sheet is subjected to a moment in order to achieve the required curvature prior to lamination. If the panels were not laminated together each ply would go back to their original geometry. However, the laminated panel now acts as a stiffer element implying that the sum of the moments is reversed and acts on the entire build-up. The spring back effect stresses are calculated by summing the moments of the separate glass plies and divide the value by the section modulus of the laminated panel. The interlayer is not included in the equation as the material softens during lamination and doesn't contribute to the stresses of the element. The spring back stresses and total moment are calculated per unit length. The highest tensile stress occurs in one ply only, therefore the spring back effect stress needs to be scaled down (Eckersley & O'Callaghan, 2018). The total stress is given by adding the cold bending stresses and the spring back effect stresses and must be significantly lower than the tensile bending stress given by the thin glass manufacture to allow for additional loading.

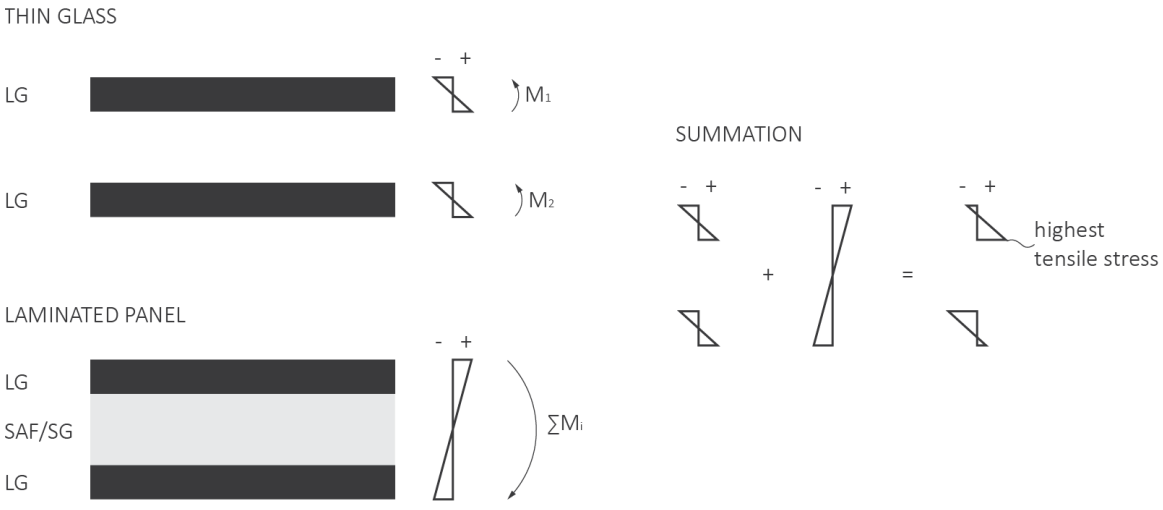

Figure 8.1: Spring back effect adapted from Eckersley & O'Callaghan (2018)

8.2.1. Circular

The most common shape that is given to glass through cold bending is the one with constant curvature (Figure 8.2). However, such a shape is perhaps one of the worst that could be applied due to strong shear stress concentrations in the interlayer at the beam ends. Especially for interlayers with a high shear modulus, such that the response of laminated glass approaches the monolithic limit, cold bending with constant curvature leads to concentrated shear forces. This can explain the delamination phenomenon that may be encountered during cold bending. Due to the viscosity of the polymer, the stress concentrations diminish with time, but the stress at the extremities of the beam always remains much higher than at midspan (Galuppi & Royer-Carfagni, 2015). The formulas to calculate the cold bending and spring back effect stresses for circular curvatures are derived in Appendix C.1.

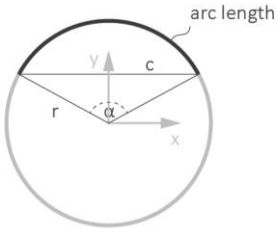

Figure 8.2: Cylindrical curvature

The minimum radius for a sheet of Leoflex glass is set by the maximum tensile bending strength of the glass or the length of the sheet. The former is obtained by adapting the formula for cold bending stresses to $r_b = \frac{Et_p}{2\sigma_b(1-v^2)}$. The latter is obtained by the formula $r_l = \frac{l}{2\pi}$ and limits the curvature to a full circle. To calculate the minimum bending radius, the used Young's modulus E is 74000 MPa, the thickness is 0.55 mm, the tensile bending stress σ_b is 260 MPa and the Poisson ratio v is 0.23. This results in a minimum bending radius r_b of 83 mm, governed by the formula of the maximum tensile stress. In order to find the total stresses in the laminated panel, caused by the production process, the cold bending stresses and spring back effect stresses are added together. This value needs to be significantly lower than the given maximum tensile bending stress of Leoflex glass to allow for additional loading (Figure C.1).

8.2.2. Catenary

A catenary corresponds to a flexible hanging cable supported at the ends. It obtains it shape by making use of gravity (Figure 8.3). No research is done into a catenary in terms of its shear stresses. The formula to calculate the cold bending stresses is derived in Appendix C.2.

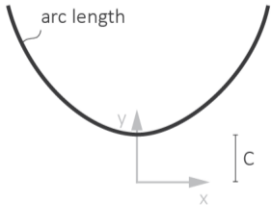

Figure 8.3: Catenary curvature

Since the highest bending stresses are obtained at x=0, the minimum curvature variable is found to be $C = \frac{Et_p}{2\sigma_b(1-v^2)}$. A similar formula to the one derived for circles. This curvature is however not limited by the sheet length, meaning that the minimum curvature variable is set by the maximum tensile bending strength of the glass. The total production stresses due to cold bending and spring back effect for different spans can be found in Figure C.1.

8.2.3. Parabolic

A parabolic curvature is similar in appearance to a catenary arc, but must not be mistaken for one (Figure 8.4). A parabolic sag causes linear or cubic shear stress distributions in the arc, depending on the formulation of the curvatures expression. The results for these distributions are slightly better compared to circular curvatures, both in terms of shear stress in the interlayer and axial stress in the glass plies (Galuppi & Royer-Carfagni, 2015). The formulas to calculate the cold bending and spring back effect stresses are derived in Appendix C.3.

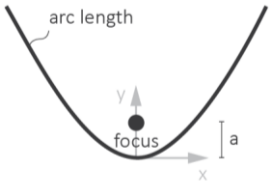

Figure 8.4: Parabolic curvature

The highest bending stresses are obtained at x=0. So the maximum curvature variable is set by adapting the formula for cold bending stresses to $a = \frac{\sigma_b(1-v^2)}{Et_p}$. To calculate the maximum curvature variable, the used Young's modulus E is 74000 MPa, the thickness is 0.55 mm, the tensile bending stress σ_b is 260 MPa and the Poisson ratio v is 0.23. This results in a maximum curvature variable a of 0.006 mm. In order to find the total stresses in the laminated panel, caused by the production process, the cold bending and spring back effect stresses are added together. This value needs to be significantly lower than the given maximum tensile bending stress of Leoflex glass to allow for additional loading. Figure C.1 shows the total production stresses due to cold bending and spring back effect for different spans.

8.2.4. Sinusoidal

The curvatures proposed above produce high shear stress concentrations in the interlayer with consequential risks of delamination. Galuppi and Royer-Carfagni (2015) recommend a sinusoidal curvature to be the optimal configuration (Figure 8.5), because it is associated with a smooth distributions of shear stress at any time of the element life. In fact, in this case there is no stress intensification in the neighbourhood of the end of the beam, even when the shear modulus of the interlayer is high. In general, for the same sag of the laminated glass beam, the shear stress in the interlayer is lower than in the other cases, even if the maximum stress in the glass plies may be slightly higher at particular times of the history.

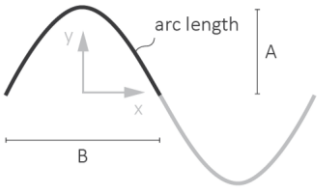

Figure 8.5: Sinusoidal curvature

The highest bending stresses are obtained at x=0, resulting in the formula $\sigma_b = \frac{A\left(\frac{\pi}{B}\right)^2 * Et_p}{2(1-v^2)}$. To calculate the amplitude (A) and span (B), the used Young's modulus E is 74000 MPa, the thickness is 0.55 mm, the tensile bending stress σ_b is 260 MPa and the Poisson ratio v is 0.23. This results in a maximum amplitude A of 160 mm and a minimum span B of 363 mm. Figure C.1 shows the total production stresses due to cold bending and spring back effect for different spans.

8.2.5. Conclusion

In any of the configurations, the differences in the deformed shape of the laminated glass panel are minimal (Figure 8.6). Consequently, the aesthetics of the curved glazing is not affected by any one of the proposed curvatures. Although the deformed shapes are very close to one another, the corresponding shear stress in the interlayer is much different. Galuppi and Royer-Carfagni (2015) demonstrated that the circular curvature shape should be avoided for cold bending, due to the associated shear stress concentrations at the panel extremities which induces a high risk of delamination. Similar results were found in parabolic curvatures and would not make for a proper alternative in terms of the shear stresses. No research is done into a catenary shape, but it follows a curvature between a circle and a parabola. Assumptions are made that this geometry will give similar significant shear stresses. Among the considered cases, even though it introduces a larger bending stress at the top, the optimal configuration is sinusoidal, because it provides the smoothest distribution of shear and therefore the least risk of delamination. The difference in curvature might be small, but the advantages are noteworthy.

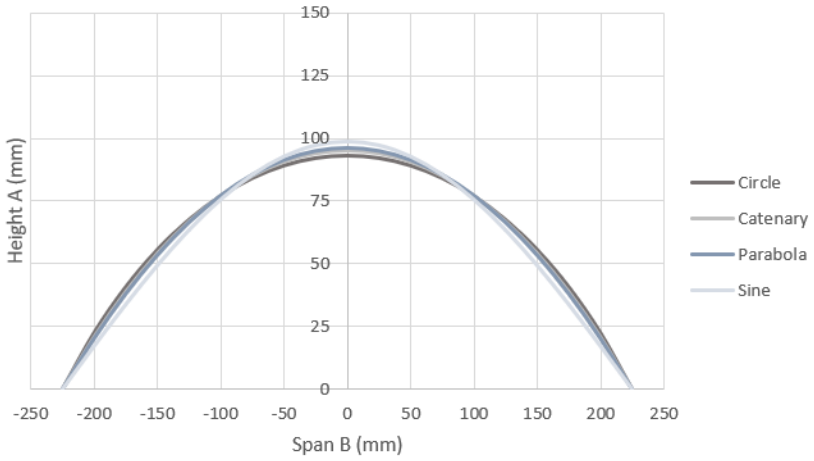

Figure 8.6: Circular, catenary, parabolic and sinusoidal curvatures with a span of 450 mm

8.3. Connections

Connections are inevitable and govern the principle of cold bent laminated thin sheets of glass due to the unknown factors of design, production, material properties, structural properties and structural behaviour. Optimal use of the cross section is only made by simply supporting the thin glass panels at the curved ends of the beam or by fixing the straight ends of the beam (Figure 8.7). When applied as a façade, the first option makes use of the bottom and top boundaries of which the upper part is connected to the roof, the bottom part is supported by the foundation and, depending on the application, the side boundaries are support free. This results in a fully transparent free formed glass façade, assuming that the support structure is self-supporting. The individual glass panels are subjected to in-plane shear and out-of-plane bending during loading. The second option requires a substructure between every panel to ensure the fixed ends where the panels rest on supports at the bottom. If weather and water tightness governs the design, a combination of the two principles can also be applied.

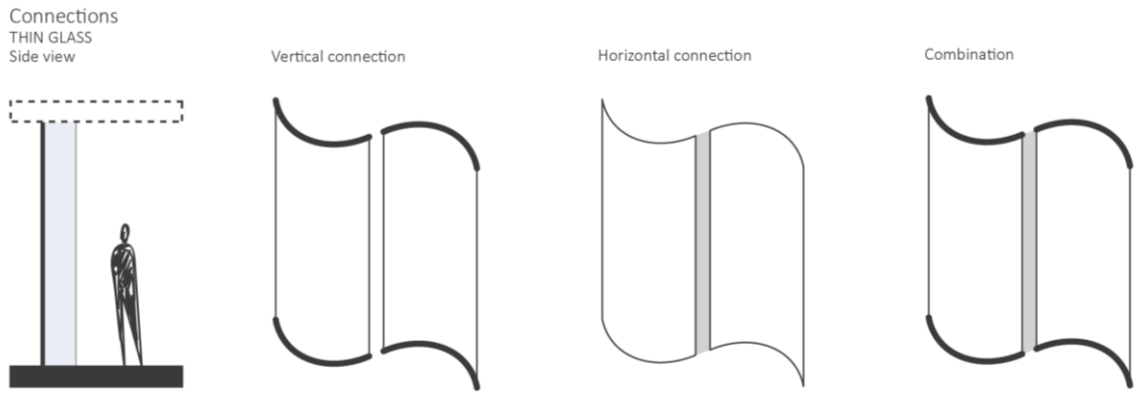

Figure 8.7: Schematic representation of vertical and horizontal connections

8.3.1. Vertical connections

The connections in vertical direction can be seen as continuous linear supports. As explained in chapter 3.5.1, they are the simplest and most widespread method of supporting a glass pane. The only difference being that the connection now needs to follow the curvature of the panel. With the frame being slightly larger than the pane, deviations from manufacturing, construction and post-installation changes are being accommodated. The out-of-plane loads are transmitted from the glass to the supporting system through a structural sealant of 6-15 mm neoprene, EPDM or silicone gaskets (Haldimann et al., 2008). By clamping the glass in between these supports up to 50 mm, a good degree of rotation of the glass edge is obtained and may be considered as a simply supported structure. The self-weight of the glass panel is transferred to the supports through plastic setting blocks located at the bottom edge. An alternative would be to use neoprene layers with a Shore A hardness ranging from 60 to 80.

8.3.2. Horizontal connections

Due to the thinness of a chemically tempered thin glass panel, the design of horizontal connections between glass panels should be approached differently than the design of connections for regular float glass in architectural applications. These connections have not been designed, simply because there has not been a need for them yet. This means that a full scale investigation must be performed in order to be certain that these connections can be safely implemented. During the lifetime of the cold bent laminated panels, the geometry changes due to relaxation and loading. If the panel is also vertically supported, the horizontal joint will broaden more in the centre of the span than at the supports. This will cause tensile stresses and eventually in tearing and leaking of the joint (Nijsse, 2008). Except for their weather and water tightness, these horizontal connections may also need to function as additional supports if the requirements for the deflections are not met. A few interesting types of horizontal connections are adhesives, Velcro, zippers, membrane-like connections and welded connections. However, this thesis focuses on the principle of cold bent laminated thin glass panels, and due to the large scale, will not take on another research into different horizontal connections types.

8.3.3. Conclusion

As a first architectural application the principle of simply supporting the thin glass panels at the curved ends of the beam without horizontal connections will be further investigated. It is however recommended to investigate the horizontal connections between thin glass panels. Especially if one would want to design a weather and water tight façade. These horizontal connections may also need to function as additional supports if the requirements for the deflections are not met by only using vertical supports.

9. Structural behaviour

After defining the preliminary principles of the design regarding composition, curvature and connections, this chapter focuses on the structural design of cold bent laminated thin glass panels. Firstly, an explanation on how to measure the structural behaviour is given. Secondly, the production process of cold bent laminated thin glass panels is defined. Lastly, numerical and experimental analysis are performed by observing different stages. The results will provide an insight into the structural behaviour of cold bent laminated thin glass panels.

9.1. Approach

The main goal of this research is to gain insight in the structural and post-breakage behaviour of cold bent laminated thin glass panels. To obtain a curvature, glass panes have to be cold bent into a certain shape. As explained in chapter 8.2, a sinusoidal curvature introduces higher bending stresses at the top, but also provides the smoothest distribution of shear and the lowest risk of delamination. The stresses in the interlayer are not accounted for, since they will be released during lamination. At this stage, the interlayer softens and glues the thin glass plies together. After laminating the panels in their curved shape and releasing them from their mould, a certain spring back effect is observed. It must be noted that the stresses at the top of the lowest thin glass ply increase a little due to a moment in opposite direction. This springing back also influences the geometry and consequently the stiffness. According to Fildhuth (2015), the initial spring back of laminated bent glass (5-20%) mainly depends on the number and thickness of glass layers and the elastic properties of the interlayer.

Hereafter, the glass panel transitions into the relaxation phase. At this moment, it's the interlayer that holds the entire panel together. The interlayer is subjected to a constant load, because the thin glass panes want to go back to their original flat shape. For long-term relaxation, the interlayer strongly depends on the shear modulus with regards to time, temperature and load duration. These variables can change the geometry and accompanying stresses significantly. Fildhuth (2015) investigated cold bent laminated glass of regular thicknesses for different configurations and concluded that at room temperature, the curvature of the two-ply PVB laminate is reduced by 40% after 8 months, whereas the SG laminates recover by 17%. Cold bent PVB laminates thus can only be used together with a shape stabilising substructure. At 20°C, the SG laminates do not noticeably relax and mostly preserve their cold bent shape.

However, due to the lower costs, better optical properties and easier manufacturing processes, a PVB is more desirable. Fildhuth (2015) investigated the difference of regular PVB's and SG's, but no research has been done into stiffer PVB's yet. Therefore, for this research, two cold bent laminated thin glass panels with a Saflex DG41 interlayer and two cold bent laminated thin glass panels with a SentryGlas interlayer are considered. AGC provided Leoflex glass of 0.55 mm thick and 500x500 mm large. Qdel provided 0.76 mm thick Saflex DG41 interlayers and Trosifol provided 0.89 mm thick SentryGlas interlayers. All the panels are cold bent into a sinusoidal curvature of:

$$y = \mathrm{A}\cos\left(\frac{\pi}{\mathrm{B}}\mathrm{x}\right) \tag{9.1}$$

where A=99 mm and B=450 mm. This curvature is chosen because it's in the middle of the spectrum in terms of its geometrical stiffness and allowance for additional loading, assuming a tensile bending strength of 260 MPa. An even larger curvature would break quite easily and a flatter one would deform significantly during loading. Additionally, a larger curvature also allows for a greater range of relaxation in which the panel can change its geometry and therefore captures the behaviour well. By adding this curvature to a single thin glass pane, the stiffness has increased from I = 7 mm^4 to a stiffness of I = 258903 mm^4. The latter is comparable to a flat panel with a thickness of 18-19 mm.

Figure 9.1 illustrates the different kind of build-ups and geometries at different stages. Four two layered glass panels with the same curvature and different interlayers (2x SAF and 2x SG) are produced. One panel from the first series didn't maintain its curvature during lamination (panel 1.2). Therefore, another series with the same interlayer is manufactured. From the second batch, one panel broke during handling (panel 2.2). Only two usable panels with an interlayer of Saflex DG41 were left. A more elaborate explanation on why this happened can be found in the following chapters. Different curvatures are measured at the bending, spring back and relaxation stage. At last, the choice is made to load the panels by a point load to validate the numerical model. Other loads, such as a distributed wind load, are harder to introduce onto the curved geometry. Only if the numerical model is verified, other types of loading can be applied. Additionally, point loads induce higher stresses at a specific area of the panel, consequently this type of loading can lead to failure and could come in handy when observing the fracture pattern. When the point load is applied in a controlled matter until failure, the post-breakage behaviour can be observed as well.

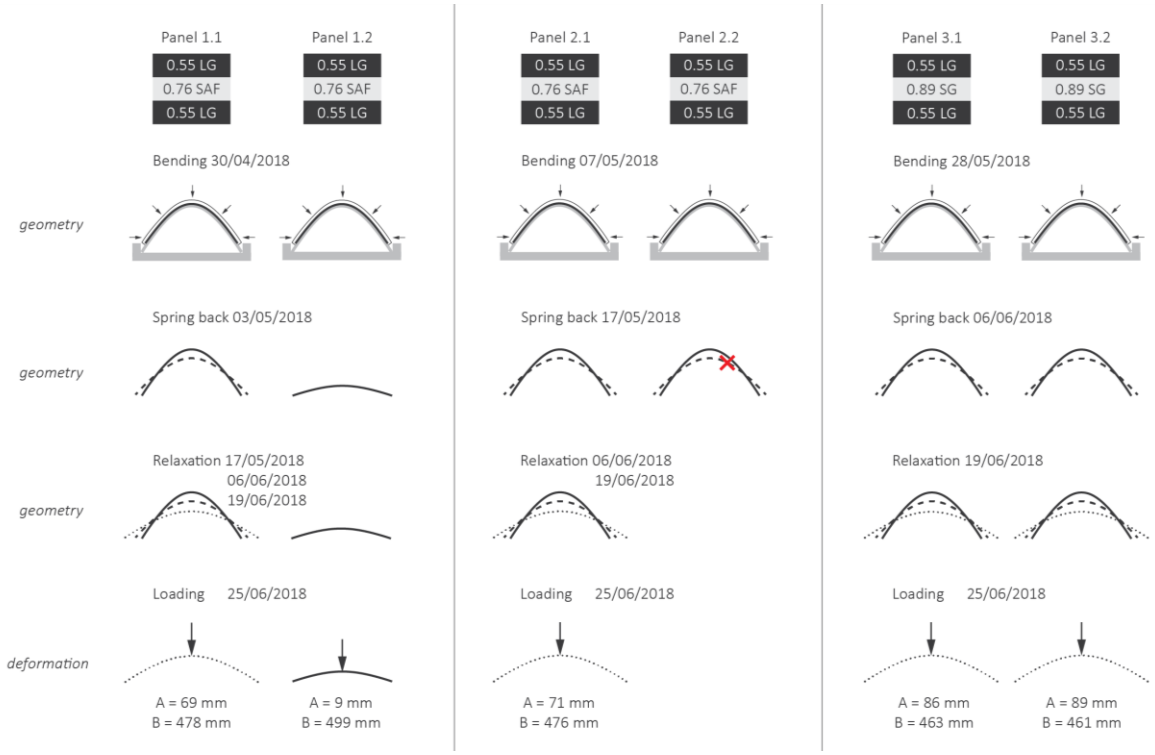

Figure 9.1: Overview of experimental specimens

9.2. Production process

The production process starts with manufacturing the mould, after which the glass panels are cold bent into the curvature of the mould. This is done in a vacuum environment where the glass is equally pressured at every point, avoiding peak stresses. The same process also aims to remove all the air from the interlayer and glass surface to make a full-surface adhesion and avoid premature separation in the autoclave process (Molnár, Vigh, Stocker, & Dunai, 2012). An autoclave completes the cycle by laminating the glass panels. Lastly, the supports acting as boundary conditions during loading are manufactured. Table D.1 lists the products and equipment used to manufacture cold bent laminated thin glass panels.

9.2.1. Mould

A mould is manufactured in order to cold bent thin glass sheets into a sinusoidal curvature. This mould needs to resist temperatures of around 140 °C in the autoclave. Thus, materials like timber that are affected by higher temperatures cannot be used. A first trial of moulds can be found in Appendix D.1. Eventually, the choice is made to manufacture an adjustable mould in aluminium. A sinusoidal curvature can be established by using the buckling principle where one support is fixed at one end and the other support can move sideways. By simply changing the distance between the supports, only one mould is needed to provide different sinusoidal curvatures. This is obtained by assembling a rectangular frame using an aluminium profile system from Boikon. One aluminium bar is fixed at one end of the frame, while another bar can slide though the cavity of the frame below using bolts as guidance. An aluminium plate of 2 mm is cut to a size larger (550x680 mm) than the thin glass sheets. This is done to prevent the glass from touching the Boikon bars located at each side during bending. Additionally, this space can also be used to attach the vacuum bag onto the aluminium plate instead of wrapping the entire mould with risks for the vacuum foil to tear. The aluminium plate is slightly curved in the middle by using a manual slip roll machine to steer the plate upwards during buckling. Clamps provide the required pressure for buckling the plate into a certain curvature. L-shaped profiles are located at the ends to prevent the plate from sliding underneath the aluminium bars. The desired curvature can be measured on the basis of distance B between the supports. After the curve is set, the bolts can be tightened and the clamps can be removed.

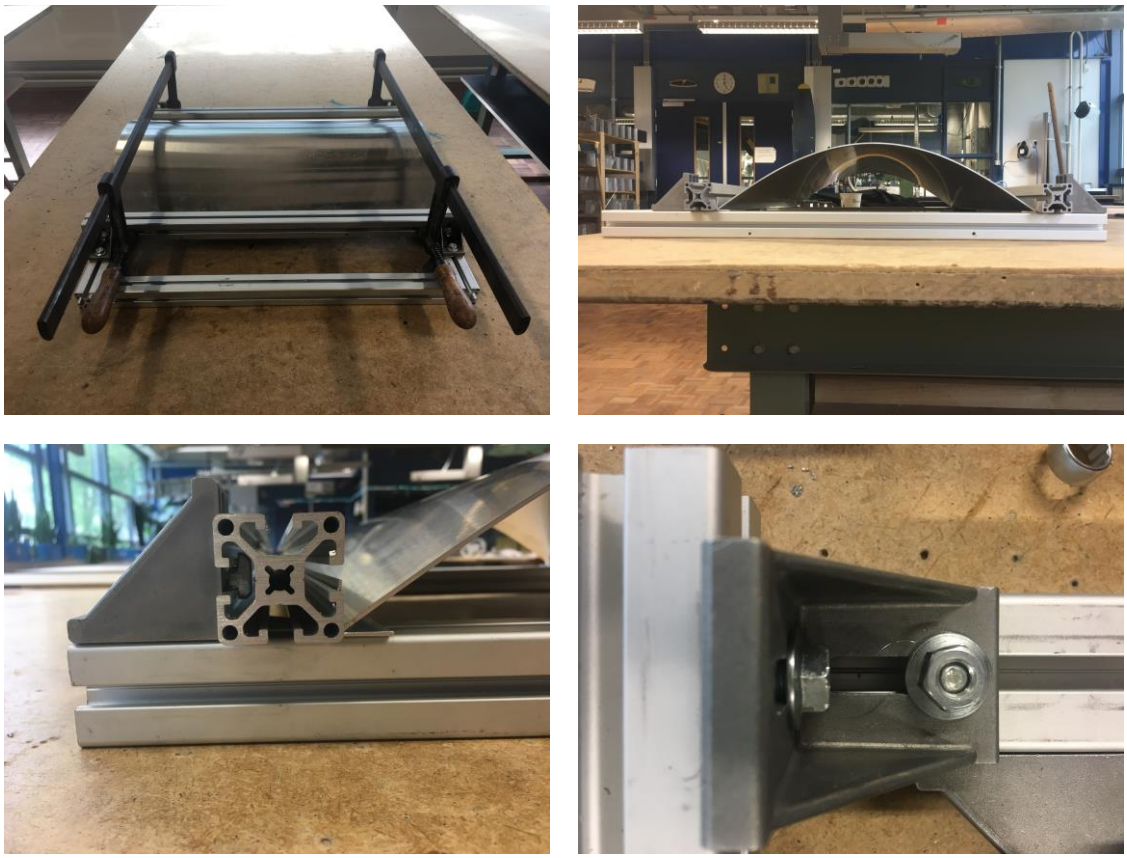

Figure 9.2: Adjustable aluminium mould

9.2.2. Bending

The bending process is completed in a clean room to prevent dust from sticking to the thin glass sheets and interlayer, thereby creating a proper laminated panel (Figure 9.3). At the end of the laminating process the glass and the interlayer are bonded chemically by hydrogen bonding bridges. The adhesion depends on the hydrogen bonding bridges between the water-compatible groups of the glass surface and the polymer. It is very important to clear the glass surface before the whole procedure (Molnár et al., 2012). To make a two-layered laminated glass plate, two thin glass sheets are thoroughly cleaned with acetone and a clean cloth, using gloves while doing so. After the glass is checked for marks, the interlayer (SAF or SG) is removed from its package and placed on top of one of the thin glass sheets. The other thin glass sheet is then added on top of the interlayer. Saflex DG41 is shipped inside a moisture barrier bag and needs, once opened, to be stored in a ventilated environment between 2-10 °C with 30 % relative humidity to minimise sticking. SentryGlas doesn't need to be stored in a room with special conditions. To prevent the build-up from sliding, blue heat resistant adhesive tape is used. The corners of the panel are covered with sealing tape and wrapped with heat resistant adhesive tape to protect the vacuum bag from sharp corners and prevent tearing.

The first series of cold bent laminated thin glass panels is produced differently from the other two following series. In the first series, two rows of black sealing tape are attached along the edges of the glass to create two areas that can be in vacuum separately. This is done to allow the middle part of the vacuum bag to be cut out and painted after lamination, while the edges are still pressurised into vacuum. The idea of this principle is that the cold bent shape can be measured first and after releasing the pressure from the edges, the spring back can be observed. The inner part is connected to a vacuum connector by a plastic straw filled with peel ply. This plastic straw is attached to the black sealing tape in the middle at the edge of the glass build-up. The bump that is created has to be symmetrically applied on the other side to make up for differences (Figure 9.3). Any leftover foil needs to be filled with sealing tape to ensure the bag is airtight. A large piece of vacuum foil needs to be cut to cover the glass and remaining areas. A vacuum foil for lower temperatures (177 °C) was used in the build-up of panel 1.1, while panel 1.2 included a vacuum foil used for higher temperatures (204 °C).

The process of separating the inner and outer parts of the panel is rather complicated and a few problems arise. A loss in vacuum is observed in panel 1.2 during the autoclave cycle. Also, it is hard to remove the black sealing tape from the glass panel. To prevent the glass from breaking, this should be done with care, but is time consuming. The choice was made to revise and simplify the production process. For the second and third batch, the vacuum bag will consist of only one area instead of two. The glass specimen will be covered with peel ply to allow for a better vacuum. Yellow sealing tape, resistant to higher temperatures, replaces the black sealing tape. Lastly, lower temperature resistant foil for all specimens will be used, because it behaves less stiff and can deform more easily around the corners.

The mould is prepared by cleaning the curved aluminium plate with acetone and a clean cloth. The areas where sealing tape will be applied are sanded to allow for a better airtight and adhesive connection. Afterwards, the mould is cleaned again. To prevent glass from touching aluminium, a protective red coloured release foil is attached to the aluminium plate. Sealing tape is applied around the edge of the aluminium plate, using two rows of tape in the second and third batch as backup. One side of the mould is used to install the vacuum connecters. The first series includes two vacuum connectors, separated by black sealing tape. As mentioned, the vacuum connector on top of the curve is linked to the inner part of the panel. While the other vacuum connecter is associated with the edges of the panel. A plastic straw filled with peel ply is used to bridge the left and right side of the first mentioned vacuum connector. Breeder blankets are placed underneath the vacuum connectors to separate the connectors and the aluminium plate and to stimulate full vacuum. The second and third series use only one vacuum connector.

When the glass is correctly positioned and fixed with heat resistant tape, the vacuum bag can be closed off at the boundaries. Before fully closing the bag, a sharp cutting knife is used to cut holes at the place of the vacuum connecters. The connectors are then positioned and mounted. Additional foil is used at the ends where the glass panel will curve the most, so that the bag can be manually pulled out to prevent foil from slipping underneath the glass panel during de-airing. To reach full vacuum, the sealing tape is pressed firmly. Figure 9.3 shows the difference in manufacturing the first, second and third series.

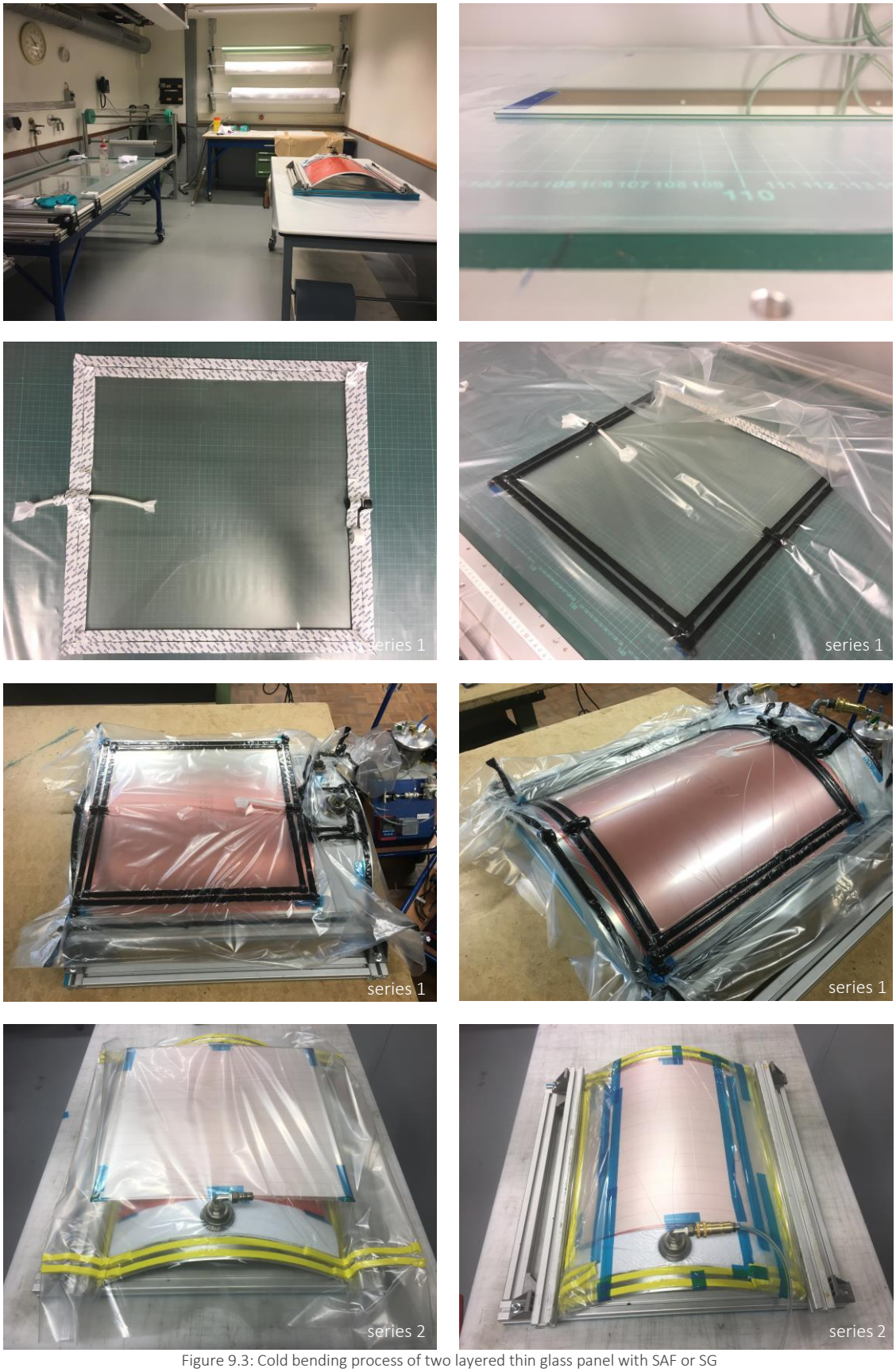

Figure 9.3: Cold bending process of two layered thin glass panel with SAF or SG

9.2.3. Lamination

The lamination process is the last step in the production of laminated glass. Autoclaving is necessary to achieve the best quality, thus the correct temperature and pressure must be chosen. The temperature is approximately 140 ˚C and the ideal pressure 12 bars. The duration of the process can last 1 to 6 hours, depending on the build-up and glass thickness (Molnár et al., 2012). For optimal results, the steps during the autoclave cycle can differ in terms of temperature, pressure and time range. Before starting the cycle, all the specimens are connected to a vacuum pump inside the autoclave to ensure full vacuum inside the bag and to maintain the geometry.

According to Eastman Chemical Company (2013) successful laminate autoclaving for a two layered thin glass panel with a Saflex DG41 interlayer depends on not permitting the high pressure air to penetrate, achieving interlayer flow and dissolving any residual air in the assembly. In order to achieve these objectives, the autoclave cycle is composed of three distinct steps: ramp up, hold and ramp down. During the ramp up phase, the temperature increases from about room temperature to the final hold temperature and pressure increases from atmospheric to the final hold pressure. If all edges of the vacuum bag are properly sealed before autoclaving, the rate of pressurisation may not have any effect on the final laminate. However, poor edges may allow interlayer movement and consequent shrinkage. Residual air in the laminate will build up its own pressure as the temperature increases, which may cause bubbles or open a previously sealed edge. During holding, viscous permanent flow of the interlayer is facilitated in order to fully develop the final laminate properties. Time and temperature are the most important factors, with pressure secondary. AGC recommended a temperature holding time of 4 hours with a pressure of 12 bar. At the end of the hold time the laminates must be cooled down while remaining under pressure to avoid bubble formation, particularly at or near the edges of the interlayer. Pressure should be maintained until temperature of the laminates is 40-50 °C or less. Figure D.2 shows that the autoclave had a hard time getting under the recommended temperature value for pressure to be released. This was due to high temperatures in the Netherlands at the time of production. Therefore, since the cycle ran partly during the night, the pressure was maintained until the next day. This may cause a poor edge seal to open in panel 1.2, releasing its vacuum and loss in curvature (Figure 9.4.). Figure D.2 shows that 270 minutes (4.5 hours) into the cycle, the vacuum was lost (graph N1, N2 and N3).

It must be noted that at 1 hour during the first cycle, a wire broke due to fatigue, releasing all the pressurised air inside the autoclave. The wire had to be fixed and the cycle had to start again from the beginning. According to AGC, this should not affect the laminate of the panels. Also, half an hour into the second cycle a hose detached from the autoclave, releasing the pressurised air from the vacuum bags. The cause of this problem was that the autoclave has three vacuum connector exits, and one of them wasn't closed properly, resulting in an air burst pushing the hose out of its place. The exit was closed and the cycle had to start from the beginning. Unfortunately, the data of the second cycle could not be retrieved due to errors in the saved file, but should be similar to the cycle of the first series.

Kuraray Trosifol (2018) recommends a similar temperature and pressure, but different steps for a two-layered thin glass panel with a SentryGlas. During the ramp up phase, the temperature increases from about room temperature to the first holding temperature of 55 ˚C and pressure increases from atmospheric to the first holding pressure of 3 bars. The temperature stays at the same level for 40 minutes and builds up to 130 ˚C where after the second holding temperature sets in. The pressure is on hold for an hour and increases to 12 bars afterwards. The second holding phase lasts 100 minutes for both the temperature and pressure. Hereafter cooling down starts. The amount of haze in the final laminate is directly related to the autoclave cycle cooling rate. The faster the cooling rate the lower the haze. However, at the time of production a heat wave hit the Netherlands. Therefore, as can be seen in Figure D.2, the autoclave had trouble cooling down. Only until the temperature hit nearly 40 ˚C, the pressure dropped. It must be noted that the delivered sheets were originally 600x600 mm, so they had to be cut to a size of 500x500 mm manually by a cutting machine. Protective measurements were taken to evenly distribute the load during cutting.

The results of the autoclave process are shown in Figure 9.4. Panel 1.1 developed perfectly, while panel 1.2 lost its vacuum during the process. Due to the high pressure, a print of the vacuum connectors is clearly visible in the breeder blanket (detail 1). The temperatures made the black sealing tape viscous and hard to remove from the mould and glass panel. The black sealing tape can still be seen at the edges of the panel from the first batch (detail 2). From this photo, it is also clear that the top thin glass layer isn't aligned with the lower thin glass layer due to difference in curvature. The second and third series both successfully completed the lamination process. Improvements could be made in terms of the distance of the breeder blanket to the glass panel. Detail 3 shows that the breeder blanket got stuck to the interlayer and had to be removed carefully. Although some setbacks were encountered during the lamination process, the panels for both SAF and SG appear to be clear and well laminated. However, the straight edges seem to slightly bent upward along the entire length in all specimens and can only be captured when the surface reflects light (detail 4). This could be caused by shrinkage of the interlayer during cooling down or vacuum foil trapped underneath the glass changing the shape at the edges. The latter could be controlled by pulling the vacuum foil sideways, and therefore seems less likely to be the cause of these deformations at the edge.

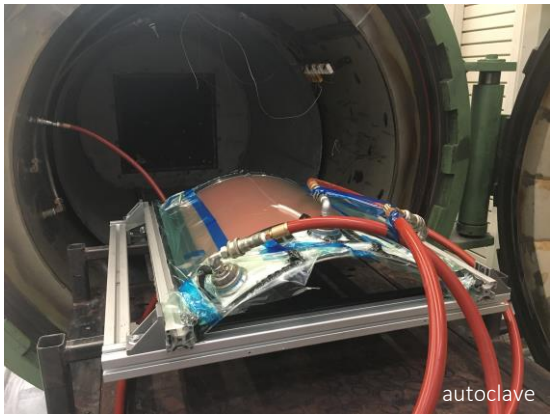

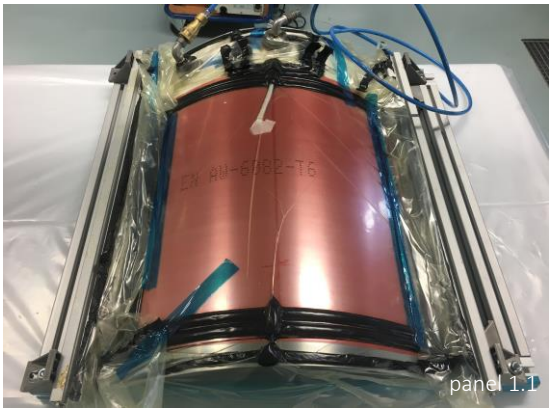

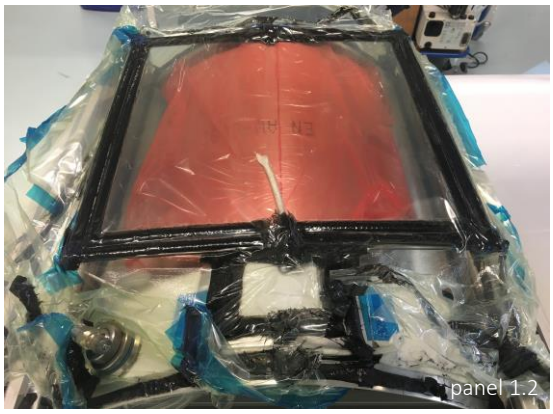

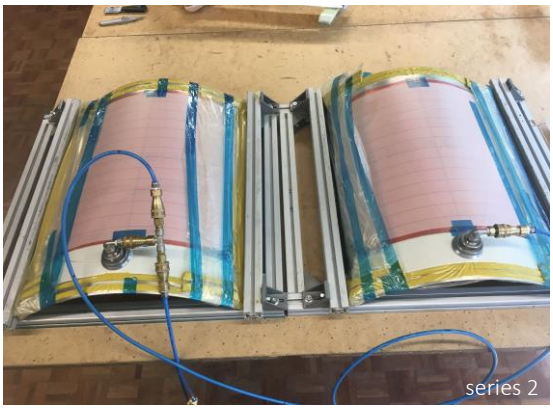

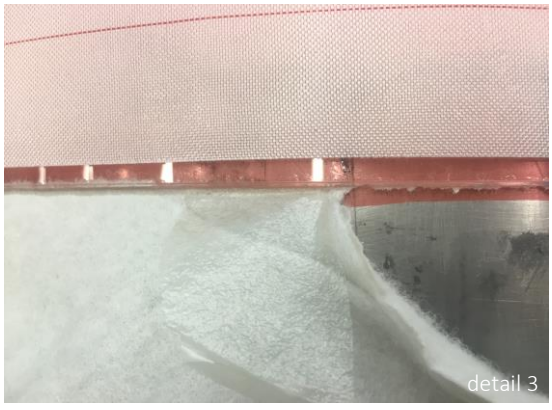

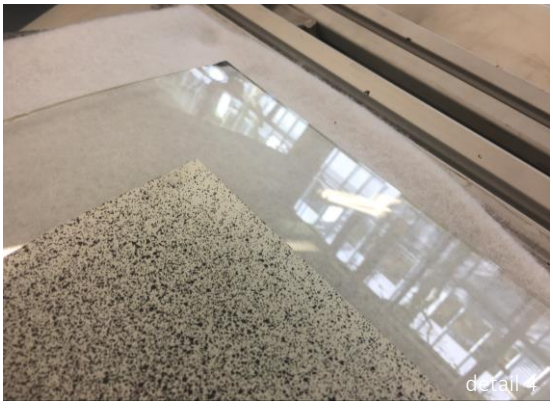

Figure 9.4: Lamination of thin glass panels

9.2.4. Supports

As explained in chapter 8.3, the choice was made to simply support thin glass panels at the curved ends of the beam without horizontal connections. At loading, the supporting frame is designed to load the panels vertically, hence the horizontal orientation (Figure 9.5). By keeping in mind the scale of the glass panels, the width of the supports is chosen to be 3 mm. Due to the differences in curvature of cold bent laminated glass panels, each support is manually made by using soft wood planks as the frame and strips of 1 mm thick rubber as a structural sealant. The latter allows for tolerances and small movements, and tries to avoid peak stresses. The glass panel rests on a timber curved element with a rubber strip in between and is kept in place by another timber curved element on top, also with a rubber strip in between. The bottom and top part are attached to each other by a piece of timber at the outer edge of the panel and fixed with screws. The top part is necessary to prevent the glass panel from going upwards during loading. Another timber element is used to attach the supports at both ends of the beam to avoid the frame from becoming unstable during loading.

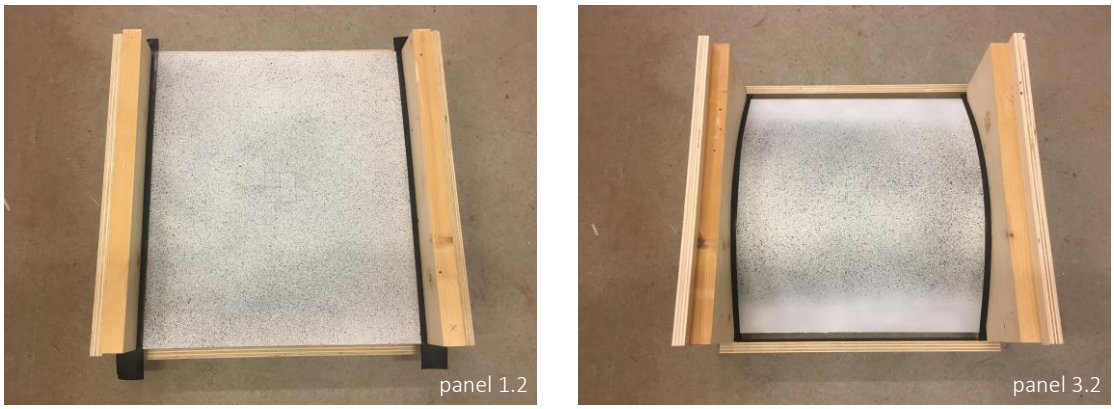

Figure 9.5: Overview of manufactured supports

9.3. Numerical analyses

The thinness of the glass panel leads to geometrically nonlinearity and influences the behaviour significantly. A linear analysis can only be performed when deformations are smaller than half the thickness of a structural element. In this case, the assumption can be made that the deformations are larger. Therefore, a numerical model is created to capture the geometry and stresses during bending, spring back, relaxation and loading. This is done in Finite Element (FE) software Strand7. The intention is that the model runs as quickly as possible and yet produces accurate results. Thus, to save computing time, the first three stages are modelled in 2D and the latter in 3D. The maximum stress in the glass during loading is calculated by adding the stresses at the end of relaxation to the ones obtained from the structural analysis at loading. Another profit can be obtained by using symmetry. Due to the curvature bending in a single direction, the problem lends itself very well for symmetry conditions. Results from the numerical analyses can be found in Appendix E.1.

9.3.1. Bending

The bending process is modelled in a two dimensional coordinate system using nodes and plates. All the plates consist of Quad8 elements to obtain a quadratic interpolation. Just as the cold bent laminated glass, the numerical model is made up of two layers of thin glass with a thickness of 0.55 mm and, depending on the build-up, an interlayer of 0.76 mm corresponding to SAF or an interlayer of 0.89 mm thick corresponding to SG. A mesh ratio of 1:1 is preferred with a recommended maximum ratio of 1:5. However, due to the thinness of the glass, the model will take indefinite to solve the problem. This is not necessarily an issue during the 2D stages, but it is in 3D. The choice is made to obtain a mesh ratio of 1:18, decreasing the computing time, but losing a certain accuracy in the results. Symmetry is also applied. Each layer divided into two elements vertically and fifty elements horizontally, results in a mesh of 50x2 elements per layer.

Numerically bending thin glass into a sinusoidal curvature is done by using the buckling principle. One end of the beam is restraint vertically and displaced horizontally at the lower corner of both glass panes, while at the other end all the nodes are restrained horizontally to make up for symmetry (Figure 9.6, Appendix E.1). The former boundary conditions are applied to the lower corner of both glass panes, as the interlayer doesn't contribute anything to the panel during bending. The interlayer only starts working from the spring back stage, thus, during bending, two options can be introduced. The first option disables the interlayer and requires morphing of the elements to translate the interlayer in between the curved thin glass panes obtained at the end of bending. The second option also involves morphing, but in addition changes properties of the interlayer from almost zero stiffness during bending to a certain level of stiffness during spring back. The latter is applied due to better results and less errors in the mesh at spring back and relaxation (Figure E.3). Both the material properties of glass and interlayer are assumed to be isotropic and elastic with a width in z-direction of 500 mm.

The system is solved using geometrical nonlinearity. Only a small load at the end where symmetry is located needs to be applied in order for the model to know the panel has to move upwards. The load has to be small in the sense that it doesn't affect the bending results (e.g. 0.01 N per node). This load is present in the first increments, after which relatively small steps are taken to let the plates buckle into a sinusoidal curve. This is done by using displacement control until a displacement of 25 mm. Consequently, the numerical model will span B=450 mm due to symmetry. The same model is used to predict the bending behaviour of panel 1.1. and panel 2.1 (SAF). Another model is used to represent panel 3.1 and panel 3.2 (SG). As European glass design methods generally assume cracks to be oriented perpendicularly to the major principal stress, this stress is assumed to be governing. The maximum tensile bending stress for the before mentioned panels is σ_{11}=82.13 MPa and can be found at the boundary for symmetry at the top of both thin glass plies (Figure E.6). Another model is created for panel 1.2, because a loss in vacuum resulted in another curvature. Note that this doesn't mean the panel is cold bent into that curvature, but it is assumed so in the numerical model to obtain the correct shape with a span of B=499.5 mm. The maximum tensile bending stress is σ_{11}=7.67 MPa and can also be found at the boundary for symmetry at the top of both thin glass plies (Figure E.5).

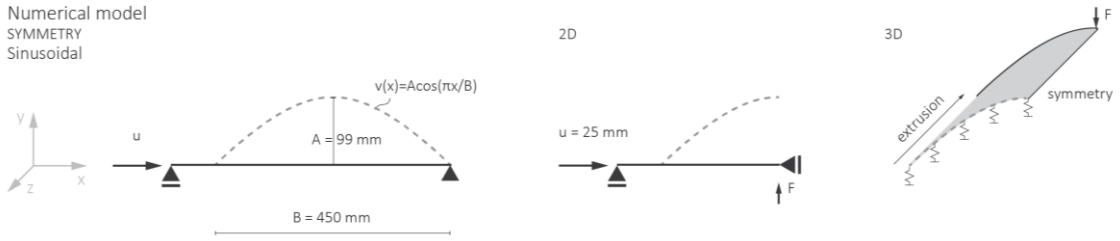

Figure 9.6: Schematisation of numerical model using symmetry to obtain a sinusoidal curvature

9.3.2. Spring back

After the numerical bending stage, spring back is captured by introducing a new stage where certain properties and supports change. At spring back, one end transforms from a vertical and displaced horizontal restraint at the lower corner of both glass panes to a single vertical support at the bottom of the laminated panel (Appendix E.1). The other end remains the same to make up for symmetry. As mentioned in the previous chapter, only morphing of the interlayer causes problems later on in the analysis due to poor results (Figure E.3). The properties therefore go from almost zero stiffness during bending to a certain level of stiffness during spring back. Both the general material properties of glass and interlayer are assumed to be the same as for bending. Appendix A.6 and Appendix A.7 show the changing Young's modulus and Poisson ratio determined by the manufacturers for a different load duration and temperature of SentryGlas and Saflex DG41. The Young's modulus and Poisson ratio used to determine spring back are defined in Table 9.1. The choice for these values is based on the highest recorded temperature during this research, which is 30 °C. The corresponding Young's modulus and Poisson ratio are taken at a load duration of one second to capture spring back. Strand7 only needs the Young's modulus and Poisson ratio, as it calculates the shear modulus.

No loads or restraints are added, so this stage only requires one increment to capture the spring back. As expected, the top goes down from 97.11 mm to 91.75 mm in vertical direction for panels containing an interlayer of SAF and from 97.10 mm to 92.62 mm in vertical direction for panels containing an interlayer of SG. As predicted in the analytical calculations in chapter 8.2, the top of the lower thin glass ply contains more stresses at spring back than at the end of bending due to a bending moment in opposite direction. The highest principal stress goes from σ_{11}=82.13 MPa to σ_{11}=88.44 MPa for SAF and from σ_{11}=82.13 MPa to σ_{11}=88.31 MPa for SG (Appendix E.1.2).

9.3.3. Relaxation

The used interlayers are highly sensitive to load duration and temperature as illustrated in Appendix A.6 and Appendix A.7. A substantial decrease in stiffness is notable for Saflex DG41 at normal environmental conditions. SentryGlas seems to be stiffer at first, but decreases to the same values as SAF at extreme conditions. During relaxation, the panels are subjected to a range of temperatures and constant loading due to the glass panes wanting to go back to their flat shape. These factors influence the geometry and stresses of the panel significantly. During testing, temperatures varied from 15 to 30 °C. To simplify the problem, an estimation is made using the highest temperature at different time intervals (Table 9.1). The Young's modulus and Poisson ratio at 1 hour, 1 day, 1 month and 10 years are adopted to numerically investigate the relaxation stage.

To capture the physical nonlinearity of the interlayer, a linear approach is applied by introducing a new stage for different load durations. The boundary conditions remain the same as for spring back, but the Young's modulus and Poisson ratio change at every stage. The top of the geometry would change from 91.75 mm at spring back to 82.92 mm at a month of loading in temperatures of 30 °C for SAF and from 92.62 mm at spring back to 92.18 mm at a month of loading in temperatures of 30 °C for SG. The accompanying stress goes from σ_{11}=88.44 MPa to σ_{11}=79.97 MPa for SAF and from σ_{11}=88.31 MPa to σ_{11}=88.04 MPa for SG. As expected, a decrease in curvature also results in a decrease of principal

stresses over time (Figure 9.7). It must be noted that the sequence of variables changes the geometry and corresponding stresses significantly. Consequently, it doesn't come as a surprise that the numerical output doesn't match the experimental results. Therefore, the choice is made to adapt the 2D numerical model to the experimental results at the end of relaxation. The numerical model is then transformed into a 3D model in order to apply loading.

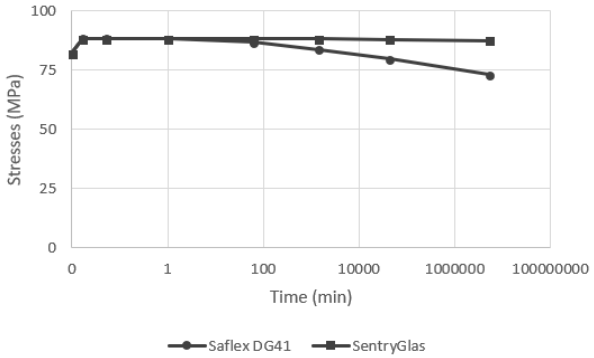

Figure 9.7: Time (min) versus maximum principal stress (MPa) for SAF and SG

9.3.4. Loading

The 2D numerical model at the end of relaxation is adapted to match the curvatures from the experimental panels. From the experimental results, it follows that the height of panel 1.1 is 69 mm and 71 mm for panel 2.1. The height of panel 3.1 is 86 mm and 89 mm for panel 3.2. To capture the behaviour during loading, the average heights are taken and converted into one 3D model for SAF and one 3D model for SG. Thus, the 2D model for SAF is converted to a height of 70 mm and to 88 mm for SG. Afterwards, the displaced geometry at this stage is saved and reopened as a new model. Note that only displacements are saved and no stresses. To obtain the correct stresses, the principal stress at the end of relaxation have to be added to the ones from loading.

The plate elements are extruded into z-direction, perpendicular to their face. Symmetry conditions can also be applied here, so the extrusion is only 250 mm. This creates Hexa8 brick elements, after which the plate elements can be removed. The same division is applied as for 2D in x and y-direction. To obtain squared brick elements, the mesh is also divided into 50 elements in z-directions, resulting in a mesh of 50x2x50 per layer (Figure E.4). Five days before loading, the panels are kept in a room at a temperature of 20 °C. When loading the panels, series one and two are 6-8 weeks old and series three is 3 weeks old. The chosen properties of the interlayer remain the same during the analysis and are therefore chosen to be loaded by its curvature for a month at 20 °C (Table 9.1). The boundary conditions at symmetry edges are the same and translationally restraint at the direction of symmetry at every node along that edge. Since the supports are at the curved edge of the panel, boundary conditions that simulate the supports will need to be designed. A translational spring of 100 N/mm is applied at the lower nodes along the full length of the curved edge. The reason to choose for springs rather than restraints is that the rubber will allow the panel to move up and downwards slightly. A rigid node, as one would have if a restraint is applied, introduces large stresses at the edge resulting in immediate failure of the panel before reaching any significant deformations. The value of 100 N/mm is chosen to prevent the edge from moving too much, but also restraining them to a decent amount of movement.

The panel will be loaded by a point load with an area of 50x50 mm. According to the Eurocode, point loads are normally applied with an area of 100x100 mm, but is reduced for this research based on the scale of the panel. To model such a point load in Strand7, a global face load is applied at the centre of the panel. To make up for symmetry, the load is introduced at an area of 25x25 mm. To simplify the process and to obtain the correct output, the given value is 0.25/TA, meaning one fourth of the load is divided by the total area. When solving the model by using geometrical nonlinearity, load factors are included in the increments. Thus, if the load factor is 50 N, the total load will be 50*0.25N*4 (symmetry) = 50 N. Note that load control is used by implementing this method and results in divergence when the load decreases after a peak load is reached. At this peak, the calculations are terminated. Arc length control has been tried to capture the behaviour after the increment that diverged, but didn't give any results. Displacement control would not be realistic for this case, since it assumes that all the nodes or bricks move the same amount, while in fact the load is gradually introduced onto the panel due to its changing geometry.

Numerical calculations are carried out for curved panels with an interlayer of SAF and SG, including panel 1.2 and reference panels. These reference panels consist of the same properties and thickness used for panels with SAF and SG, but are completely flat in order for the output to be compared with curved panels. The results are taken at a load of 400 N (Table E.1, Appendix E.3.3). From these results, it can be concluded that, for every panel configuration, the highest principal stress occurs at the bottom node where the load is applied. The stress in this node does not have to be superimposed, because the principal stress at the end of relaxation is close to zero. However, the numerical model for

panel 1.1 and 2.1 shows a slightly different behaviour. At first, the model does develop the highest stresses at the same location, but at a load of 370 N, the location shifts to a part in the middle between the top and unsupported edge. In terms of the deflections, the curved panels behave significantly better than the flatter ones. Of the curved configurations, it can be concluded that panels with SG are stiffer than panels with SAF. Although the panels develop stresses due to cold bending, the stresses during loading develop at the area where almost no stress is introduced during bending. Thus, due to higher deflections in reference panels, the stresses in these panels are actually higher at the same load.

	Leoflex glass	Saflex DG41 (SAF)	SentryGlas (SG)	
Temperature		30	30	°C
BENDING 0 seconds				
Young's modulus	74000	0.001	0.001	MPa
Poisson ratio	0.23	0	0	-
SPRING BACK 1 second				
Young's modulus	74000	449	442	MPa
Poisson ratio	0.23	0.476	0.463	-
RELAXATION 1 hour				
Young's modulus	74000	4.1	178	MPa
Poisson ratio	0.23	0.476	0.485	-
RELAXATION 1 day				
Young's modulus	74000	2.1	148	MPa
Poisson ratio	0.23	0.476	0.488	-
RELAXATION 1 month				
Young's modulus	74000	1.5	34.7	MPa
Poisson ratio	0.23	0.476	0.487	-
RELAXATION 10 years				
Young's modulus	74000	0.8	15.9	MPa
Poisson ratio	0.23	0.476	0.499	-
RELAXATION 3D				
Young's modulus	74000	0.965	2.0	MPa
Poisson ratio	0.23	0.476	0.500	-
LOADING 1 month				
Temperature	-	20	20	°C
Young's modulus	74000	5.3	330	MPa
Poisson ratio	0.23	0.476	0.473	-

Table 9.1: Physical properties input during bending, spring back, relaxation and loading

9.4. Experimental analyses

Digital Image Correlation (DIC) is used to measure the geometry during bending, spring back and relaxation. In order to measure these conditions, the glass panels are painted white with black dots on top (Figure E.21). The strains could not be captured, because they were too small from bending to spring back and therefore included too much noise, resulting in inaccurate results. While bending and spring back are measured on the same day, the strains for relaxation are measured at different time intervals over a certain period. Consequently, different DIC set-ups were build up and calibrated. Strain is calculated by the transformation and gradients of deformation. Without matching calibration images, and comparable speckle images, the strain could not be measured during relaxation. It is assumed that the curvature corresponds to stresses obtained from the numerical analysis. Results from the experimental analyses can be found in Appendix E.2.

9.4.1. Bending

Several coordinates of the bent aluminium plate are roughly measured with a measuring tape and plotted in Figure E.19 to compare the curvature of both moulds to the analytical curvature. It follows that the aluminium plates capture the analytical sinusoidal curvature quite well. The only remark would be that the curvature at a quarter and three-quarters is larger than at the ends of a sinusoidal curvature. This could be improved, since the panel exactly starts at these curved points and assumes that bent laminated glass panels are more prone to delamination at more curved ends.

Figure 9.8 shows analytical, numerical and experimental curvatures of the thin glass panels obtained after cold bending and lamination. The points for the experimental curvature are plotted in 2D, but originate from a 3D surface. It turns out that the panels are not perfectly curved into one direction, consequently resulting in the graphs to show a range in curvature of the panel in z-direction. In order to measure the bending and spring back stage, the first series is fabricated with two compartments to allow the middle part of the vacuum bag to be cut out and painted after lamination, while the edges are still pressurised into vacuum. The cold bent shape can be measured first and after releasing the pressure from the edges, spring back can be observed (Figure E.21). This could only be measured for panel 1.1, because panel 1.2 exhibited a loss in vacuum, hence the severe difference in shape compared to the other panels (Appendix E.2.1). It seems that panel 1.2 is not curved in one direction anymore, but slightly twisted. Additionally, the panel doesn't seem to relax after 3 weeks due to its minor curvature.

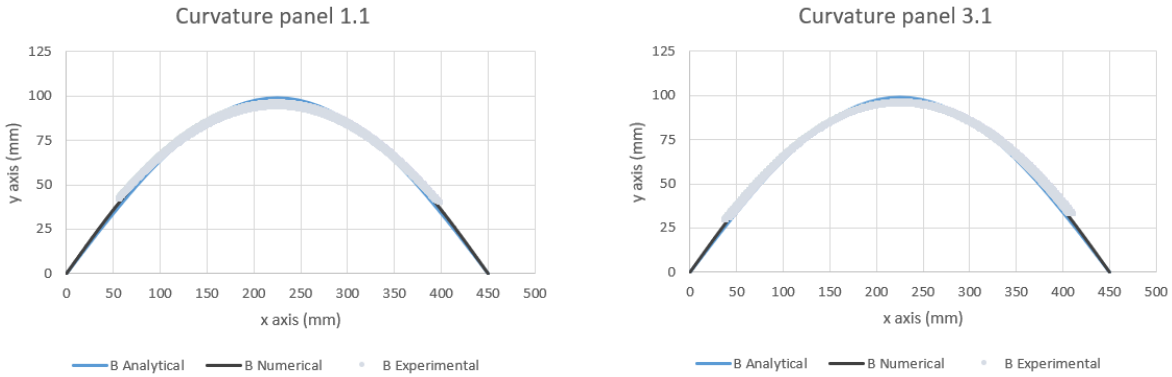

Figure 9.8: Analytical, numerical and experimental geometry obtained during bending

It must be noted that the second series was completely released from its mould, painted and measured after several hours. One panel, panel 2.2, broke during handling. The geometry of this panel is therefore not the cold bent shape, but a shape obtained after cracking and during relaxation (Appendix E.2.1). The remaining laminated panel from the second series was then pushed onto the mould to capture the bent state and must therefore not be mistaken for the actual geometry obtained from cold bending. For this reason, the choice is made to fix the panels from the third series with timber beams and clamps before releasement from the mould (Figure E.21). Breeder blanket is used between glass and timber to avoid peak stresses. After fixation, the middle part of the vacuum foil is cut away in order to measure bending and subsequently spring back.

9.4.2. Spring back

Spring back of panel 1.1 is measured immediately after releasement from the mould. The experimental results match the numerical results quite well (Figure 9.9). However, due to the complex system and room for improvement after losing vacuum in one of the panels, only one compartment is used while manufacturing the latter two series. The second series has been released from the mould an hour before capturing the results, thus, no spring back could be observed. The results capture the start of the relaxation process, as can be seen from the slighter curvature in the graph (Appendix E.2.2). The panels are under a constant load due to the thin glass wanting to go back to its original flat shape, starting from the moment of releasement. Therefore, only within a short time frame, spring back can be captured. The process had to be adapted when releasing the third series from their moulds. By fixing the straight end of the panel with timber and clamps, spring back could be observed.

Panel 2.2 cracked during handling of the panels from the second series (Figure E.20). No significant pressure was applied when a straight crack appeared in the middle between the top and the edge of the panel. Although the lower pane is subjected to higher stresses, it was the upper pane that cracked. This crack probably initiated from a flaw at the edge that opened up in a straight line towards the other end of the panel. The panel itself was still intact due to lamination. After a few days, the crack pattern had grown. Similar cracks had appeared at the top of the pane and near the ends where the stress is introduced from applying a sinusoidal curvature. Other cracks appeared perpendicular to these cracks at the curved top and bottom of the panel. Without any further loading, the panel continued to crack and even delaminate. A possible explanation for this phenomenon could be sub-critical crack growth, explained by Haldimann et al. (2008) as stress corrosion that causes existing surface flaws to grow slowly in size prior to failure. This means that a

glass element that is stressed below its strength, will still fail after the time necessary for the most critical flaw to grow to its critical size at a particular stress level.

9.4.3. Relaxation

The geometry of the panels is measured at two, five and seven weeks for panel 1.1, at three and five weeks for panel 2.1 and at two weeks for panel 3.1 and panel 3.2. During this period, two panels are stored on top of the mould with breeder blanket underneath the glass panel as shown in Figure E.21. The other panels are safely stored on top of a rolled-up breeder blanket so that the edges are free to move. An important observation is that the panels with a SAF interlayer relax significantly, but seem to come to a standstill after a certain period (Figure 9.9). The measured geometries of panel 1.1 at two, five and seven weeks are more or less the same, just as the geometries of panel 2.1 at three and five weeks. The panels with a SG interlayer do not seem to relax after spring back. The measured geometries of this series are the same at spring back and after two weeks. All the results at different time intervals are captured in Appendix E.2.3.

From the results, it is clear that the numerical approach doesn't correlate with the experimental curvatures, especially for panels with SAF as the interlayer. Other methods to capture the relaxation of the panel have been tried, but do not result in an accurate outcome. In addition to the geometry, no other variables are measured. However, many factors can influence the behaviour during relaxation. It could depend on varying temperatures or the variability in properties of the interlayer. The values represented by the manufacturer of the interlayer could be conservative or maybe the tolerances effect the panel significantly. In other words, it is recommended to further investigate this part of the process thoroughly.

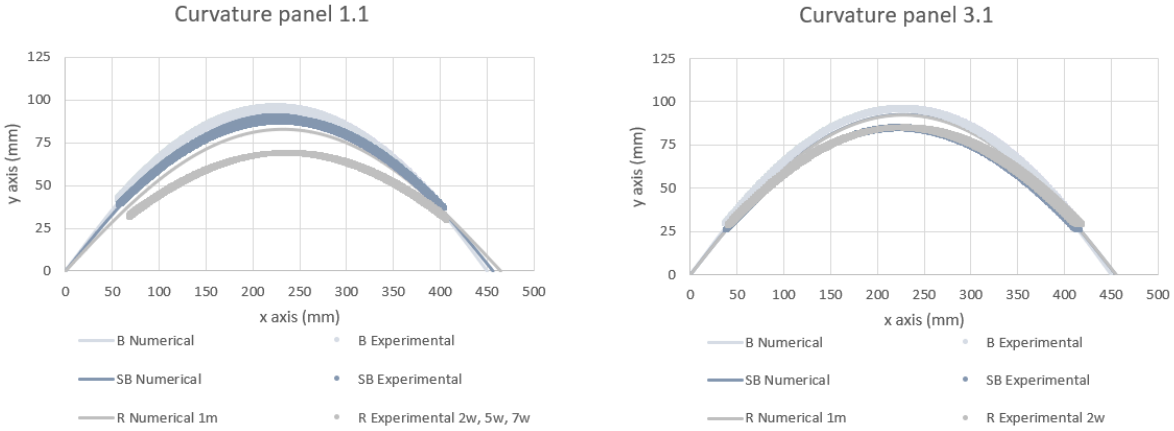

Figure 9.9: Numerical and experimental geometry obtained during bending, spring back and relaxation

9.4.4. Loading

The panels are moved into a room with constant temperatures of 20 °C five days before testing. On the day of the experiments, the panels are loaded with a point load applied in the middle of the upper surface. This point load is applied by machinery onto a surface of 50x50 mm consisting of 2 mm aluminium, which gives in more than steel during testing, and 6 mm of hard rubber. For every experiment, a new set of aluminium and rubber plates are introduced. Chapter 9.2.4 clarifies how the boundary conditions are translated to actual supports for testing. The set-up consists of three point bending controlled by displacement with the load recorded by a load cell. Six lasers are used to measure the displacement at certain points on the panel and are placed underneath the glass on top of the moving table. At induced point load area, the displacement is also measured, but includes the compression of rubber. A schematisation of the experimental set-up with the location of these lasers is illustrated in Figure 9.11. Due to restrictions in the experimental set-up, not all the lasers could be correctly positioned. The choice for using lasers was based on numerical analyses predicting the panels to deflect at least 15 mm. The lasers can measure a range of 50 mm.

An additional construction from soft wood is fabricated to support the frames holding thin glass panels and to provide some distance between the panels and lasers. During loading, it can be observed that the timber deflects as well. Consequently, the results are slightly affected by this deflection of the supporting structure. The load became large enough for one of the screws of panel 3.1 to break and for the supports to fail (Figure E.25). The glass was still intact and seemed to go back into its original curvature, thus, the supports and additional construction were fixed by adding larger screws and extra timber planks to increase the stiffness. Hereafter the panel was loaded again until failure. In fact, all the panels are loaded until failure. Panel 1.1 is one of the first to be tested and failed in such a way that glass spalled off in an aggressive manner. Therefore, the choice was made to add a very thin plastic foil as protection. The speed of loading differed per panel. Panel 1.2 was loaded 1 mm/min, panel 1.1 was loaded 2 mm/min. To speed up the process, panel 2.1 was loaded 5 mm/min. The same speed was applied for panels from series three to see if the speed had an influence on

the cracking pattern. Panel 3.1 was loaded 2 mm/min before failure of the supports, and 5 mm/min during the second run. Panel 3.2 was loaded 2 mm/min. Since panel 3.1 and panel 3.2 failed in a similar matter, it could be concluded that the speed did not influence the cracking pattern.

From the results in Figure 9.10 it is clear that the experimental data doesn't match the numerical model in terms of magnitude, but does show its global behaviour when subjected to a point load. Other numerical and experimental data obtained during loading is shown in Appendix E.3.4. The reason for this difference is probably governed by estimations of input variables. Just as for relaxation, the behaviour of the interlayer is hard to predict and hardly any information on the properties is available at this stage. Due to the curvature of panel 1.2 being rather flat, all the measured points go downward and change direction at a certain load. According to the experiments performed with highly curved panels, points T and L1 to L4 move downward during the entire loading process. Points L5 and L6 start to move upward, but change direction at a certain load level. The panels with a SAF interlayer displace more at the same load than panels with a SG interlayer. The lower stiffness can be explained by the difference in interlayer, but also a smaller curvature due to a higher degree of relaxation for panels with SAF. The graph of panel 3.1 at the first loading cycle shows additional deformation in the supports. This can be seen from a larger displacement compared to the second cycle, where the overall set-up behaves stiffer. Optical distortions in the glass couldn't be observed due to the panel being painted white. Nevertheless, it can be assumed that the deflections do result in optical distortions.

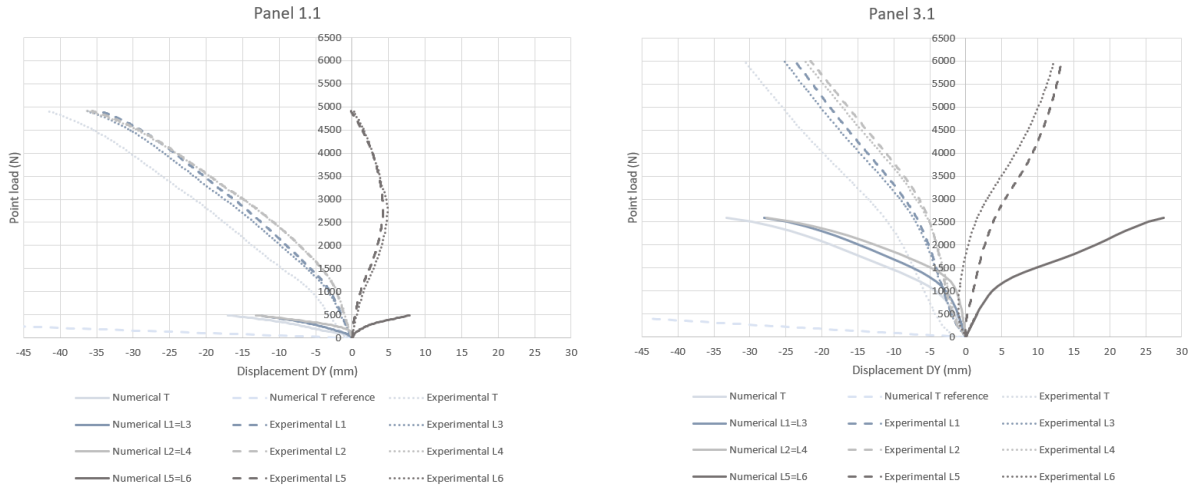

Figure 9.10: Numerical and experimental point load vs displacement obtained during loading

9.4.5. Cracking

Different cracking patterns are observed during the experiments as shown in Figure 9.14, with their origin as illustrated in Figure 9.12. The different crack patterns are all captured in Appendix E.3.5. After failure, panel 1.2 is still intact and doesn't show any signs of glass spalling. The crack pattern is asymmetrical and seems to originate from a flaw on the surface of the lower ply. Failure of panel 1.1 resulted in a loud bang and spalling of glass. The upper ply cracked and spalled at a specific region of the panel. Except from this region, the overall panel remained intact. A close-up of this region shows that thin glass is visible rather than the interlayer. Chapter 4.4.1 already briefly touched the topic of frangibility, a failure mode where the centre tension created by ion exchange results in spalling. This type of failure is extremely dangerous when applied in architectural applications and must therefore be extensively investigated.

The remaining panels failed with a loud bang as well and all cracked in a pattern that is more or less the same. The lower ply failed from accumulating stresses in the middle in line with the applied point load. This load caused the panel to deform equivalent to a circle in the middle. The direction differs at the area just around this circle, explaining the sudden change in pattern. The fragmentation of all the panels is high, indicating high stress releasement. The fragmentation size is less than a millimetre to several centimetres. Nevertheless, only one sheet broke for every panel, allowing the panel to remain its shape after failure due to lamination. Small cracking noises suggest that all the panels continued to crack for a while after removing the load. No delamination is observed, even after a few days.

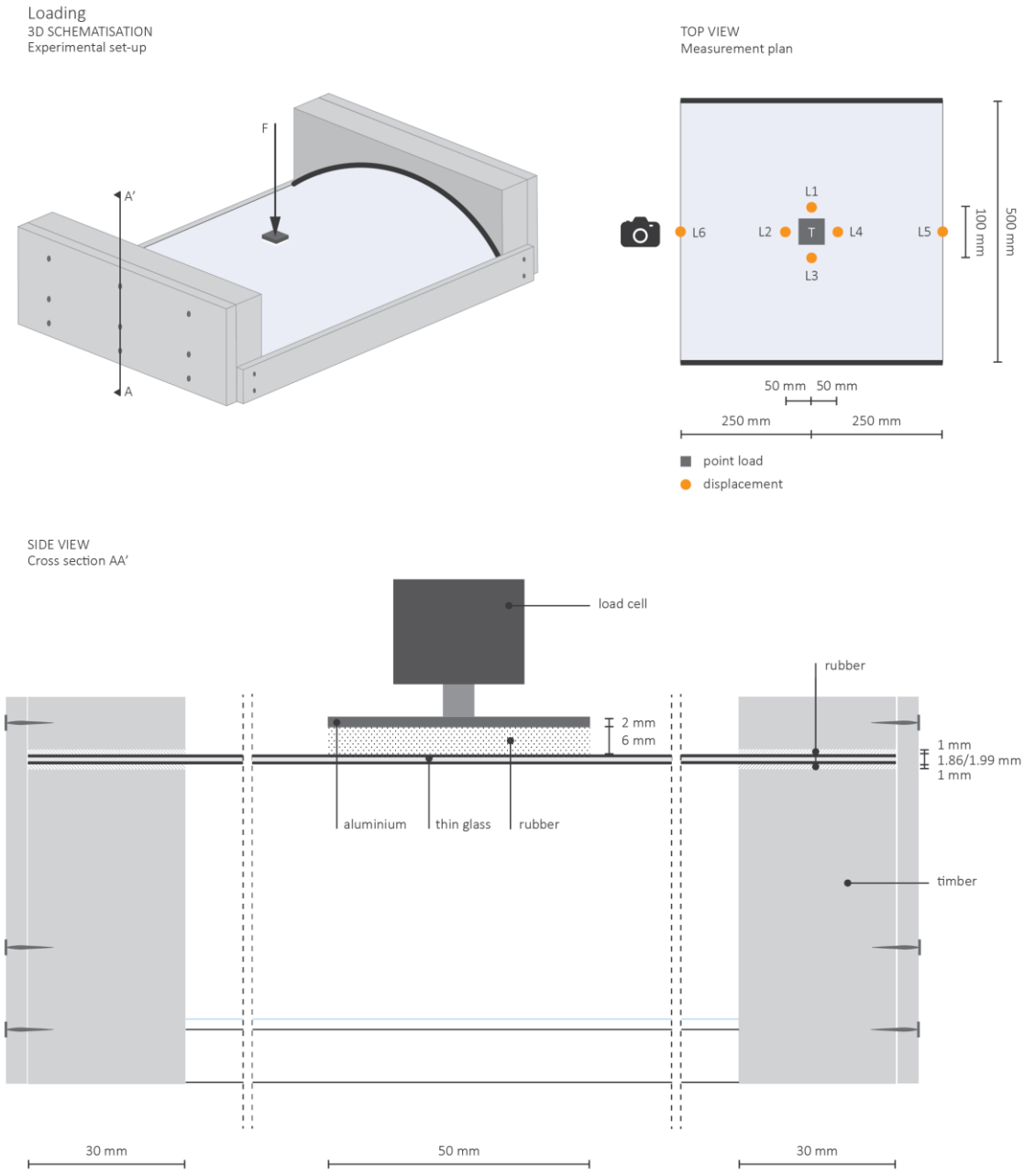

Figure 9.11: Schematisation of experimental set-up

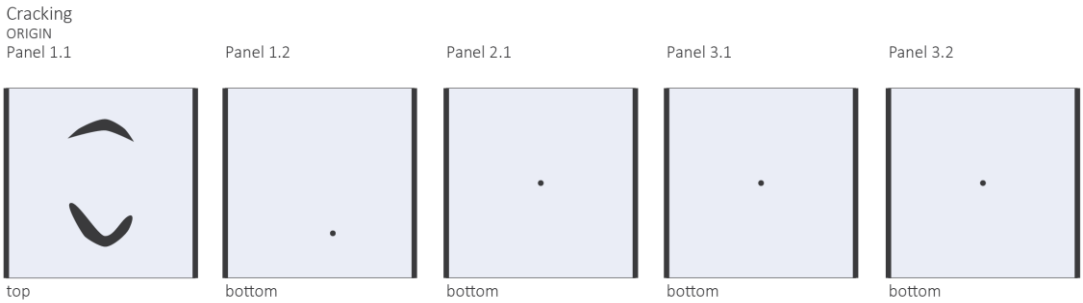

Figure 9.12: Origin of cracking and consequently failure for different panels

9.5. Discussion

This chapter discusses and compares the results from the analytical analysis at bending and the numerical and experimental analyses at bending, spring back, relaxation and loading. It must be noted that it will not be possible to reliably quantify the strength of cold bent laminated thin glass panels from these tests due to using low sample numbers.

9.5.1. Bending

A sinusoidal curvature is pursued during bending with an analytically calculated height of 99 mm from top to bottom and a corresponding span of 450 mm. The numerical model uses the principle of buckling to obtain a similar sinusoidal curvature. At this stage, the interlayer doesn't contribute to the panel and the properties are assumed to be almost zero. Geometrical nonlinearity is introduced to bend the glass sinusoidally. The height obtained from the numerical model is 97 mm. The difference between analytical and numerical results is less than 5%, which means that the results sufficiently correlate. Compared to the experimental curvature, the numerical results correlate better than the analytical results. For every manufactured panel, the height is also measured at 97 mm.

9.5.2. Spring back

Spring back is numerically captured by changing the boundary conditions of the panel and material properties of the interlayer in a new stage after bending. In the numerical model, the top of the geometry is measured at 91.73 mm for panels with SAF. In reality panel 1.1 captures a height of 90.23 mm, observed immediately after releasement from the mould. The height of panel 2.1 is measured at 86.47, but with the note that the panel was released from the mould an hour before testing. Figure 9.13 shows the panels from the second series after releasement from the mould, just before painting the geometry. Consequently, the process of relaxation already started. According to the numerical model, the height for panels with SAF after an hour of relaxation is 89.97 mm. Both panels are still within a 5% difference, which is acceptable. The loss in curvature at spring back for panel 1.1 is around 7%. The loss in curvature at an hour of relaxation for panel 2.1 is around 11%. For panels 3.1 and 3.2, the loss at spring back is around 11% and 8% respectively.

The experimental curvature of panel 3.1 and 3.2 don't follow the numerical curvature accurately due to a delay in measurement. Although the process has been adapted compared to the second series, parts of the laminated panel were stuck to the mould and had to be released without damaging the glass edges in order to measure the correct shape. Panel 3.2 could be removed from the mould by moving the panel carefully up and down. Panel 3.1 had to be removed from the mould with air pressured in between the mould and glass. Since the numerically calculated height for panels with an SG interlayer is 92.60 mm and panel 3.1 measured a height of 86.01 mm, this additional pressure could have resulted in a smaller curvature. The experimental height of panel 3.2 is 88.94 mm. To conclude, small differences between the numerical and experimental results are observed, with the numerical model consistently underestimating the spring back effect.

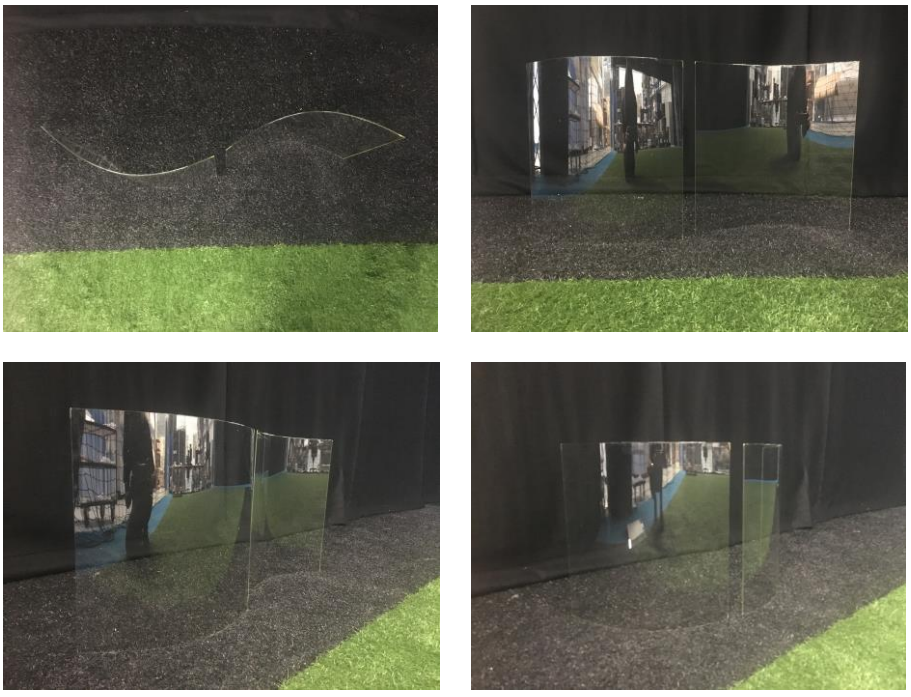

Figure 9.13: Cold bent laminated thin glass panels from series 2

9.5.3. Relaxation

To numerically capture relaxation, a linear approach is applied by introducing a new stage for different load durations. The boundary conditions remain the same, but the Young's modulus and Poisson ratio change at every stage. This method doesn't seem to be in line with the experimental results. As can be seen from Figure E.11 the numerical model consistently underestimates relaxation for panels containing a SAF and SG interlayer. The top of the geometry is numerically measured at 82.92 mm for panels with SAF, while panel 1.1 captures a height of 69 mm and panel 2.1 a height of 71 mm. For panels with SG, the top is numerically measured at 92.18 mm, while for panel 3.1 a height of 86 mm is observed and 89 mm for panel 3.2. A difference in curvature is especially noticeable with a SAF interlayer.

Many factors influence the relaxation behaviour that aren't captured in the model due to a lack of information. Only the Young's modulus and Poisson ratio are known for a certain load duration and temperature. The manufacturer however doesn't state what kind of load and magnitude the interlayer is subjected to in order to obtain the values from Appendix A.6 and Appendix A.7. Furthermore, the values used for the numerical analysis are from temperatures at 30 °C at certain time intervals given by the manufacturer. Thus, numerical results at only a day or a month could be obtained while the panels are measured at two, three, five of seven weeks. Assuming a constant temperature of 30 °C and constant loading, would seem as a conservative approach. But as it turns out, the numerical model still underestimates relaxation effects. Another method has been tried to narrow the gap. This method applies the same approach as before by introducing a new stage and changing the properties of the interlayer, but instead of using the values at constant temperatures, the temperature pattern during relaxation is included. According to Dutch weather stations the temperature fluctuated between 10-30 °C. The Young's modulus and Poisson ratio corresponding to these temperatures aren't exact, because the table only includes rounded temperatures. This could be important for a SAF interlayer, because the stiffness decreases significantly at higher temperatures and higher load duration. The stiffness for SG is rather constant, except for extreme conditions. Nevertheless, the model didn't come close to the experimental results, but did show that the history of stiffness is important and has an impact on the current result. Imagine two different cycles of which one starts at room temperature, changes to 50 degrees, then cools back to room temperature. The other cycle start at room temperature, heats up to 30 degrees and comes back down to room temperature. Both cases end at room temperature, but the output is different. In other words, the loading and temperature history of the interlayer define its creeping behaviour. It could also be that not only loading or temperature are variables that govern the difference in both the numerical and experimental model, but other variables control the behaviour of the cold bent laminate thin glass panel as well. Take for example the influence of different curvatures, interlayer thickness, tolerances or other physical properties. Basically, the input parameters for this problem are still unknown and need further investigation to properly model the relaxation stage.

One of the conclusions that can be drawn from this investigation is that a large relaxation of the curve can be observed for a cold bent laminated thin glass panel with SAF, but that it seems to come to a standstill. The geometries measured at two, five and seven weeks for panel 1.1 are the same. The same applies to the curvatures of panel 2.1 at three and five weeks. The loss in curvature from bending to stand still for panel 1.1 is around 28%. This loss for panel 2.1 is similar from bending to standstill and is measured to be around 27%. This standstill is not accounted for in the numerical model. The series with SG laminates doesn't even seem to relax after spring back. The curvature measured at two weeks is the same as at spring back. For panels 3.1 and 3.2, the loss in curvature from bending to two weeks of relaxation is around 11% and 8% respectively. The loss in curvature from spring back to two weeks of relaxation is for both panels close to zero. In terms of maintaining its shape, a SG laminate seems to behave better than a SAF laminate. To conclude, the numerical model does show that panels with SAF relax more than panels with a SG. However, it does not capture the magnitude and standstill of panels with SAF or SG.

9.5.4. Loading

In the numerical model, the properties of the interlayer are estimated to be at a room temperature of 20 °C and loaded for a month. Just as for relaxation, this estimation doesn't seem to be correct and needs to be further investigated. However, the numerical model consistently underestimates the curvature at relaxation as if the stiffness of the interlayer is lower, while the model underestimates structural behaviour during loading as if the stiffness is higher. The values given by the interlayer manufacturer don't say anything about what kind of load is applied or the load intensity. Experimentally, panel 1.2 failed at 0.5 kN with a maximum displacement of around 17 mm. Panel 1.1 failed at 4.9 kN with a maximum displacement of around 42 mm, panel 2.1 failed at 4.1 kN with a maximum displacement of around 30 mm. For the panels with SG as the interlayer, panel 3.1 failed at 6 kN with a maximum displacement of around 32 mm and panels 3.2 failed at 5.8 kN with a maximum displacement of around 30 mm. For comparison, Dillon (2002) investigated human loading on barriers and concluded that a single point load due to a person pushing on glass is only 0.3 kN on an area of 50x50 mm. Of the activities examined, kicking produced the largest load equivalent to 3 kN. Although kicking produces a peak load in a short time interval and is therefore different from the load applied in this research, these loads are well within the values obtained from experimental analyses. Furthermore, a slight drop near 6 kN in the graph of panel 3.1 where the supports failed and the graph of panel 3.2 indicates the machine reaching its weight limit of 600 kg (Figure E.26). Before reaching this value the table moves upwards, pushing against a rigid block. From this value the table needs to push the block upwards as well, explaining the shift in measured loading.

From the numerical model, it was expected that the panel would behave symmetrically, resulting in similar deflections at L1=L3, L2=L4 and L5=L6. These values for the experimental model differ a little due to unsymmetrically placement of the lasers governed by the experimental set-up. Still, panel 1.2 shows equal sagging at T and L1 to L4 around the applied load. Points L5 and L6 move equally downward as well. The deformation of the other, more curved panels is a bit different. Around the applied load, a sagging pattern close to a circle arises. Both the numerical and experimental model show that points L1 to L4 move downward and change its slope at a certain load, showing a change in stiffness. Points L5 and L6 move upward and also show a changing slope in the numerical and experimental model. During the experiments, these points start moving down again at a certain load. This isn't captured in the numerical model.

The numerical models generally deflect more and fail at far lower loads if a tensile bending stress of 260 MPa is assumed. This conservative value is given by the manufacturer, the tensile bending strength of thin glass tends to be higher according to recent studies at Delft University of Technology. In terms of the stiffness, it can be concluded that the experiments estimate the panels with a SAF interlayer to be 5 times stiffer than the numerical model and the panels with a SG interlayer to be 2 times stiffer than the numerical model. In other words, the numerical model is too conservative in terms of the output values, but it does provide a better insight in the structural behaviour of cold bent laminated thin glass panels. Particularly interesting is the shift in governing stresses, both shown in numerical and experimental models. As described in chapter 9.3.4, the position of governing principal stresses in panels with a SAF interlayer change at a certain load (Figure E.15 and Figure E.16). The highest stress goes from the bottom node at the top of the lower ply to an area in between the top and unsupported edge at the upper ply. Experimentally, panel 1.1 failed exactly at this position at a higher load than panel 2.1. Panel 2.1 and the panels from series three all started cracking from the bottom node at the top of the lower ply. Figure 9.14 shows the similarities in structural behaviour between the numerical and experimental models. The difference in output is governed by the fact that the patterns for the numerical models are obtained at a lower applied point load than the experimental patterns.

It seems that the failure mode starting at the bottom ply should occur first, but if this somehow doesn't happen, the failure mode shifts to the second failure mode. An explanation for this phenomenon could be that the lower ply of panel 1.1 had a higher tensile bending strength than the upper ply and didn't crack at a given load. Loading continued until the upper ply failed with the consequence of glass spalling. The latter failure mode is concerning in terms of safety and should be further investigated. The change in position of highest stresses wasn't numerically captured for SG panels due to divergence, but could be a problem at higher loads as well. The numerical model also shows higher stresses at supports. Although not observed during experiments, this could be a third failure mode. To conclude, the numerical model does predict structural behaviour for SAF and SG laminated panels well, but cannot be used to obtain acceptable output values. Further investigation into the interlayer needs to be performed in order to find adequate input variables.

9.5.5. Conclusion

According to Eurocode EN16612, the major influences on the bending strength and load resistance of glass are the rate and duration of loading, area of surface stressed in tension and the surface condition. The bending strength and load resistance of laminated glass is also influenced by the interlayer properties, rate and duration of loading giving rise to creep of the interlayer and temperature affecting the stiffness of the interlayer. In the case of cold bent laminated thin glass panels, all of these factors plus the influence of different curvatures should be taken into account. Not everything has been explored during this research. The results from the numerical and experimental analysis show that these factors certainly have an influence, but it is not known yet to what extent. It is therefore recommended to further investigate the principle of cold bent laminated thin glass. Focus should be towards factors influencing the interlayer and different failure modes. From the analyses, it can be concluded that a SG interlayer performs better in terms of its stiffness during relaxation and loading. However, due to a higher curvature of panels with a SG interlayer at loading, the stiffness of the panel is also higher and may have influenced the stiffness as well. Note that the studies are performed on a small scale and cannot simply be extrapolated to full scale applications. Therefore, it is necessary to perform an investigation on full scale panels.

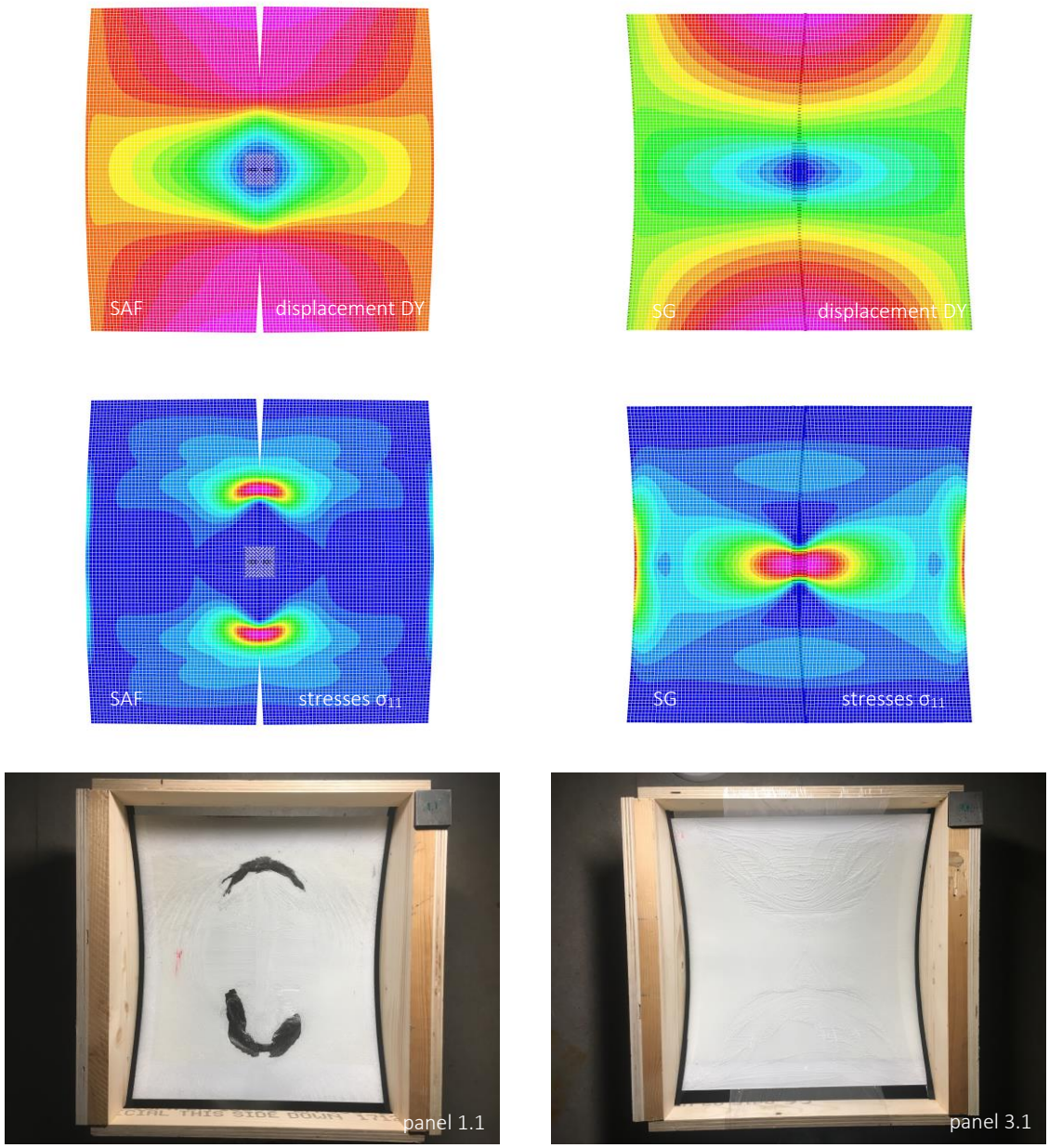

Figure 9.14: Symmetrically combined numerical results at 400 N and experimental crack patterns at failure for panels with an interlayer of SAF (left) and SG (right)

10. Final design

Reference models are regularly used to validate newly designed innovations. Comparable existing curved glass structures can be found in the Casa di Música in Porto and the MAS museum in Antwerp. Both use hot bent float glass for their façades and follow a constant curvature. Substituting float glass for thin glass in these structures doesn't necessarily mean the structure performs better. Thin glass has other characteristics than float glass and, as mentioned, thin glass will only excel in areas where float glass doesn't work. Thin glass as a cold bent free form curved element is a new principle and can't be compared to existing structures. The aim of this thesis is to use cold bent laminated aluminosilicate glass as a more free formed and lighter alternative. Therefore, the main focus will be to demonstrate to what extend thin glass can be used and show the public what this material is capable of. So instead of limiting the investigation by replacing float glass in existing structures for thin glass, a new design for a small pavilion is made.

10.1. Pavilion

Originally designed for special occasions, pavilions can be described as temporary or permanent architectural open structures, situated in a public area to invite people to come in and spend some time. They allow the public to comment on architecture and interact with the discipline. Pavilions are the perfect medium for exploring new architectural ideas, methods and materials, without the limitations of established functions and their economics. Take for example the Serpentine Gallery Pavilion. Every year they commission a temporary pavilion by a leading architect that is completed within six months and open for the public for three months in Hyde Park central London. Although the pavilions were constructed and designed as temporary structures, a number of them have been reconstructed in different locations and times. Their nomadic nature results in some common characteristics such as flexible use, standardization of each element and easy transportation, construction and dismantling.

Since there is no exact definition of what a pavilion exactly is, or what the limitations and the boundaries are, architects redefine and set up their own rules while designing pavilions by analysing the space and combining new materials with changing tendencies in architecture to create an innovative experience. They have the potential to set up new techniques in the production of architecture, pioneering of new architectural generation processes, and directing the exploration and experiencing of new concepts, method and materials. The definition of the term pavilion changes with respect to the architect's perception (Tunçbilek, 2014). Therefore, a pavilion might be used as a shelter, meeting point, cafe, small theatre or sports building. In other words, pavilions provide the opportunity to present radical ideas and a creative laboratory for testing bold innovations in design and building technology. They are the perfect instrument to demonstrate what cold bent laminated thin glass can do with its geometrical form.

10.1.1. Geographical location

If such a pavilion would be build, assumptions are made that the geographical location is limited to an area at the Technical University of Delft in the Netherlands.

10.1.2. Dimension

Pavilions are designed to be prototype buildings, explaining the smaller size of the structure. An area of 10x10 m^2 is reserved to build the pavilion on.

10.1.3. Geometry

In the case of applying thin glass as a new structural material, focus is directed towards a load-bearing element that only withstands wind loads. As discussed in chapter 8.3, only top and bottom boundaries are applied of which the upper part is connected to the roof, the bottom part is supported by the foundation and the side boundaries are support free. The pavilion is therefore designed as a free standing concrete structure where a horizontal roof is carried by columns. Since the cold bent laminated thin glass panels are not connected, they don't function as a façade. The panels are simply designed to play with the surrounding space in a free formed way (Figure 10.2).

10.2. Thin glass panels

The glass type that suits a cold bent laminated thin glass pavilion best is Falcon glass from AGC. Although the sheets have less strength, they are cheaper, available in larger sizes and easier to obtain as they are produced in Belgium (Appendix A.5). Falcon glass is especially created to bridge the gap between soda lime and aluminosilicate glasses in the most cost-efficient way and tries to expand its market to architectural applications. This chapter focusses on the dimension of the panels, composition, curvature and connections.

10.2.1. Dimension

Falcon glass comes in different sizes and corresponding thicknesses as illustrated in Figure 10.1. All panels are produced as flat elements and have the same length but differ in width depending on the thickness. The width doesn't differ that much and isn't a limiting factor when using the panes in an architectural pavilion. In terms of the thickness, thinner glass provides more bendable panes, but also decreases the stiffness and increases deflections. It also may not be needed to bend the glass to a very small radius. Float glass can be cold bent to a radius of approximately 1 m nowadays, so as long thin glass can be held beneath that value, the material has a major advantage over float glass. Although the substrate after production is 3120 mm long, the actual length is limited by the chemical tempering batch to a maximum of 2500 mm.

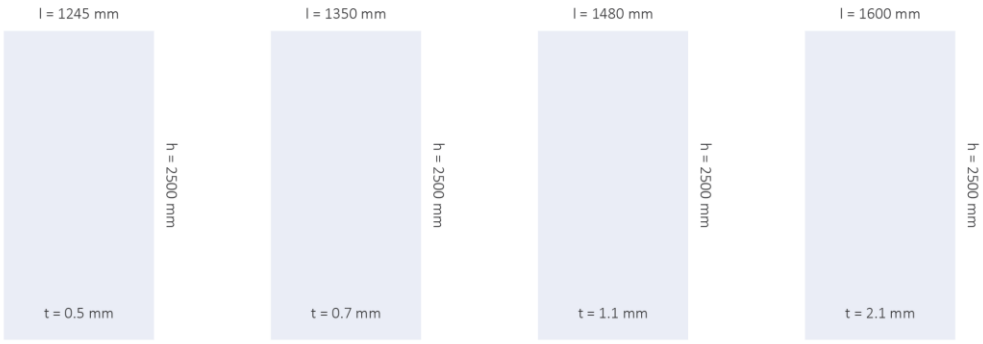

Figure 10.1: Different Falcon glass sheet sizes with corresponding thicknesses

10.2.2. Composition

Saflex DG41 and SentryGlas are both viscoelastic materials with the physical properties strongly depending on temperature and load duration. As seen from the experiments, the relaxation phase causes some of the panels to deform significantly. After releasement from the mould, the SAF panels experience a higher loss of curvature in two weeks compared to the panels produced with SG. In fact, the panels with an interlayer of SG do not seem to relax at all after spring back. However, when measuring the geometry of the SAF panels at 5 weeks, they seem to have come to a standstill. Nevertheless, the deformation can be larger in more extreme conditions for both interlayers. Be aware of this phenomenon when designing for different typologies and areas. According to the experiments done concerning relaxation and loading, SG also behaves better in terms of stiffness. It is therefore recommended to use an interlayer of SentryGlas to produce cold bent laminated thin glass panels. The composition of these panels used to design the pavilion will therefore consists of two plies of 0.7 mm Falcon glass and one ply of 0.89 mm thick SentryGlas.

10.2.3. Curvature

As mentioned in chapter 8.2, single curved panels are preferred in the case of cold ben laminated thin glass due to their ability to enable the structure to transfer long term loads purely by axial membrane forces and minimises constant bending moments. In chapter 8.2, a set of different curvatures is proposed to introduce a range in which the thin glass can bend. These curvatures and their corresponding minimum and maximum variables for different sheets of Falcon glass are analytically calculated. The stress induced by production, create cold bending and spring back effect stresses. As expected, a Falcon glass sheet with a thickness of 2.1 mm quickly introduces high stresses during bending, while a sheet with a thickness of 0.5 mm will bent further at lower stresses. However, a thicker sheet of Falcon glass does enables a larger moment of inertia and therefore a stiffer panel. Falcon glass with a thickness of 0.7 mm and dimensions 1350x2500 mm is chosen to provide a balance between stresses and stiffness.

Among the considered curvatures, even though it introduces a larger bending stress at the top, the optimal configuration is sinusoidal, as it provides the smoothest distribution of shear and therefore the lowest risk of delamination. The difference in curvature might be small, but the advantages are noteworthy. The sinusoidal spans used in this design are set to 900, 1000, 1100 and 1200 to minimise the number of different panels and necessary moulds.

10.2.4. Connections

As described before, the designed pavilion will consist of a free standing structure with a horizontal roof carried by columns and cold bent laminated thin glass panels simply designed to play with the surrounding space. The upper part of the thin glass panel is connected to the roof, the bottom part is supported by the foundation and the side boundaries are support free (Figure 10.2). Horizontal connections could be necessary to function as additional supports if the requirements for the deflections are not met by only using vertical supports. Research into horizontal connections is not covered by this thesis.

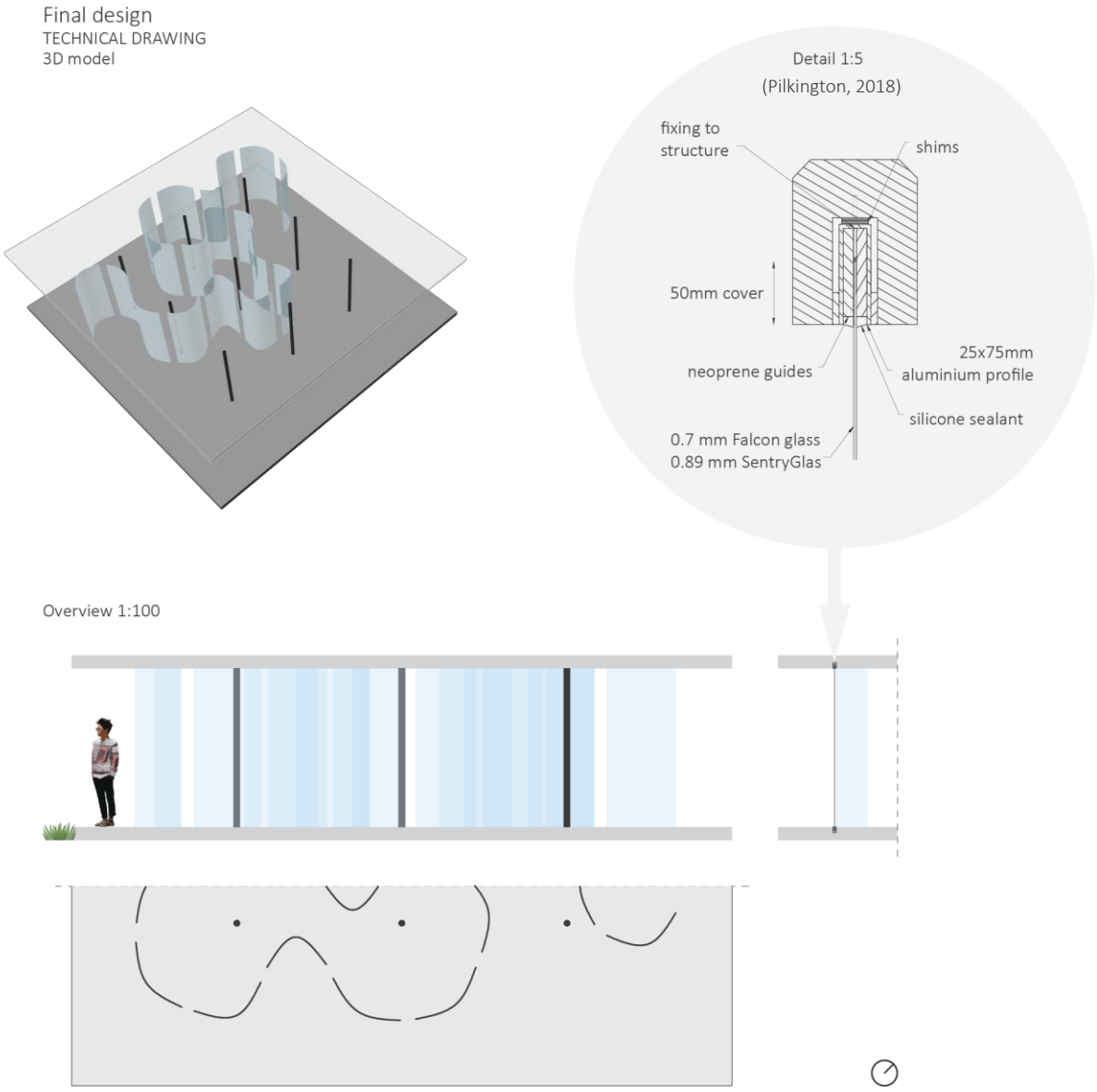

Figure 10.2: (3D) Overview and details of final design for pavilion using cold bent laminated Falcon glass

10.3. Structural behaviour

This chapter covers the structural behaviour of cold bent laminated thin glass panels on a full scale. Note that the numerical model isn't validated and the exact magnitude cannot be extracted from this model, but it does give an indication of the behaviour of the panel. From the four proposed panels, it has been chosen to investigate the panel with a span of 1200 mm. Based on its geometry, this configuration is expected to deflect most during loading. Not the stresses, but the deflections are anticipated to govern the design. The same properties as for the numerical analyses are used during bending, spring back and relaxation. At loading, a wind load instead of a point load is applied. As explained before, a convex shape is weaker and deforms easier than a concave shape. Therefore, the worst case scenario of wind loading is applied in a convex matter. The tensile bending strength of Falcon glass is assumed to be 200 MPa.

10.3.1. Bending

The bending process is modelled exactly the same as for the experiments by using a two dimensional coordinate system with nodes and plates. This time, the model is made up of two layers of thin glass with a thickness of 0.7 mm and an interlayer of 0.89 mm corresponding to SG. Due to the larger size of the panel, the choice is made to obtain a mesh ratio of 1:71. Symmetry is also used, so each layer is divided into two elements vertically and forty-five elements horizontally, resulting in a mesh of 45x2 elements per layer. The system is solved using geometrical nonlinearity and displacement control until a displacement of 75 mm. Thus, the numerical model will span B=1200 mm due to symmetry. The maximum tensile bending stress is σ_{11}=40.93 MPa at the top of both thin glass plies (Appendix F.2.4).

10.3.2. Spring back

Spring back is captured by introducing a new stage where properties and supports change. These properties remain the same as for the numerical model from chapter 9.3. The top goes down from 275.86 mm at bending to 259.45 mm at spring back in a vertical direction. The top of the lower thin glass ply contains more stresses at spring back than at the end of bending due to a bending moment in opposite direction. The highest principal stress goes from σ_{11}=40.93 MPa to σ_{11}=44.11 MPa (Appendix F.2.5).

10.3.3. Relaxation

To capture the physical nonlinearity of the interlayer, a linear approach is applied by introducing a new stage for different load durations. The boundary conditions remain the same as for spring back, but the Young's modulus and Poisson ratio change at every stage. The values are kept the same as for the previous numerical model. The top of the geometry changes from 259.45 mm at spring back to 259.28 mm at a month of loading in temperatures of 30 °C. The accompanying stress goes from σ_{11}=44.11 MPa to σ_{11}=44.09 MPa (Appendix F.2.6). Previously, an extra stage is added to adapt the 2D numerical model to the experimental results at the end of relaxation. The same is done for this analysis. At this stage, the top of the geometry is 257.04 mm and the accompanying stress goes to σ_{11}=43.71 MPa.

10.3.4. Loading

The plate elements are extruded into z-direction, perpendicular to their face. Symmetry conditions can also be applied here, so the extrusion is only 1250 mm. A full size panel is 1350x2500 mm and scaled down to 675x1250 mm with symmetry conditions. The bricks are divided into 50 elements in z-directions, resulting in a mesh of 45x2x50 elements per layer. The boundary conditions and properties of the interlayer remain the same as for the previous conducted numerical analysis. Due to larger expected deformations for convex shapes, the wind load is applied as a face load normal to its surface at the convex side of the panel (Figure F.2). The given value is 0.25/TA with load factors included in the increments.

The wind actions are calculated according to the general Dutch standard NEN 1991 and concluded to be 3.14 kN on an area of 1.35x2.5 m (Appendix F.1). From the results at a load of 3.2 kN it can be seen that the highest stress accumulates at the supported edge. With a stress of 81.90 MPa, this stress is well below the maximum stress of 200 MPa, even with stresses added from production. However, the edges of a glass panel are more prone to cracking than the surface. The edge strength completely depends on the edge quality, which is determined by flaws introduced by cutting the glass. As mentioned in chapter 3.4, these flaws cause stress concentrations and are the starting point for crack propagation.

A distributed wind load results in the top of the panel to move upwards, while the unsupported edge goes down. The latter is governing with a deflection of 34.41 mm. According to EN16612, there is no specific requirement of glass to limit the deflection of glass under load. However, consideration should be given to ensure the glass is not excessively flexible when subjected to applied loads, as this can cause alarm to users. Therefore, the deflections shall be limited to:

$$v; max = \frac{h}{65} = \frac{2500}{65} = 38.46\, mm \qquad (10.1)$$

The deflection obtained from the numerical model is within this value. Actual deflections may be even lower, because the numerical model tends to be conservative. It seems that no horizontal connections are necessary to minimise deflections. However, the numerical model isn't validated and the exact magnitude cannot be extracted from this model. No real conclusions can be drawn in terms of large scale applicability and the model can only give an indication of the structural behaviour of cold bent laminated thin glass panels.

Figure 10.3: Visualisation for pavilion using cold bent laminated Falcon glass

FINAL REMARKS

11. Conclusion

This chapter presents the conclusions drawn from research regarding the applicability of chemically tempered thin glass in architectural applications. During the investigation, focus was directed towards cold bent laminated thin glass panels. First, a general conclusion is given on the process of how to transform thin glass sheets into cold bent laminated panels. Hereafter, the research questions are answered as presented in chapter 2.2.

11.1. General

How thin chemically tempered aluminosilicate glass in combination with a stiffening material and/or geometry is produced, wasn't included in the research questions, simply because at the time of formulating the questions the stiffening principle was not known. Thereby, the importance of this process also wasn't known. For this reason, an additional chapter is developed to draw conclusions and create a link to a larger scale on the production process of cold bent laminated thin glass panels.

11.1.1. Production process

An adjustable mould is manufactured in order to cold bent thin glass sheets into a sinusoidal curvature using the buckling principle. Aluminium is the main material of this mould due to sufficient resistance against a high temperature and pressure in the autoclave. By simply changing the distance between the supports, only one mould is needed to provide different sinusoidal curvatures. Hereby saving material, labour and cost compared to static moulds produced for only a single curvature. In this case, a larger aluminium plate is used to prevent the glass from touching the bars located at each side during bending and to use the additional space to attach the vacuum bag onto the aluminium plate. The desired curvature can simply be obtained by measuring the distance B between the supports. Figure E.19 shows the accuracy of the sinusoidal curvature into the aluminium plate. Improvements could be made by perforating this plate and wrapping vacuum foil all around it to allow for better vacuum during bending and lamination. Also, the curvature at a quarter and threequarters is larger than at the ends. This could be revised, since the panel exactly starts at these curved points, assuming that bent laminated glass panels are more prone to delamination at more curved ends. Nevertheless, no delamination occurred during testing, and it can be concluded that this principle to create a sinusoidal mould works well.

Flaws seem to govern cold bent laminated thin glass panels, as shown in panel 1.2 and panel 2.2. Thus, it is highly recommended to thoroughly check the thin glass sheets for flaws while preparing them for bending. By choosing vacuum bagging as the principle to bent two plies of thin glass with an interlayer in between, the process of bending is controlled and entrapped air is released. At first, research into the stages of bending and spring back demanded the mould and thin glass build-ups to be manufactured a certain way. Due to a loss in vacuum in one of the panels during the lamination process of the first series, a few improvements were made and adopted in the second and third series. For example, yellow sealing tape, resistant to higher temperatures, instead of black sealing tape needed to be used. Just as replacing higher temperature resistant foil for lower temperature resistant foil, as it behaves less stiff and can deform more easily around the corners. Additionally, it is recommended to leave enough space between the breeder blanket and glass due to the interlayer becoming viscous during lamination and getting stuck to the breeder blanket. This is easily solved by enlarging the aluminium plate into the direction perpendicular to its curvature. Although preparing the vacuum bagging is time consuming, successful lamination of the second and third series resulted in the conclusion that this process has the potential to be translated to large scale production. Saflex DG41 interlayers were recommended by AGC due to lower costs, better optical properties and easier manufacturing processes. However, no noticeable differences in manufacturing with a SAF or SG interlayer were observed.

11.2. Research question

The following subchapters present the research questions set at the beginning of this thesis. First, the sub questions are answered to ultimately answer the main research question.

11.2.1. Sub questions

What kind of stiffening material and/or geometry can be used to create a load-bearing structure out of thin chemically tempered aluminosilicate glass panes?

Chapter 5 introduces three different ways to stiffen thin glass of which an overview of the design configurations is shown in Figure 7.1. Thin glass can be stiffened by using composite panels with transparent or semi-transparent cores. Laminating the glass to other materials is a means to add out-of-plane stiffness by adding material thickness. The second option of stiffening thin glass is to apply a curvature by assembly or lamination. Shaping a curved surface is a means to add global out-of-plane stiffness through geometrical form. The third option involves tensioning sheets of thin glass by following the principles of membrane structures, pneumatic structures of cable systems. The material is hereby treated as fabric glass and is a means to add out-of-plane stiffness through membrane action (Lambert & O'Callaghan, 2013).

A rating system is created to determine which design configurations has the most potential to be further explored (Appendix B.3). Boundaries and demands are translated into requirements concerning optical quality, geometry, mechanical properties, sustainability and economic properties. This list is not binding, but gives an indication on the performances of each design configuration. Every principle has its advantages and disadvantages and could be further explored. Nevertheless, the results indicate that a composite panel combining float glass with thin glass, a composite panel combining polymers with thin glass, a curved panel with only thin glass and a curved panel combining polymers with thin glass are the most promising concepts. The most important demands concern larger transparent panels, minimal weight, more free formed architecture and high thermal insulation. Cold bending and laminating sheets of thin glass encourages transparency, lightweight structures and free formed architecture. Furthermore, the flexible nature of thin glass is an important and promising characteristic and shouldn't be compromised by introducing stiffening techniques. However, applying thin glass as load-bearing structures, deflections become governing and should be minimised to prevent causing alarm to users. Cold bent laminated thin glass panels use this flexibility to create a stiffer structure and therefore seems to be the perfect configuration to further explore.

What are the physical and structural properties of thin chemically tempered aluminosilicate glass and the chosen stiffening material and/or geometry?
Due to better tempering conditions, an aluminosilicate glass mixture is used to produce thin glass. This mixture consists of silica sand (SiO_2), soda (Na_2O), lime (CaO), magnesia (MgO), alumina (Al_2O_3) and boron-oxide (B_2O_3). The focus is specifically directed to alkali aluminosilicate glasses since high alkali content prepares the glass better for ion exchange and thus improves the surface compressive strength significantly. This type of glass has a high transformation temperature and outstanding mechanical properties, such as hardness and scratch behaviour (Schott, 2014). The optical properties depend on the glass thickness, chemical composition, applied coatings and the way the glass is fabricated. Especially the minimal thickness causes thin glass to be clear, lightweight and in combination with chemical tempering, flexible but still very strong.

Just as for float glass, no warning is given before failure. Whether or not fracture will occur depends on the presence of flaws, the stress level and the duration of the load. As stated in chapter 3.3.1, the core doesn't contain flaws, but the surface and edges of the glass do and may arise from the production, handling or from environmental processes. During the production process, almost all glass panels are cut. These cuts create severe flaws that make the edges of the panel weaker than the surface. As flaws do not grow or fail in compression, the compressive strength is much larger than the tensile strength (Haldimann et al., 2008). Therefore, exceeding the tensile strength of glass will cause the glass pane to break. For this research the tensile bending strength, as recommended by the manufacturer, was set to 260 MPa. The cold bent laminated panels are bent to a value well below the recommended tensile bending strength to allow for an increase in stress at spring back and loading. The applied curvature during bending is sinusoidal because it provides the smoothest distribution of shear and therefore the least risk of delamination at the ends. From the moment the panels are released from their mould, a certain spring back can be observed causing higher stresses at the top of the lower ply. Afterwards the relaxation phase is initiated. During this stage, the panels are under a constant load due to thin glass wanting to go back to its original flat shape. From the experiments, it can be concluded that the panels with a SAF interlayer relax significantly, but seem to come to a standstill after a certain period. The loss in curvature from bending to stand still for panel 1.1 is around 28%. This loss for panel 2.1 is similar from bending to standstill and is measured to be around 27%. The panels with a SG interlayer do not seem to relax after spring back. The measured geometries of this series are more or less the same at spring back and after two weeks of relaxation. For panels 3.1 and 3.2, the loss in curvature from bending to two weeks of relaxation is around 11% and 8% respectively. The loss in curvature from spring back to two weeks of relaxation is for both panels close to zero. It is important to note that the assumptions regarding the development of the interlayer during relaxation and loading of cold bent laminated thin glass panels seem to be incorrect. The viscosity and properties of the interlayer during these stages should therefore be further investigated.

Glass doesn't yield plastically, meaning that the stresses are not being reduced through stress redistribution, and exhibits brittle failure. The fragmentation pattern depends on the generated stresses. In general, a higher degree of prestressing results in finer dicing at failure. Chemically tempered thin glass has a residual stress profile, whose case depth, although still shallow in terms of micrometres, is significant in terms of percentage of the overall glass thickness. The failure pattern then depends on the stresses introduced in thin glass sheets. Flat thin glass normally fails into large pieces, while bent thin glass fails into smaller pieces due to the introduced bending stresses. The latter pattern could be seen from the experiments. A fragmentation size of less than a millimetre to several centimetres was observed. Lamination prevents the glass from dropping, but a small fracture patterns causes the glass pane to have almost no load-bearing capacity after failure.

What is the structural behaviour of thin chemically tempered aluminosilicate glass panels for the chosen principle when subjected to a point load or a static distributed load?
Numerical and experimental analyses are performed on a smaller scale panel for a point load applied in the middle of the upper bent surface. The curved edges are simply supported, while the straight edges are able to move freely. From these analyses, it can be concluded that the middle area moves downward in a circular manner for panels with an interlayer of SAF and SG. Points in the middle of the unsupported edges start by moving upward, but change direction at a certain load level. During the experiments, large deflections are measured, but at rather high point load. Panels with SAF interlayers could reach loads up to 4.9 kN with a maximum deflection of 42 mm. Panels with a SG interlayer could reach a point load up to 6.0 kN with maximum deflections of 32 mm. Panels with a SAF interlayer seem to behave less stiff compared to panels with a SG interlayer. However, due to a higher curvature of panels with a SG interlayer at loading, the stiffness of the panel is also higher and may have influenced the stiffness as well. Particularly interesting is the shift in governing stresses, both shown in numerical and experimental models. As described in chapter 9.3.4, the position of governing principal stresses in panels with a SAF interlayer change at a certain load (Figure E.15 and Figure E.16). The highest stress goes from the bottom node at the top of the lower ply to an area in between the top and unsupported edge at the upper ply. Experimentally, one of the panels failed exactly at this position at a higher load than a panel with a similar geometry and build-up. The other panel fabricated with SAF and the panels fabricated with SG failed in a similar matter at the first mentioned location, namely at the bottom node at the top of the lower ply.

The numerical models could not be validated due to cold bent laminated panels generally deflecting more and failing at far lower loads if a tensile bending stress of 260 MPa is assumed. In terms of the stiffness, it can be concluded that the experiments estimate the panels with a SAF interlayer to be 5 times stiffer than the numerical model and the panels with a SG interlayer to be 2 times stiffer than the numerical model. It seems that the assumptions made concerning the material properties of the interlayer and tensile bending strength of thin glass are conservative and should be further investigated. It does however provide a better insight in the structural behaviour of cold bent laminated thin glass panels. Therefore, an additional analysis is performed into the effect of distributed loads representing wind loads on larger panels with an SG interlayer. From the results, it can be seen that the highest stress accumulates at the supported edge. This stress is well below the maximum stress, even with stresses added from production. A distributed wind load causes the top of the panel to move upwards, while the unsupported edges go down. The latter is governing with a deflection of 34.41 mm. According to EN16612, this is still in line with the maximum allowed deformations.

How can safety be guaranteed when designing with thin chemically tempered aluminosilicate glass?
Lamination normally ensures a certain degree of safety. However, different cracking patterns are observed during the experiments with all of the examined panels failing with a loud bang due to high releasement of stresses (Figure E.27). One of the panels resulted in failure by spalling of the top layer. The upper ply cracked and spalled at a specific region of the panel, similar to the shift in stresses from the top of the bottom ply to the middle of the upper ply. Except from this region, the overall panel remained intact. A close-up shows that thin glass is visible rather than the interlayer (Figure E.27). Chapter 4.4.1 already briefly touched the topic of frangibility, a failure mode where the centre tension created by ion exchange results in spalling. The remaining panels failed from accumulating stresses in the middle in line with the applied point load. This load caused the panel to deform equivalent to a circle in the middle. The direction differs at the area just around this circle, explaining the sudden change in crack pattern. No spalling was observed and the panels remained intact.

It seems that the failure mode starting at the bottom ply should occur first, but if this somehow doesn't happen, the failure mode shifts to the second failure mode. An explanation for this phenomenon could be that the lower ply had a higher tensile bending strength than the upper ply and didn't crack at a given load. Loading continued until the upper ply failed with the consequence of glass spalling. The latter failure mode is concerning in terms of safety and, in combination with a high fragmentation observed in all the panels, must be extensively investigated. Nevertheless, only one sheet broke for every panel, allowing the panel to remain its shape after failure due to lamination. Small cracking noises suggest that all the panels continued to crack for a while after removing the load. Transparent coatings could be added to prevent the glass from spalling or splintering and thereby reducing the risk of injuries. No delamination is observed, even after a few days.

11.2.2. Main question

To what extend can thin chemically tempered aluminosilicate glass panes be applied on an architectural scale as a load-bearing element to create a structurally safe and transparent panel?
Thin chemically tempered aluminosilicate glass definitely has the potential to be applied as a load-bearing element on an architectural scale. The architectural scale in this research is restricted to glass as a load-bearing element in the marine or building industry. Several configurations are proposed that all could benefit from further research. While thin glass embraces the characteristic of being a rather flexible material, these configurations focus on stiffening principles due to the industries mainly being governed by loads and deflections. It is the composition and thinness that give thin glass its distinctive properties of being lightweight, optically outstanding and a high tensile bending strength. The choice was made to further investigate single cold bent laminated panels in order to use thin glass to its full potential by adding stiffness through bending.

Cold bending by lamination creates a completely transparent panel that can be adopted in a free formed façade. The advantage over cold bending float glass, is that thin glass can bent to a higher curvature, is more lightweight and has better optical properties. Lamination ensures the structural safety of the panel, but certain failure modes demand more research into the applicability on a larger scale. Glass panels laminated with SG are stiffer than panels laminated with SAF during the relaxation and loading stage. It is therefore recommended to use SG as the interlayer in cold bent laminated thin glass panels. Note however that cold bent laminated thin glass panels can behave differently in more extreme environmental conditions due to the interlayer being highly sensitive to load duration and temperature. Due to relaxation, the supports for this research are manually made and adapted to every single curvature just before loading. This clearly can't be done for large scale applications. Panels with a SG interlayer seem to relax significantly less than panels with a SAF interlayer. The curvature of an SG interlayer at spring back seems to be more or less the same as for two weeks into relaxation. Therefore, if the geometry is known at spring back, supports can be made based on that curvature in order to speed up production and save cost. Sufficient tolerances need to be taken into account to prevent the panel to be forced into its position.

12. Recommendation

Applying thin chemically strengthened aluminosilicate glass in architectural applications is relatively new and especially applying cold bent laminated thin glass panels as an architectural feature has never been investigated. Evidently, this leads to the recommendation for further research into thin glass itself and thin glass as cold bent laminated panels.

12.1. Thin glass

The tensile bending strength used in this research is based on values presented by AGC, the manufacturer of Leoflex and Falcon glass. However, experiments conducted at Delft University of Technology show that much higher bending stresses can be obtained. It is therefore recommended to further investigate the tensile bending strength of thin glass to determine a representative characteristic value in order to use thin glass to its full structural potential. In addition, it is recommended to investigate the influence of flaws on the (post) breakage behaviour of thin chemically strengthened aluminosilicate glass panels. When laminated, special focus must be directed to the frangibility of the material. The centre tension created by ion exchange causes spalling, resulting in an unsafe failure mode. Lastly, to increase the market of thin glass applied on a larger scale in the marine of building industry, other design configurations as presented in this thesis could be investigated to explore their potential and applicability.

12.2. Cold bent laminated thin glass

Major influences on the bending strength and load resistance of glass are the rate and duration of loading, area of surface stressed in tension and the surface condition. The bending strength and load resistance of laminated glass is also influenced by the interlayer properties, rate and duration of loading giving rise to creep of the interlayer and temperature affecting the stiffness of the interlayer. In the case of cold bent laminated thin glass panels, all of these factors plus the influence of different curvatures should be taken into account during relaxation and loading. Due to simplified assumptions, the numerical results tend to underestimate the change in curvature during relaxation and underestimate the stiffness during loading. These findings are contradictory to one another and it is therefore highly recommended to further investigate the (long term) behaviour and influence of the interlayer on cold bent laminated panels for different curvatures.

The influence of relaxation becomes even more important once the panels are set in their supports and subjected to changing environmental conditions. The vertical supports follow the curved edges, fixing the ends of the panel with the middle of the panel still free to move. This could cause additional unwanted stress with a risk of exceeding the tensile bending strength at a lower level than estimated. Horizontal connections could be added to prevent the glass from significantly changing its curvature during relaxation and loading. Due to the thinness of thin glass, existing connections to attach float glass can't be used. It is recommended to further investigate horizontal connections between thin glass panels. Especially if one would want to design a weather and water tight façade. These horizontal connections may also need to function as additional supports if the requirements for the deflections are not met by only using vertical supports.

Lastly, the failure modes and cracking patterns for cold bent laminated thin glass should be investigated due to concerning findings related to the frangibility of the material. Both failure modes, when applying a point load, also continued to crack after unloading the panel. The question arises what this means for the experience of the user. Delamination of the panels has not been observed for the applied load case, nor for the consecutive days after failure. Furthermore, it is advised to investigate other load cases, such as impact loads, to obtain additional knowledge into the structural behaviour of cold bent laminated thin glass panels.

Bibliography

Aalco. (2005). Aluminium - Specifications, Properties, Classifications and Classes. Retrieved January 31, 2018, from https://www.azom.com/article.aspx?ArticleID=2863

Albus, J., & Robanus, S. (2014). Glas in der Architektur: Neue Entwicklungen (1). Retrieved January 15, 2018, from https://www.detail.de/artikel/glas-in-der-architektur-neue-entwicklungen-1-12954/

Berger, H. (1999). Form and function of tensile structures for permanent buildings. *Engineering Structures*, *21*, 669–679. https://doi.org/10.1016/S0141-0296(98)00022-4

Bricknell, D. (2009). *Float: Pilkington's Glass Revolution*. Crucible Books.

Bruijn, P., & Maas, N. (2005). *Innovatie in de bouw*. Delft.

Carpenter, J., & Lowings, L. (2012). Fluid Glass: design proposal. Retrieved January 22, 2018, from https://carpenterlowings.com/portfolio_page/fluid-glass/

Coenders, J. L. (2008). *CT5251: Structural Design - Special Structures*. Delft.

Dillon, P. (2002). Human loading on barriers. *Structures and Buildings*, *152*(4), 381–393.

Eames, P. C. (2008). Vacuum glazing: Current performance and future prospects. *Vacuum*, *82*(7), 717–722. https://doi.org/10.1016/j.vacuum.2007.10.017

Eastman Chemical Company. (2013). *Architectural Lamination Guide*. https://doi.org/10.1002/ejoc.201200111

Eckersley, B., & O'Callaghan, J. (2012). Corning Museum of Glass. Retrieved February 15, 2018, from https://www.eocengineers.com/project/corning-museum-of-glass-184

Eckersley, B., & O'Callaghan, J. (2018). *Personal documents*. London.

Eekhout, M. (2016). Towards 50% saving of embedded energy in glass envelops. In *Engineered Transparency* (pp. 199–211). Ernst & Sohn.

Elhedhli, S., & Merrick, R. (2012). Green supply chain network design to reduce carbon emissions. *Transportation Research Part D: Transport and Environment*, *17*(5), 370–379. https://doi.org/10.1016/j.trd.2012.02.002

Enkel, E., & Gassmann, O. (2010). Creative imitation: Exploring the case of cross-industry innovation. *R and D Management*, *Volume 40*(3), 256–270. https://doi.org/10.1111/j.1467-9310.2010.00591.x

Feijen, M., Vrouwe, I., & Thun, P. (2012). Cold-Bent Single Curved Glass; Opportunities and Challenges in Freeform Facades. In *Challenging Glass 3*. https://doi.org/10.3233/978-1-61499-061-1-829

Feng, R., Wu, Y., & Shen, S. (2007). Working Mechanism of Single-layer Cable Net Supported Glass Curtain Walls. *Advances in Structural Engineering*, *10*(2), 183–195. https://doi.org/10.1260/136943307780429734

Fildhuth, T. (2015). *Design and Monitoring of Cold Bent Lamination - Stabilised Glass*. Universität Stuttgart.

Galuppi, L., Massimiani, S., & Royer-Carfagni, G. (2014). Buckling phenomena in double curved cold-bent glass. *International Journal of Non-Linear Mechanics*, *64*, 70–84. https://doi.org/10.1016/j.ijnonlinmec.2014.03.015

Galuppi, L., & Royer-Carfagni, G. (2015). Optimal cold bending of laminated glass. *International Journal of Solids and Structures*, *67–68*, 231–243. https://doi.org/10.1016/j.ijsolstr.2015.04.023

Gomez, S., Dejneka, M. J., Ellison, A. J., & Rossington, K. R. (2011). A look at the chemical strengthening process: alkali aluminosilicate glasses vs. soda-lime glass, 61–66.

Gy, R. (2008). Ion exchange for glass strengthening. *Materials Science and Engineering B: Solid-State Materials for Advanced Technology*, *149*(2), 159–165. https://doi.org/10.1016/j.mseb.2007.11.029

Haldimann, M., Berger, E., & Bern, A. G. (2007). Diagnostic interpretation of glass failure. *Structural Engineering International*, (2), 151–158.

Haldimann, M., Luible, A., & Overend, M. (2008). *Structural Use of Glass*. International Association for Bridge and Structural Engineering.

Herwijnen, F. Van. (2008). Warm en koud gebogen glas. *Cement*, 32–37.

Hundevad, J. (2014). Super lightweight glass structures – a study. *GlassCon Global - Innovation in Glass Technology*, 324–337.

Hynd, W. C. (1984). Flat glass manufacturing processes. *Glass: Science and Technology*, *Volume 2*, 46–106.

Kloss, T. (1996). Microfloat technology to improve borosilicate flat glass potential. *Glass Technology International*, (2), 82–85.

Kozlowski, M., & Bao, M. (2016). Cold-bent laminated glass for Marine Applications. In *Engineered Transparency* (pp. 275–283). Ernst & Sohn.

Kruijs, R. (2009). De sterkte van glas (1). *Glas in Beeld*, (1), 40–42.

Kumar, R., & Buckett, J. (2002). Float Glass. *Encyclopedia of Materials: Science and Technology*, (February 2015), 1–8. https://doi.org/10.1016/B978-0-12-803581-8.01850-6

Kuraray Trosifol. (2018). *SentryGlas Ionoplast Interlayer Lamination Guide*.

Lambert, H., & O'Callaghan, J. (2013). Ultra-thin High Strength Glass Research and Potential Applications. *Glass Performance Days Finland 2013*, 95–99.

LeBourhis, E. (2014). *Glass: Mechanics and Technology, 2nd Edition*. *Glass: Mechanics and Technology, 2nd Edition*. https://doi.org/10.1002/9783527679461

Leonhard, T., Cleary, T., Moore, M., Seyler, S., & Fisher, W. K. (2015). Novel Lightweight Laminate Concept with Ultrathin Chemically Strengthened Glass for Automotive Windshields, *8*(1), 95–103. https://doi.org/10.4271/2015-01-1376

Macrelli, G. (2016). Critical evaluation of chemically strengthened glass in structural glazing applications. In *Engineered Transparency* (pp. 451–457). Ernst & Sohn.

Mainil, T. (2015). *Exploratory investigation on the cold bending of thin glass*. Ghent.

Martienssen, W., & Warlimont, H. (2005). *Springer Handbook of Condensed Matter and Materials Data*. https://doi.org/10.1007/3-540-30437-1

Molnár, G., Vigh, L. G., Stocker, G., & Dunai, L. (2012). Finite element analysis of laminated structural glass plates with polyvinyl butyral (PVB) interlayer. *Periodica Polytechnica Civil Engineering*, *56*(1), 35–42. https://doi.org/10.3311/pp.ci.2012-1.04

Mureau, M. D. A. (2017). *Thin glass; A Study on the Applicability in Greenhouse Coverings*. Delft University of Technology, Delft.

Nascimento, M. L. F. (2014). Brief history of the flat glass patent - Sixty years of the float process. *World Patent Information*, *38*, 50–56. https://doi.org/10.1016/j.wpi.2014.04.006

Neugebauer, J. (2017). Untersuchung alternativer Testszenarien zur Bestimmung der Biegezugfestigkeit von Dünnglas. *Ce/papers*, *1*(1), 168–180. https://doi.org/10.1002/cepa.18

Nijsse, R. (2008). Corrugated glass as improvement to the structural resistance of glass. In F. Bos, C. Louter, & F. Veer (Eds.), *Challenging Glass* (pp. 399–412). Delft: IOS Press.

Nijsse, R., & Wenting, R. (2014). Designing and constructing corrugated glass facades, *2*, 123–131. https://doi.org/10.3233/FDE-140014

O'Regan, C. (2014). *Structural use of glass in buildings (Second edition)*. IStructE Ltd.

Oristep Consulting. (2015). *Global Flat Glass Market - By Regions and Vendors - Market Size, Demand Forecasts, Industry Trends and Updates, Supplier Market Shares 2014- 2020*.

Ottens, R. (2018). *High strength thin glass as stiff structural fabric*. Delft University of Technology.

Overend, M., Butchart, C., Lambert, H., & Prassas, M. (2014). The mechanical performance of laminated hybrid-glass units. *Composite Structures*, *110*(1), 163–173. https://doi.org/10.1016/j.compstruct.2013.11.009

Pepi, J. (2002). *Strength properties of glass and ceramics*. Washington: Spie Press.

Pilkington. (2018). Technical Detail PDFs. Retrieved July 1, 2018, from http://www.pilkington.com/en-gb/uk/architects/types-of-glass/structural-glazing/technical-information/technical-detail-pdfs

Pilkington, L. A. B. (1969). Review Lecture. The Float Glass Process. *Proceedings of the Royal Soceity of London. Series A, Mathematical and Physical Sciences*, *Volume 314*(1516), 1–25.

Raynaud, J. (2014). Smooth free-formed glass skin. In C. Louter, F. Bos, J. Belis, & J.-P. Lebet (Eds.), *Challenging Glass 4 & COST Action TU0905 Final Conference* (pp. 57–65). CRC Press.

Robinson-Gayle, S., Kolokotroni, M., Cripps, A., & Tanno, S. (2001). ETFE foil cushions in roofs and atria. *Construction and Building Materials*, *15*(7), 323–327. https://doi.org/10.1016/S0950-0618(01)00013-7

Rohrig, B. (2015). Smartphones. Smart chemistry. *ChemMatters*, 10–12.

Schmitz, A., Kamiński, J., Maria Scalet, B., & Soria, A. (2011). Energy consumption and CO2 emissions of the European glass industry. *Energy Policy*, *39*(1), 142–155. https://doi.org/10.1016/j.enpol.2010.09.022

Shute, R. L., & Badger, A. E. (1942). Effect of iron oxide on melting of glass, *51*(1938), 355–357.

Silveira, R. R. (2016). *Flexible Transparency*. Delft University of Technology, Delft.

Simoen, C. (2016). *Thin Glass*. Delft University of Technology, Delft.

Sitte, S., Brasseur, M. J., Carbary, L. D., Wolf, A. T., Wolf, A., & Dean, S. W. (2011). Preliminary Evaluation of the Mechanical Properties and Durability of Transparent Structural Silicone Adhesive (TSSA) for Point Fixing in Glazing. *Journal of ASTM International*, *8*(10), 104084. https://doi.org/10.1520/JAI104084

Spitzhüttl, J., Nehring, G., & Maniatis, I. (2014). Investigations on determining the bending strength of thin glass. *Challenging Glass 4 & COST Action TU0905 Final Conference*, *169*, 521–530. https://doi.org/doi:10.1201/b16499-75

Talimian, A. (2016). *Strengthening of Soda-Borosilicate Glasses by Ion Exchange Processes*. Trento.

Teixidor, C. (2016). The Berkeley glass pavillion. In *Engineered Transparency* (pp. 317–25). Ernst & Sohn.

Teotia, M., & Soni, R. K. (2014). Polymer Interlayers for Glass Lamination-A Review, *3*(8), 1264–1270.

Topçu, Ö. (2017). *Kinetic Thin Glass Façade*. Delft University of Technology, Delft.

Tunçbilek, G. Z. (2014). Temporary architecture. In *Proceedings of the 2nd ICAUD International Conference in Architecture and Urban Design*.

Van der Weijde, I. (2016). *Ultra lightweight, insulating thin glass facade panel*. Delft University of Technology, Delft.

Varshneya, A. K. (2001). Chemical Strengthening of Glass Products. *Transactions of the Indian Ceramic Society*, *60*(1), 1–6. https://doi.org/10.1080/0371750X.2001.10799951

Varshneya, A. K., & Bihuniak, P. P. (2017). Cover screens for personal electronic devices: Strengthened glass or sapphire? *American Ceramic Society Bulletin*, *96*(5), 20–25.

Veer, F. A. (2007). The strength of glass, a nontransparent value. *Heron*, *52*(1–2), 87–104.

Veer, F. A., Louter, P. C., & Bos, F. P. (2009). The strength of annealed, heat-strengthened and fully tempered float glass. *Fatigue and Fracture of Engineering Materials and Structures*, *32*(1), 18–25. https://doi.org/10.1111/j.1460-2695.2008.01308.x

Weber, F. (2009). Curved glass structures. *GPD - Glass Performance Days*, 375–380.

Wegert, K. (2010). Magic of microfloat. *Glass Magazine*, (July/August), 60–62.

Weimar, T. (2012). Design of Glass-Polycarbonate Composite Panels. In F. Bos, C. Louter, R. Nijsse, & F. Veer (Eds.), *Challenging Glass 3* (pp. 759–767). Delft: IOS Press.

Whitehouse, D., & Corning Museum Of Glass. (2004). *Roman Glass in the Corning Museum of Glass, Volume 3*. New York: Corning Museum of Glass Inc.,U.S.

Wurm, J. (2007). *Glass structures: design and construction of self-supporting skins*.

Yussof, M. (2015). *Cable-Net Supported Glass Facade Systems*. Surrey.

APPENDICES

Appendix A

Appendix A shows the datasheets of thin glass manufacturers and the datasheets of interlayer manufacturers. Datasheets from the manufactures Schott, Corning and AGC off thin glass are used. Datasheets from the interlayer manufacturer Trosifol and Eastman are used.

A.1. Schott Xensation glass

Thermal Properties	
Thermal Conductivity $\lambda_{(25\,°C)}$	0.96 W/(m · K)
Specific Heat Capacity $C_{p(20\,°C;\,100\,°C)}$	0.84 KJ/(Kg · K)
Coefficient of Mean Linear Thermal Expansion $\alpha_{(20\,°C;\,300\,°C)}$	8.8 · 10^{-6} K^{-1}*
Transformation Point Tg	615 °C*
Annealing Point (10^{13} dPas)	635 °C
Softening Point ($10^{7.6}$ dPas)	880 °C
Working Point (10^{4} dPas)	1265 °C

* cooled according to DIN

Chemical Properties		
Hydrolytic Resistance	DIN ISO 719	Class HGB 1
Acid Resistance	DIN 12116	Class S 4
Alkali Resistance	DIN ISO 695	Class A 1

Optical Properties			
Refractive Index at	**588 nm (n_d)**	**633 nm**	**780 nm**
Core Glass	1.508	1.506	1.502
Compression Layer			
KNO_3 pure	1.516	1.514	1.510
Transmittance τ (Glass Thickness 0.7 mm)			
840 nm			> 91.5 %
560 nm			> 91.5 %
380 nm			> 90 %
Photoelastic Constant			29.2 nm/cm/MPa

Electrical Properties*		
Frequency	**Dielectric Constant**	**Loss Tangent**
MHz	**ε′**	**tanδ**
1	7.74	0.011
54	7.49	0.008
480	7.40	0.009
825	7.38	0.010
912	7.38	0.010
1977	7.35	0.012
2170	7.35	0.012
2986	7.34	0.012
Electric Volume Resistivity ϱ_D for A.C. at 50Hz		
υ = 250 °C		1.5 · 10^{6} Ω · cm
υ = 350 °C		8.9 · 10^{4} Ω · cm

Sheet Dimensions	
Sheet Size*:	1150 x 950 mm
	475 x 575 mm
Thickness Range:	0.5 - 3.0 mm

* other sizes on request

Mechanical Properties	
Density	2.477 g/cm³*
Young's Modulus E	74 kN/mm²
Poisson's Ratio	0.215
Shear Modulus	30 kN/mm²
Knoop Hardness $HK_{0.1/20}$	
Non-strenghtened	534
Strengthened	639
Vickers Hardness $HV_{0.2/20}$	
Non-strengthened	617
Strengthened	681

* cooled according to DIN

Chemical Strengthening	
Compressive Stress	capable > 900 MPa
Depth of Layer	capable > 50 µm
4-Point Bending Strength	cap. > 800 MPa

A.2. Corning Gorilla glass

Corning® Gorilla® Glass is Big, Bold, and Beautiful

Corning® Gorilla® Glass is an ideal cover glass for the most innovative large-format displays, including interactive white boards, digital signage, and other large-size public displays. It is elegant, lightweight, and durable enough to resist many real-world events that commonly cause glass damage and failure.

The unique composition of Gorilla Glass allows for a deep layer of high compressive stress created through an ion-exchange process. This compression layer makes the glass exceptionally tough and damage resistant. The composition also helps to prevent the deep chips and scratches that degrade appearance and can cause glass to break.

Additionally, Gorilla Glass is formed using the same proprietary fusion process as all of Corning's high-technology display substrates. This extraordinarily precise, highly-automated process produces glass with exceptionally clean, smooth, flat surfaces and outstanding optical quality.

Gorilla Glass is also remarkably thin and clear, which reduces weight, helps reduce the appearance of parallax, enables more sensitive and accurate touch responses, creates a more precise and professional display, and helps deliver on the promise of high-definition and 3D technologies.

Product Information

Display Screen Diagonal Size

Typical sizes	32 inches to 84 inches

Finished Part Dimensions

Width (max)	2020 mm
Length (max)	1365 mm @ 1 mm thickness 1200 mm @ 2 mm thickness
Thickness (mm)	2.0, 1.5, 1.0, 0.7, 0.55

Viscosity

Softening Point ($10^{7.6}$ poises)	896 °C
Annealing Point ($10^{13.2}$ poises)	627 °C
Strain Point ($10^{14.7}$ poises)	573 °C

Mechanical Properties

Density	2.39 g/cm³
Young's Modulus	68.0 GPa
Poisson's Ratio	0.22
Shear Modulus	27.9 GPa
Vickers Hardness (200 g load)	
Un-strengthened	551 kgf/mm²
Strengthened	654 kgf/mm²
Fracture Toughness	0.69 MPa $m^{0.5}$

Thermal

Coefficient of Expansion (0 °C - 300 °C)	75.5 x 10^{-7}/°C

Optical

Refractive Index (590 nm)	
Core index (no ion-exchange)	1.50
Compression layer	1.51

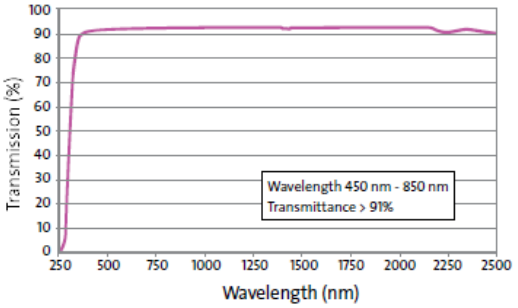

Chemical Strengthening

Compressive stress	≥ 650 MPa @ 40 µm DOL
Depth of Layer	≥ 40 µm

Note: Additional surface treatments are available, such as screen printing, optical films, and anti-glare finishes. For more information please contact Corning with your specific requirements.

Greater retained strength for Gorilla® Glass after scratch

Error bars represent 95% CI

Greater retained strength for Gorilla® Glass enables use of thinner glass

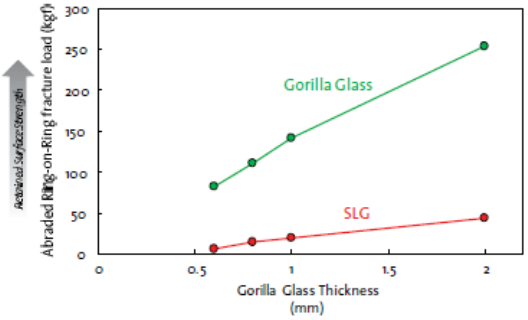

A.3. AGC Dragontrail glass

Dragontrail

Datasheet for coverglass and 2in1(OGS) substrate

Mechanical property	Density [g/cm³]		2.48
	Young's Modulus [GPa]		74
	Shear Modulus [GPa]		30
	Poisson's Ratio		0.23
	Vickers hardness (before CS)		595
	Vickers hardness (after CS)		673
Thermal property	CTE(50-350deg.x10^{-7}) [deg.]		98
	Softening Point [deg.]		821
	Annealing Point [deg.]		606
	Strain Point [deg.]		556
Optical property	Refraction Index (Nd)		1.51
	Photoelastic constant [nm/cm/MPa]		28.3
Electrical property	Dielectric constant Loss tangent	1M Hz	7.4 0.019
		2400MHz	7.4 0.011
Chemical durability	Weight loss [mg/cm^2]	HCl 0.1mol/l 90° for 20hrs	0.03
		NaOH 0.1mol/l 90° for 20hrs.	0.56
		HF 5% 25° for 20min.	11.8

Application	typical CS value	typical DOL value
Coverglass	More than 600MPa	35< DOL <45 (0.7t)
2in1(OGS)	700±50MPa	21±3um (0.7t)

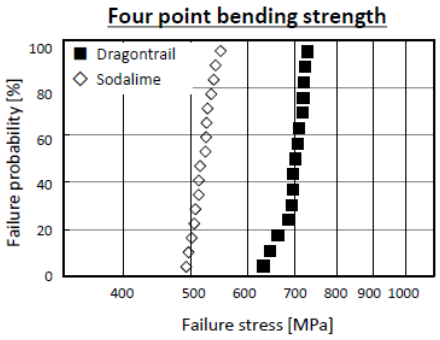

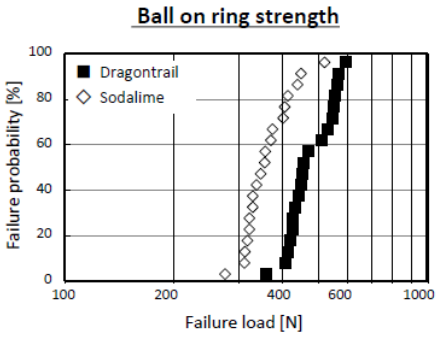

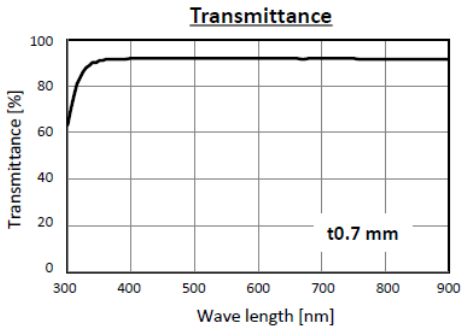

A.4. AGC Leoflex glass

AGC Leoflex™ opens the door to new groundbreaking opportunities for glass. Leoflex™ is very thin, chemically strengthened aluminosilicate glass, offering higher strength compared to tempered soda lime. This results in new opportunities for designers to create thinner or curved designs, while maintaining the beauty of glass.

This next-generation glass presents additional benefits in the industrial and building environment: superior clarity without any green tint, flexibility as well as scratch resistance. Whether you are an architect, designer or builder or an industrial product manufacturer, you can now get the weight benefits of plastic sheets with the superior performance and durability of glass.

Leoflex™ is produced using AGC technology that ensures the highest quality product.

Technical specifications

LEOFLEX™

Leoflex™ is the ideal solution for applications requiring very thin glass with high mechanical resistance.

	Clear float glass (with thermal tempering)		Leoflex™ (with chemical tempering)				
	3 mm	4 mm	0.55 mm	0.85 mm	1.1 mm	1.3 mm	2 mm
Weight (kg/m²)	7.5	10.0	1.4	2.1	2.7	3.2	5.0
Max Compressive Strength (MPa)	max 150	max 150	> 800	> 800	> 800	> 800	> 800
Compressive marginal stress (MPa)	80	80	260	260	260	260	260
Theoretical min radius curvature* (mm)	1500	2000	90	130	170	200	400
Vickers Hardness	527	527	673	673	673	673	673
Ug value EN 673 (W/m².C)	5.79	5.76	5.87	5.86	5.85	5.84	5.82
Light transmission EN 410 (D65.2°) LT %	90.3	89.8	91.3	91	90.8	90.6	89.9
Solar energy transmission EN 410 (D65.2°) TE %	85.7	84.4	91.6	91.5	91.4	91.3	91
Solar Factor EN 410 (D65.2°) SF %	87.5	84.9	91.7	91.6	91.5	91.4	91.2

(*) approx. value, depending on application

Processing options

Safety	Laminating (PVB or EVA), after chemical tempering
Cutting	Straight or circular, before and after chemical tempering
Shaping and edge finishing	Edge grinding (chamfering), before and after chemical tempering
	Grinding, before chemical tempering
	Drilling, before and after chemical tempering
Special treatments	Acid-etching, before and after chemical tempering
	Silk screen printing, after chemical tempering
	Painting and silvering, after chemical tempering
	Cold bending, after chemical tempering
Insulated glazing units	Double or triple glazing

NOTE: Some glass treatments are subject to limitations and must be carried out in specific conditions. Please contact AGC for more information (see contact details at the back).

Material Properties:

	Property	Measurement	Leoflex™	Soda Lime
Mechanical	Density	g/cm³	2.48	2.50
	Young's Modulus	GPa	74	73
	Shear Modulus	GPa	30	30
	Poisson's Ration		0.23	0.21
	Vickers Hardness	before CT	595	533
	Vickers Hardness	after CT	673	580
Thermal	CTE	[10⁻⁷](50~200°C)	98	85
	Tg	°C	604	550
	Softening Point	°C	831	733
	Annealing Point	°C	606	554
	Strain Point	°C	556	511
Optical	Refaction Index	Nd	1.51	1.52
	Photoelastic Constant	nm/cm Mpa	28.3	25.6
Electrical	Volume Resistivity	log (Ω * cm)	8.4	8.5

Weather Resistance Test

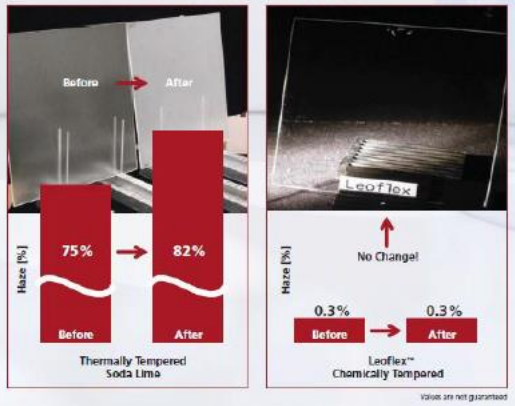

Values are not guaranteed

Toughness Ring-on-Ring Test

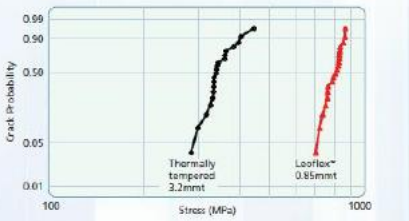

Values are not guaranteed

Chemical Tempering Performance

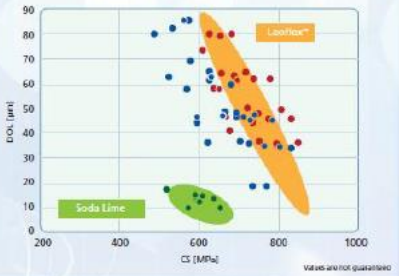

Values are not guaranteed

A.5. AGC Falcon glass

The highest performances, made affordable.

Here is the commitment of AGC's new **Falcon™ glass**.

Falcon™ glass is a new type of alumino-silicate glass, which is produced by the very high quality and cost efficient float process. Dedicated to chemical strengthening, this new generation glass opens new possibilities in the design of high resistance and lightweight structures at a reasonable cost. Its superior optical properties and its ease to thermoform make it especially well suited whenever aesthetics and design matters.

From mobile and portable devices to high-performance assemblies in building and transportation, Falcon™ is the unbeatable choice for tomorrow's high tech glass applications.

Performances

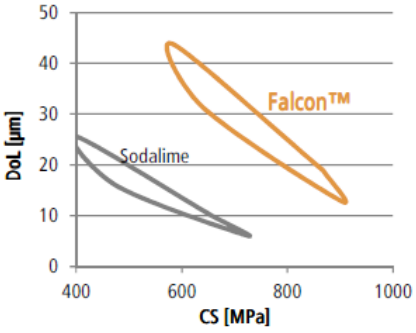

Mechanical properties

Density (g/cm³)	~2.48
Young Modulus (GPa)*	~73
Poisson's Ratio*	~0.22
Shear Modulus (GPa)*	~30

Chemical strengthening properties

Compressive stress	capable of >800MPa	(@ 20µm DoL)
Depth of Layer	capable of >40µm	(in 8h)
Reinforcement	capable of >600MPa	(for 15µm native defect)
Warpage	capable of <0.05%	(in 0.7mm – 420°C/4h)

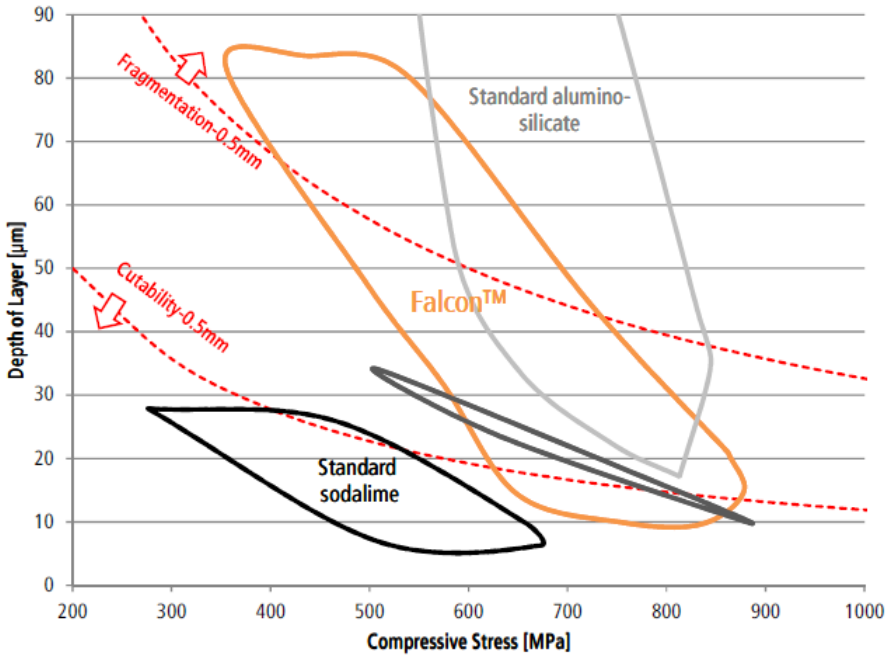

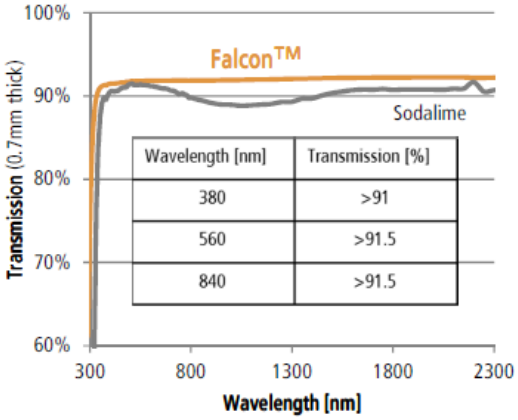

Wavelength [nm]	Transmission [%]
380	>91
560	>91.5
840	>91.5

Optical properties

Refractive index(630nm)*	1.514	
Photoelastic constant (nm/cm/MPa)*	~27.2	

Thermal properties

Softening point (°C)	~ 665	
Tg (°C)	~ 575	
Coefficient of thermal expansion	$\sim 9.10^{-6}$	(25-300°C)
Thermal conductivity(W/(m.°C))*	~0.95	

Chemical resistance

Hydrolytic class*	2

* Computed values

Applications and availability

Thickness	Max size	Quality grade
0.5mm 0.5mm AW*	1245*3210mm	Building, Automotive and Touch Panel
0.7mm 0.7mm AW*	1350*3210mm	
1.1mm	1480*3210mm	
2.1mm	1600*3210mm	

Processing options

- AGC's antiwarp
- Cutting
- Grinding
- Drilling/Forming
- Printing, Painting
- Chemical tempering
- Single or double acid etching
- UV gluing
- Wet coating application

Availability

Falcon glass will be available from July 2016

Standard thickness of 0.5, 0.7, 1.1 and 2mm, for thin and lightweight applications

Sheet sizes up to 3210*1600mm allows wide design possibilities

Falcon™ glass

A.6. SentryGlas

SentryGlas®

IONOPLAST INTERLAYER

SPECIFYING AND TECHNICAL DATA

The following information is presented to help you evaluate or order SentryGlas® ionoplast interlayers.
SentryGlas® interlayer is available on roll or as sheet and has a Yellowness-Index (YID) of < 2.5.

SHEET DIMENSIONS

Caliper mm (mil)	Width cm (in) Ordered, -0 +10 mm (-0 +0.4 in)	Length m (ft)
0,89 (35)	61-216 (24-85)	up to 600 (up to 236)
1,52 (60)	61-216 (24-85)	up to 600 (up to 236)
2,28 (90)	61-216 (24-85)	up to 600 (up to 236)
2,53 (100)	61-183 (24-72)	up to 600 (up to 236)
3,04 (120)	61-183 (24-72)	up to 600 (up to 236)

In addition to the standard stock sizes above, SentryGlas® can be ordered as 'cut-to-size', 'cut-to-fit' or 'cut-to-form' sheet, which means that none of the material is wasted. In all cases, sheet thickness is 0.89 mm (35 mil), 1.52 mm (60 mil) or 2.28 mm (90 mil). As these custom sizes require special handling/cutting, lead times are longer.

For details about the 'cut-to-size', 'cut-to-fit' or 'cut-to-form' sheet offering feel free to contact us.

ROLL DIMENSIONS

Caliper mm (mil)	Width cm (in) Ordered, -0 +10 mm (-0 +0.4 in)	Length m (ft)
0,76 (30)	122 (48)	200 (656)
0,76 (30)	153 (60)	200 (656)
0,76 (30)	183 (72)	200 (656)
0,76 (30)	153 (60)	50 (164)
0,89 (35)	122 (48)	200 (656)
0,89 (35)	153 (60)	200 (656)
0,89 (35)	183 (72)	200 (656)
0,89 (35)	153 (60)	50 (164)
0,89 (35)	225 (88)	50 (164)
0,89 (35)	225 (88)	200 (656)
0,89 (35)	240 (96)	50 (164)
0,89 (35)	240 (96)	200 (656)

In general, 0,76 mm (30 mil) is specified for easy processing when double stacking and not intended to be used as a single ply. Single ply use has not been tested to determine performance against any safety glazing codes or standards. 0,89 mm (35 mil) interlayers typically require high quality tempered glass for flatness. 1.52 mm (60 mil) interlayers are specified as the standard thickness for minimally supported applications. 2.28 mm (90 mil) thickness interlayers are normally specified for anti-intrusion, hurricane and other types of security applications. Glass producers and laminators require interlayers to be supplied either in sheet form or on rolls. SentryGlas® Ionoplast interlayers are available in both formats. For faster deliveries, SentryGlas® ionoplast interlayer is stocked in standard thicknesses (calipers) of 0.89 mm (35 mil), 1.52 mm (60 mil) and 2.28 mm (90 mil) sheets. SentryGlas® ionoplast interlayer on roll is available in 0,76 mm (30 mil) and 0.89 mm (35 mil) thickness.

TABLE 1 — LAMINATE PROPERTIES

Property	Units Metric (English)	Value	Test
Haze	%	< 2	ASTM D1003
Impact test 0,23 kg (0.5 lb)	m (ft)	> 9.14 (> 30)	ANSI Z26.1
Boil test 2 hr	-	No defects	ANSI Z26.1
Bake test 2 hr/100 °C	-	No defects	ANSI Z26.1

TABLE 2 — INTERLAYER TYPICAL PROPERTIES

Property	Units Metric (English)	Value	ASTM Test
Young's Modulus	Mpa (kpsi)	300 (43.5)	D5026
Tear Strength	MJ/m3 (ft lb/in3)	50 (604)	D638
Tensile Strength	Mpa (kpsi)	34.5 (5.0)	D638
Elongation	% (%)	400 (400)	D638
Density	g/cm3 (lb/in3)	0.95 (0.0343)	D792
Flex Modulus 23 °C (73 °F)	Mpa (kpsi)	345 (50)	D790
Heat Deflection Temperature (HDT) @ 0.46 MPa	°C (°F)	43 (110)	D648
Melting Point	°C (°F)	94 (201)	(DSC)
Coeff. of Thermal Expansion (-20 °C to 32 °C)	10-3 cm/cm °C (mils/in °C)	10 - 15 (0.10 - 0.15)	D696
Thermal Conductivity	W/M-K (BTU-in/hr-ft2 °F)	0.246 (1.71)	

POISSON RATIO: SENTRYGLAS®

		Load Duration						
Poisson Ratio, ν		1 s	3 s	1 min	1 h	1 day	1 mo	10 yrs
Temperature	10 °C (50 °F)	0.442	0.443	0.446	0.450	0.454	0.458	0.463
	20 °C (68 °F)	0.448	0.449	0.446	0.459	0.464	0.473	0.479
	24 °C (75.2 °F)	0.452	0.453	0.458	0.465	0.473	0.482	0.489
	30 °C (86 °F)	0.463	0.466	0.473	0.485	0.488	0.497	0.499
	40 °C (104 °F)	0.481	0.484	0.492	0.498	0.499	0.499	0.499
	50 °C (122 °F)	0.491	0.493	0.497	0.499	0.499	0.500	0.500
	60 °C (140 °F)	0.497	0.498	0.499	0.500	0.500	0.500	0.500
	70 °C (158 °F)	0.499	0.499	0.500	0.500	0.500	0.500	0.500
	80 °C (176 °F)	0.500	0.500	0.500	0.500	0.500	0.500	0.500

YOUNG`S MODULUS: SENTRYGLAS®

Young's Modulus E MPa (psi)		Load Duration 1 s	3 s	1 min	1 h	1 day	1 mo	10 yrs
Temperature	10 °C (50 °F)	692. (1.00 E+05)	681. (98745)	651. (94395)	597. (86565)	553. (80185)	499. (72355)	448. (64960)
	20 °C (68 °F)	628. (91060)	612. (88740)	567. (82215)	493. (71485)	428. (62060)	330. (47850)	256. (37120)
	24 °C (75 °F)	581. (84245)	561. (81345)	505. (73225)	416. (60320)	327. (47415)	217. (31465)	129. (18705)
	30 °C (86 °F)	442. (64090)	413. (59885)	324. (46980)	178. (25810)	148. (21460)	34.7 (5032)	15.9 (2306)
	40 °C (104 °F)	228. (33060)	187. (27115)	91.6 (13282)	27.8 (4031)	13.6 (1972)	9.86 (1430)	8.84 (1282)
	50 °C (122 °F)	108. (15660)	78.8 (11426)	33.8 (4901)	12.6 (1827)	8.45 (1225)	6.54 (948.3)	6.00 (870)
	60 °C (140 °F)	35.3 (5119)	24.5 (3553)	10.9 (1581)	5.10 (739.5)	3.87 (561.2)	3.24 (469.8)	2.91 (422)
	70 °C (158 °F)	11.3 (1639)	8.78 (1273)	5.64 (817.8)	2.52 (365.4)	1.77 (256.7)	1.44 (208.8)	1.35 (195.8)
	80 °C (176 °F)	4.65 (674.3)	3.96 (574.2)	2.49 (361.1)	0.96 (139.2)	0.75 (108.8)	0.63 (91.4)	0.54 (78.3)

A.7. Saflex DG41

Saflex® DG41 Young's Modulus

Load Duration	Temp 20°C	25°C	30°C	35°C	40°C	45°C	50°C	55°C	60°C
	MPa								
1 sec	1101	782	449	154	27	6.8	3.2	2.4	2.1
3 sec	1007	700	319	80	11	3.8	2.4	2.1	1.8
30 sec	812	466	115	13	3.0	2.4	1.8	1.8	1.5
1 min	735	387	74	8.3	2.7	2.1	1.8	1.5	1.5
5 min	596	213	20	3.5	2.1	1.8	1.5	1.5	1.2
30 min	413	83	5.6	2.4	1.8	1.5	1.2	1.2	0.9
1 hour	316	47	4.1	2.1	1.8	1.5	1.2	0.9	0.6
1 day	65	5.0	2.1	1.5	1.2	0.9	0.6	0.3	0.3
5 days	19	2.7	1.8	1.5	0.9	0.6	0.3	0.3	--
1 week	14	2.7	1.8	1.5	0.9	0.6	0.3	--	--
3 weeks	6.8	2.1	1.5	1.2	0.9	0.6	0.3	--	--
1 month	5.3	2.1	1.5	1.2	0.6	0.3	0.3	--	--
1 year	2.4	1.7	1.2	0.6	0.3	--	--	--	--
10 years	1.9	1.4	0.8	0.3	--	--	--	--	--
15 years	1.9	1.3	0.7	0.3	--	--	--	--	--
50 years	1.8	1.2	0.6	--	--	--	--	--	--

Young's modulus E' is calculated using formula E'= 2G'(1+v) where v = Poisson's ratio of approximately 0.476 for isotropic polymeric material as measured in accordance with ASTM D638.

2

	Property	Test Method	Units	Test Conditions	Saflex® DG
Mechanical	Elongation at Failure	JIS K6771	%	23°C / 50% RH	190
	Tensile Strength	JIS K6771	Kg/cm^2	23°C / 50% RH	330
	Shear Modulus	See table below			
	Young's Modulus	See table below			

Optical	Haze	ASTM D 1003	-	3 mm clear glass (laminate)	0.92
	Refractive Index	ASTM D 542	-	23°C	1.488
	Yellowness Index	ASTM D313	-	3 mm clear glass (laminate)	0.30

Thermal	Coefficient of Thermal Expansion	Thermal Mechanic	in/(in°F)	-40 °C -5 °C	189
	Thermal Conductivity, K	ASTM F 433	$W/m / (m^2°C)$	32 °C – 90 °C	0.205
	Emissivity	ASTM C 1371		19.5 °C	0.94

Solar	Solar Transmittance		D65	0.76 mm Saflex® DG Clear 3 mm Glass	76%
	Solar Reflectance				7%
	Solar Absorptance				17%
	Visible Transmittance				89%
	Visible Reflectance				8%
	Solar Heat Gain Coeffient		SHGC (G value)		0.81
	Light to Solar Gain		LSG		1.10
	UV Screening		280 – 380 nm		>99%

Appendix B

Appendix B includes the rating system developed according to the literature study for different conceptual designs.

B.3. Design conclusion

		Composite panels				Curved glass				Tensioned structures			
		Transparent		*Semi-transparent*		*Assembly*		*Lamination*		*Membrane*	*Pneumatic*		*Cable*
		Float and thin glass	Polymer and thin glass	Metals and thin glass	Non-metals and thin glass	Single curved	Double curved	Thin glass	Polymer and thin glass	Tensioned	Inflate	Deflate	Cable net system
Optical quality	Transparency	3	3	1	1	2	2	3	3	2	2	1	2
	Light transmittance	3	3	2	2	3	3	3	3	3	3	3	3
	Distortions	3	3	1	1	2	2	2	3	3	2	2	2
	Colour	3	2	2	2	3	3	3	2	3	3	3	3
Geometry	Curvature	1	3	1	1	3	3	3	3	1	1	1	2
	Manufacturing	3	3	1	1	3	1	3	3	3	1	1	2
	Lightweight	1	2	1	2	2	2	3	2	3	2	2	3
	Connections	3	3	2	2	2	2	1	3	1	2	2	1
Mechanical	Strength	3	2	3	3	2	2	2	2	1	2	2	2
	Stiffness	3	2	3	3	2	2	2	2	2	2	2	1
	Load bearing	3	3	3	3	2	2	3	3	1	1	1	2
	Post-breakage	3	3	3	3	2	2	2	3	1	2	2	2
	Redundancy	3	3	3	3	1	1	1	3	1	1	1	2
Sustainability	Production	1	1	2	2	2	2	3	1	3	1	2	2
	Heat transfer	2	2	1	1	1	1	1	2	1	3	3	1
	Durability	3	3	1	1	3	3	3	3	3	2	2	2
	Material efficiency	2	2	3	3	2	2	3	2	3	2	2	3
	Material recycling	1	1	1	1	3	3	2	1	3	3	3	3
	Panel recycling	2	2	2	2	3	3	2	2	3	3	3	2
Economical	Costs	2	1	2	2	2	2	2	1	2	1	1	2
	Market	3	3	2	2	2	2	3	3	2	1	3	2
	Innovation	1	2	2	2	1	1	3	2	3	1	3	1
Total value		**52**	**52**	**42**	**43**	**48**	**46**	**53**	**52**	**48**	**41**	**45**	**45**

Figure B.1: Requirements vs design configurations rating system from 1 to 3 of which 1 is not good and 3 is very good

Appendix C

Appendix C includes the derivations of formulas for different curvatures. The moment of inertia (I), section modulus (W) and their ratio are shown below.

$$\frac{I}{W} = \frac{lt^3}{12}\frac{6}{lt^2} = \frac{1}{2}t \quad (C.1)$$

C.1. Circular curvature

General formula for circles:

$$r^2 = x^2 + y^2 \quad (C.2)$$

Translated to parametric equations:

$$x = rcos(x),\ y = rsin(x) \quad (C.3)$$

$$x' = -rsin(x),\ y'(t) = rcos(x) \quad (C.4)$$

$$x" = -rcos(x),\ y" = -rsin(x) \quad (C.5)$$

Translated to curvatures:

$$K = \frac{x'*y"-x"*y'}{\left(x'^2+y'^2\right)^{\frac{3}{2}}} = \frac{r^2\sin^2(x)+r^2\,cos^2(x)}{-r^2\sin^2(x)+r^2\cos^2(x)} = \frac{1}{r} \quad (C.6)$$

Translated to bending moments by making use of the Kirchhoff Love plate theory:

$$M(x) = \frac{EI}{1-v^2}K = \frac{EI}{1-v^2} * \frac{1}{r} \quad (C.7)$$

Translated to cold bending stresses:

$$\sigma_b = \frac{M(x)}{W} = \frac{I}{W}\frac{E}{r(1-v^2)} = \frac{Et_p}{2r(1-v^2)} \quad (C.8)$$

With σ_b as the tensile bending stress, E as the modulus of elasticity, t_p as the thickness of a glass ply and r as the bending radius and v as the Poisson ratio.

Derivation of the spring back stresses:

$$M_{total} = \frac{EI}{r(1-v^2)} = \frac{E\sum t_p^3}{12r(1-v^2)} \quad (C.9)$$

$$\sigma_{sb} = \frac{M_{total}}{W} = \frac{E\sum t_p^3}{12r(1-v^2)} * \frac{6}{t_{eff,\sigma}} = \frac{E\sum t_p^3}{2r(1-v^2)t_{eff,\sigma}} \quad (C.10)$$

$$\sigma_{sb} = \left(1 - \frac{t_{pt}}{0.5*t_{total}}\right)\frac{E\sum t_p^3}{2r(1-v^2)t_{eff,\sigma}} \quad (C.11)$$

With σ_{sb} as the spring back effect tensile bending stress, t_{pt} as the thickness of a glass ply on the tension side, t_{total} as the panel thickness, E as the modulus of elasticity, t_p as the thickness of a glass ply, r as the bending radius, v as the Poisson ratio and $t_{eff,\sigma}$ as the effective stress thickness.

C.2. Catenary curvature

General formula for catenaries:

$$y = C * \cosh\left(\frac{x}{C}\right) \quad (C.12)$$

Translated to curvatures:

$$K = \frac{x'*y"-x"*y'}{\left(x'^2+y'^2\right)^{\frac{3}{2}}} = \frac{\operatorname{sech}^2\left(\frac{x}{C}\right)}{C} \quad (C.13)$$

Translated to bending moments by making use of the Kirchhoff Love plate theory:

$$M(x) = \frac{EI}{1-v^2}K = \frac{EI}{1-v^2} * \frac{\operatorname{sech}^2\left(\frac{x}{C}\right)}{C} \quad (C.14)$$

Translated to cold bending stresses:

$$\sigma_b = \frac{M(x)}{W} = \frac{I}{W}\frac{\operatorname{sech}^2\left(\frac{x}{C}\right)E}{C(1-v^2)} = \frac{\operatorname{sech}^2\left(\frac{x}{C}\right)Et_p}{2C(1-v^2)} \quad (C.15)$$

With σ_b as the tensile bending stress, C as the curvature variable, E as the modulus of elasticity, t_p as the thickness of a glass ply, v as the Poisson ratio and x as the position on the parabola.

C.3. Parabolic curvature

General formula for parabolas:

$$y = ax^2 \quad (C.16)$$

Translated to parametric equations:

$$x = x,\ y = ax^2 \quad (C.17)$$

$$x' = 1,\ y' = 2ax \quad (C.18)$$

$$x" = 0,\ y" = 2a \quad (C.19)$$

Translated to curvatures:

$$K = \frac{x'*y"-x"*y'}{\left(x'^2+y'^2\right)^{\frac{3}{2}}} = \frac{2a}{(1+4(ax)^2)^{\frac{3}{2}}} \quad (C.20)$$

Translated to bending moments by making use of the Kirchhoff Love plate theory:

$$M(x) = \frac{EI}{1-v^2}K = \frac{EI}{1-v^2} * \frac{2a}{(1+4(ax)^2)^{\frac{3}{2}}} \quad (C.21)$$

Translated to cold bending stresses:

$$\sigma_b = \frac{M(x)}{W} = \frac{I}{W}\frac{2aE}{(1-v^2)(1+4(ax)^2)^{\frac{3}{2}}} = \frac{aEt_p}{(1-v^2)(1+4(ax)^2)^{\frac{3}{2}}} \quad (C.22)$$

With σ_b as the tensile bending stress, a as the curvature variable, E as the modulus of elasticity, t_p as the thickness of a glass ply, v as the Poisson ratio and x as the position on the parabola.

Derivation of the spring back stresses at x=0:

$$M_{total} = \frac{2aEI}{(1-v^2)} = \frac{aE\sum t_p^3}{6(1-v^2)} \quad (C.23)$$

$$\sigma_{sb} = \frac{M_{total}}{W} = \frac{aE\sum t_p^3}{6(1-v^2)} * \frac{6}{t_{eff,\sigma}} = \frac{aE\sum t_p^3}{(1-v^2)t_{eff,\sigma}} \quad (C.24)$$

$$\sigma_{sb} = \left(1 - \frac{t_{pt}}{0.5*t_{total}}\right)\frac{aE\sum t_p^3}{(1-v^2)t_{eff,\sigma}} \quad (C.25)$$

With σ_{sb} as the spring back effect tensile bending stress, t_{pt} as the thickness of a glass ply on the tension side, t_{total} as the panel thickness, a as the curvature variable, E as the modulus of elasticity, t_p as the thickness of a glass ply, v as the Poisson ratio and $t_{eff,\sigma}$ as the effective stress thickness.

C.4. Sinusoidal curvature

General formula for sinusoidal waves:

$$y = \mathrm{A}\cos\left(\frac{\pi}{\mathrm{B}}\mathrm{x}\right) \quad (C.26)$$

Translated to parametric equations:

$$x = x,\ y = \mathrm{A}\cos\left(\frac{\pi}{\mathrm{B}}x\right) \quad (C.27)$$

$$x' = 1,\ y' = -\mathrm{A}\frac{\pi}{\mathrm{B}}\sin\left(\frac{\pi}{\mathrm{B}}\mathrm{x}\right) \quad (C.28)$$

$$x'' = 0,\ y'' = -\mathrm{A}\left(\frac{\pi}{\mathrm{B}}\right)^2\cos\left(\frac{\pi}{\mathrm{B}}\mathrm{x}\right) \quad (C.29)$$

Translated to curvatures:

$$K = \frac{x'*y''-x''*y'}{\left(x'^2+y'^2\right)^{\frac{3}{2}}} = \frac{\mathrm{A}\left(\frac{\pi}{\mathrm{B}}\right)^2\cos\left(\frac{\pi}{\mathrm{B}}\mathrm{x}\right)}{\left(1+\left(\mathrm{A}\frac{\pi}{\mathrm{B}}\sin\left(\frac{\pi}{\mathrm{B}}\mathrm{x}\right)\right)^2\right)^{\frac{3}{2}}} \quad (C.30)$$

Translated to bending moments by making use of the Kirchhoff Love plate theory:

$$M(x) = \frac{EI}{1-v^2}K = \frac{EI}{1-v^2} * \frac{\mathrm{A}\left(\frac{\pi}{\mathrm{B}}\right)^2\cos\left(\frac{\pi}{\mathrm{B}}\mathrm{x}\right)}{\left(1+\left(\mathrm{A}\frac{\pi}{\mathrm{B}}\sin\left(\frac{\pi}{\mathrm{B}}\mathrm{x}\right)\right)^2\right)^{\frac{3}{2}}} \quad (C.31)$$

Translated to cold bending stresses:

$$\sigma_b = \frac{M(x)}{W} = \frac{I}{W}\frac{\mathrm{A}\left(\frac{\pi}{\mathrm{B}}\right)^2\cos\left(\frac{\pi}{\mathrm{B}}\mathrm{x}\right)*E}{(1-v^2)\left(1+\left(\mathrm{A}\frac{\pi}{\mathrm{B}}\sin\left(\frac{\pi}{\mathrm{B}}\mathrm{x}\right)\right)^2\right)^{\frac{3}{2}}} = \frac{\mathrm{A}\left(\frac{\pi}{\mathrm{B}}\right)^2\cos\left(\frac{\pi}{\mathrm{B}}\mathrm{x}\right)*Et_p}{2(1-v^2)\left(1+\left(\mathrm{A}\frac{\pi}{\mathrm{B}}\sin\left(\frac{\pi}{\mathrm{B}}\mathrm{x}\right)\right)^2\right)^{\frac{3}{2}}} \quad (C.32)$$

With σ_b as the tensile bending stress, A as the amplitude, B as length of half a period, E as the modulus of elasticity, t_p as the thickness of a glass ply, v as the Poisson ratio and x as the position on the sinusoidal wave.

Derivation of the spring back stresses at x=0:

$$M_{total} = \frac{\mathrm{A}\left(\frac{\pi}{\mathrm{B}}\right)^2 EI}{1-v^2} = \frac{\mathrm{A}\left(\frac{\pi}{\mathrm{B}}\right)^2 E\sum t_p^3}{12(1-v^2)} \quad (C.33)$$

$$\sigma_{sb} = \frac{M_{total}}{W} = \frac{\mathrm{A}\left(\frac{\pi}{\mathrm{B}}\right)^2 E\sum t_p^3}{12(1-v^2)} * \frac{6}{t_{eff,\sigma}} = \frac{\mathrm{A}\left(\frac{\pi}{\mathrm{B}}\right)^2 E\sum t_p^3}{2(1-v^2)t_{eff,\sigma}} \quad (C.34)$$

$$\sigma_{sb} = \left(1-\frac{t_{pt}}{0.5*t_{total}}\right)\frac{\mathrm{A}\left(\frac{\pi}{\mathrm{B}}\right)^2 E\sum t_p^3}{2(1-v^2)t_{eff,\sigma}} \quad (C.35)$$

With σ_{sb} as the spring back effect tensile bending stress, t_{pt} as the thickness of a glass ply on the tension side, t_{total} as the panel thickness, A as the amplitude, B as length of half a period, E as the modulus of elasticity, t_p as the thickness of a glass ply, v as the Poisson ratio and $t_{eff,\sigma}$ as the effective stress thickness.

C.5. Conclusion

The figure below shows the total production stresses caused by cold bending and laminating thin glass for different curvatures at different spans. The graphs represent both the build-ups with Saflex DG41 and SentryGlas, as they experience very similar stress distributions. It can be concluded that the lowest stresses are induced by a circular curvature with a constant stress distribution along the curve. The highest stresses are induced by a sinusoidal curvature with the highest value being at the top of the curve.

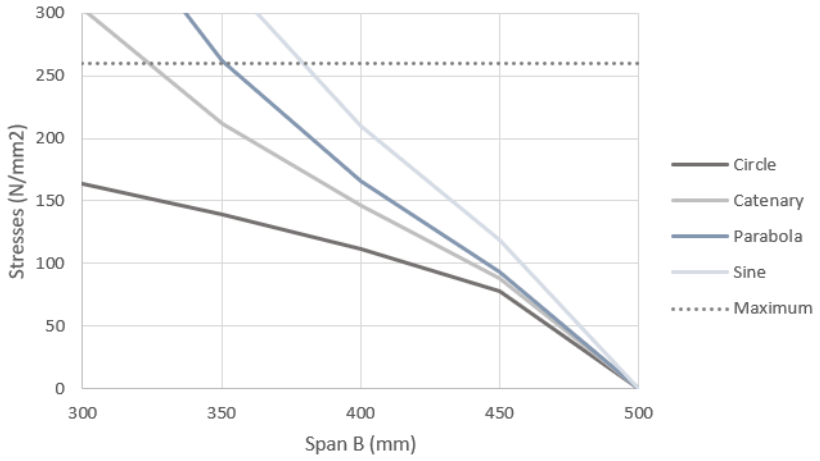

Figure C.1: Span (B) vs total production stresses (σ_{tot}) for cold bending a single sheet of Leoflex glass

Appendix D

Appendix D covers the production process of cold bent laminated thin glass panels.

D.1. Production process

The table below lists the products and equipment used to manufacture cold bent laminated thin glass panels. A distinction is made between the mould, equipment for bending, equipment for lamination and supports.

Products	Size (mm)	Material/Colour	Type	Max. temperature/pressure
MOULD				
Boikon elements	>680x700	Aluminium	-	-
Rectangular plate	550x680	Aluminium	-	-
L shaped profiles	680	Aluminium	-	-
Glue clamps	>500	-	-	-
BENDING				
Glass	500x500	Leoflex glass	-	-
Interlayer	500x500	SAF/SG	-	-
Cleaning liquid	-	Acetone	-	-
Vacuum foil	-	Nylon	WL5400/WL7400	177 °C/204°C
Seal tape	-	Black/Yellow	LTS90B/AT200Y	180 °C/204°C
Peel Ply	-	Nylon	Stitch Ply A	232 °C
Breeder blanket	-	Nylon	Air weave N10	204 °C
Release foil	-	Red FEP foil	A 4000 FEP	260 °C
Tape	-	-	Blue tape 25 mm	204 °C
Vacuum connector	-	-	-	-
Vacuum pump	-	-	-	-
LAMINATION				
Autoclave	1080x1700	-	-	250 °C/20 bar
Hose	-	-	-	-
SUPPORTS				
Timber	>3x500	Softwood	-	-
Rubber	>3x500	-	-	-
Screws	-	-	-	-

Table D.1: List of used products and equipment

E.3.1. Mould

To obtain a sinusoidal curvature, an initial mould is made from timber using the buckling principle. A sheet of thin glass is brought into a slight curved position to force the glass to buckle upwards. One support is fixed at one end and the other support can move sideways by tightening the clamps and allow for the glass to go into the correct position. Measurements of the geometry conclude that the sinusoidal curvature is in fact obtained by this principle. However, a great disadvantage of this type of mould is that, although timber is a softer material, large peak stresses can be introduced at the supported edges of the glass. This could result in sudden failure before reaching the desired curvature. The first tests were done with a single sheet of glass, but could cause problems when wanting to curve two plies of thin glass with an interlayer in between. The question also arises on how to apply the vacuum bagging around the specimen without tearing the bag during tightening of the boundaries. Furthermore, timber as a material cannot go into the autoclave.

Another way to manufacture a sinusoidal curve is to use a static aluminium mould. By rolling an aluminium sheet in a manual slip roll machine, the desired curvature can be obtained. This is time consuming and doesn't necessarily give the anticipated geometry. Two aluminium plates following the curvature at both sides of the curved edge, are welded onto the rolled aluminium plate. A test is performed with a piece of carbon to get a first impression on the vacuum bagging process by using a distributed pressure to curve the plate. It is clear from the picture below that the pressure causes the aluminium plates on the sides to buckle inwards, consequently changing the geometry of the entire mould. As explained in chapter 9.2.1, a combination of the previous designed moulds is used to design the final mould.

Figure D.1: Adjustable timber mould and nonadjustable aluminium mould

E.3.2. Lamination

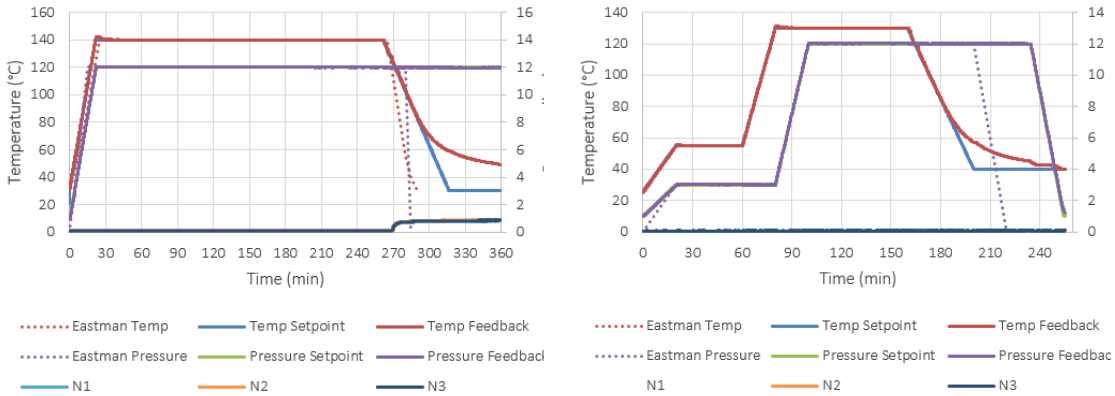

Figure D.2: Autoclave cycle for Saflex DG41 series 1 (left) and SentryGlas series 3 (right)

Appendix E

Appendix E shows the model and results for numerical and experimental analyses.

E.1. Numerical analysis

The numerical model used is illustrated below. One end of the beam is restraint vertically and displaced horizontally at the lower corner of both glass panes, while at the other end all the nodes are restraint horizontally to make up for symmetry. During spring back and relaxation the boundary conditions change. The problems shown in Figure E.3 at the curvatures end get worse when refining the mesh.

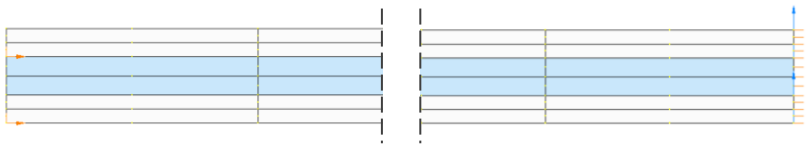

Figure E.1: Strand7 model during bending

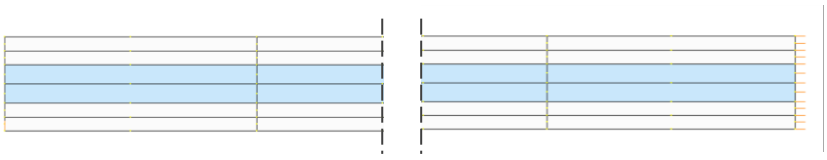

Figure E.2: Strand7 model during spring back and relaxation

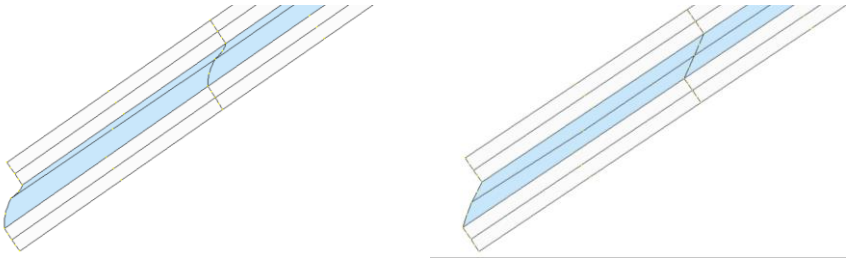

Figure E.3: 2D Plane stress elements at end only with morphing (left) and changing stiffness with morphing of the interlayer (right)

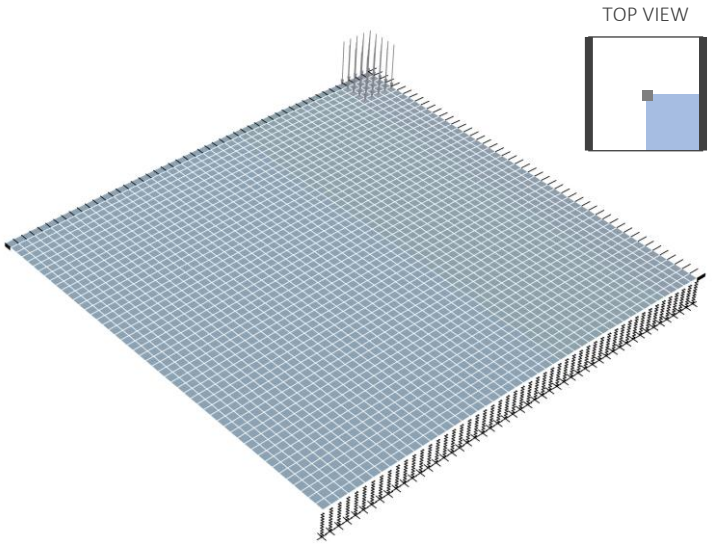

Figure E.4: Strand7 model during loading using symmetry conditions in 3D

	Relaxation	Loading	Total		Location
REFERENCE SAF					
Deflection DY	-	-70.36	-	mm	Bottom
Principal stresses	-	267.14	267.14	MPa	ply at top
REFERENCE SG					
Deflection DY	-	-43.96	-	mm	Bottom
Principal stresses	-	217.57	217.57	MPa	ply at top
PANEL 1.2					
Deflection DY	-	-72.19	-	mm	Bottom
Principal stresses	0	269.20	269.20	MPa	ply at top
PANEL 1.1/2.1					
Deflection DY	-	-10.38	-	mm	Bottom
Principal stresses	0	156.06	156.06	MPa	ply at top
Deflection DY	-	-12.26	-	mm	Top ply at
Principal stresses	41.21	192.38	233.59	MPa	middle
PANEL 3.1/3.2					
Deflection DY	-	-1.18	-	mm	Bottom
Principal stresses	0	43.75	43.75	MPa	ply at top

Table E.1: Numerical output for deflection and stresses at a load of 400 N

E.1.1. Bending

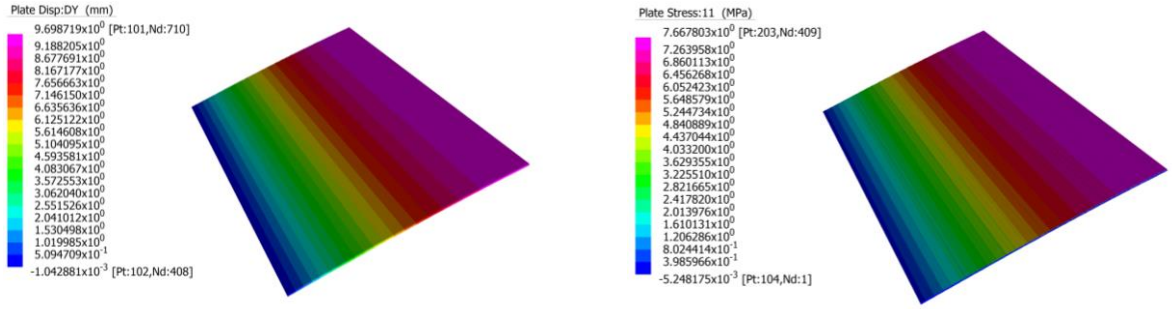

Figure E.5: Vertical displacement (DY) and principal stress (σ_{11}) of panel 1.2 using symmetry top view

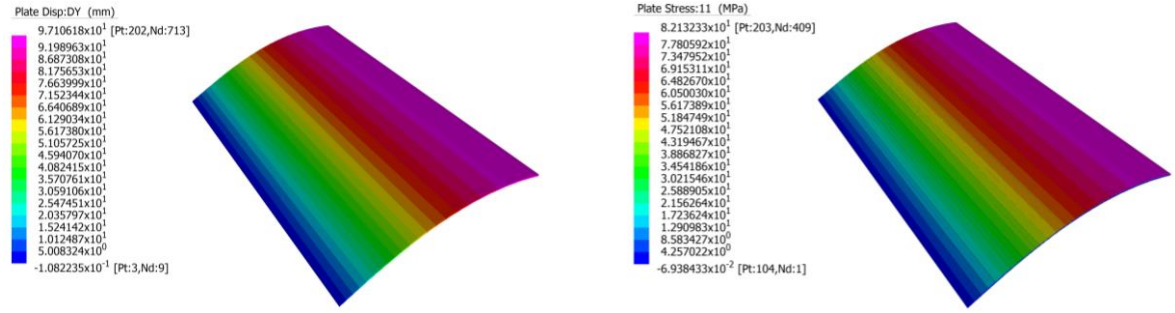

Figure E.6: Vertical displacement (DY) and principal stress (σ_{11}) of panels 1.1, 2.1, 3.1 and 3.2 using symmetry top view

E.1.2. Spring back

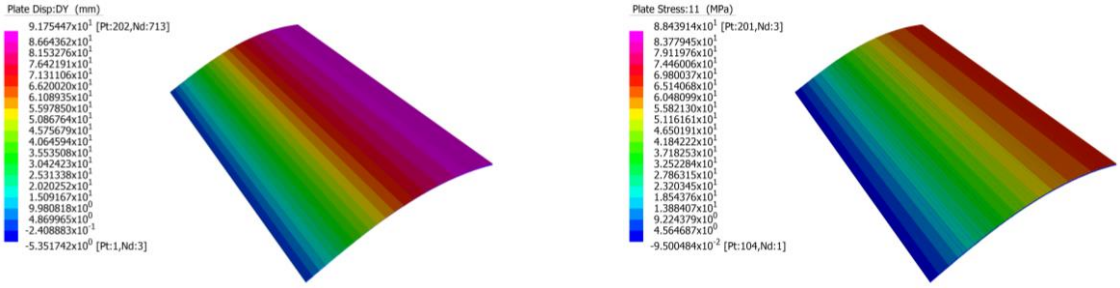

Figure E.7: Vertical displacement (DY) and principal stress (σ_{11}) of panels 1.1 and 2.1 using symmetry top view

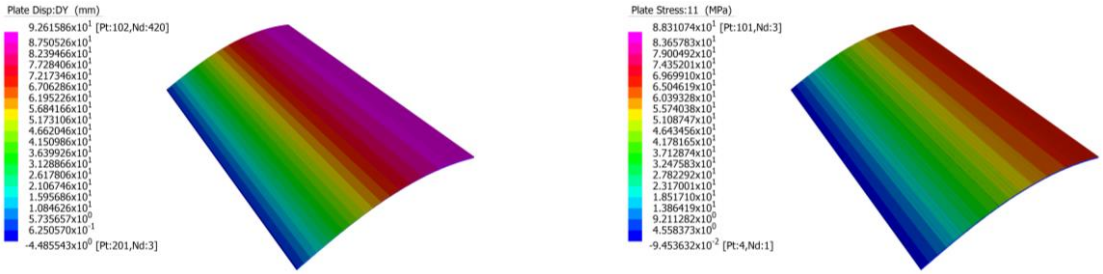

Figure E.8: Vertical displacement (DY) and principal stress (σ_{11}) of panels 3.1 and 3.2 using symmetry top view

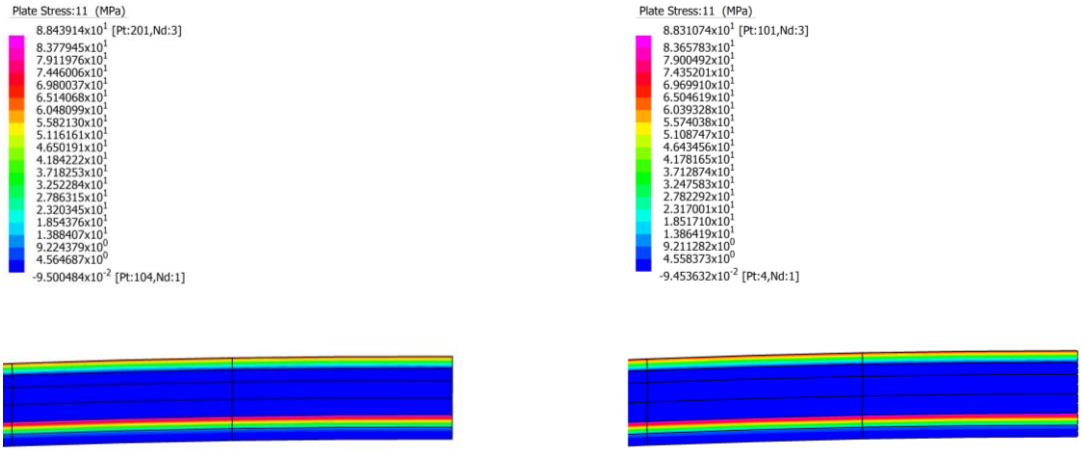

Figure E.9: Principal stress (σ_{11}) at top of panels 1.1, 2.1 (left), 3.1 and 3.2 (right)

E.1.3. Relaxation

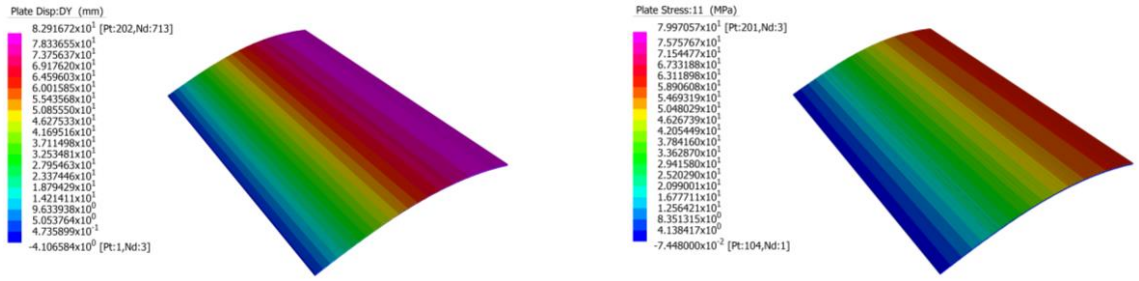

Figure E.10: Vertical displacement (DY) and principal stress (σ_{11}) of panels 1.1 and 2.1 using symmetry top view

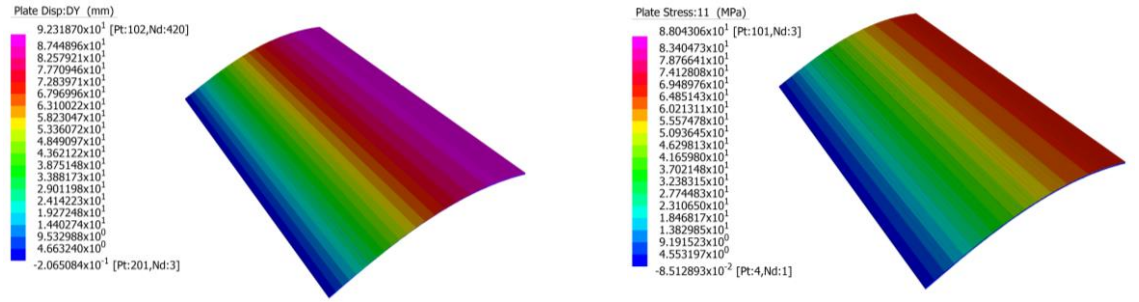

Figure E.11: Vertical displacement (DY) and principal stress (σ_{11}) of panels 3.1 and 3.2 using symmetry top view

E.3.3. Loading

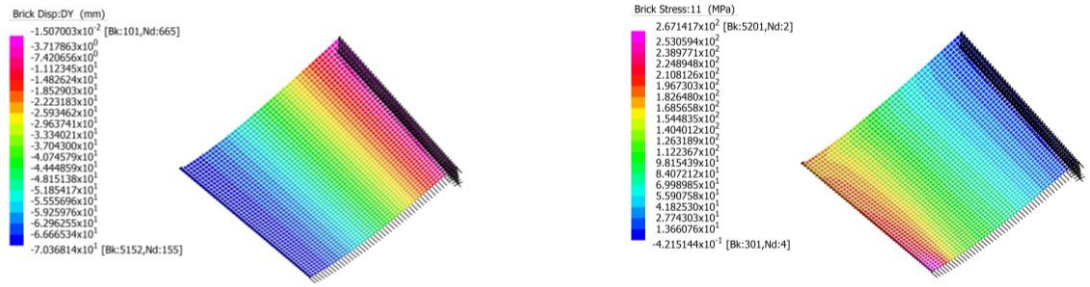

Figure E.12: Vertical displacement (DY) and principal stress (σ_{11}) at 400 N of reference panels with SAF using symmetry bottom view

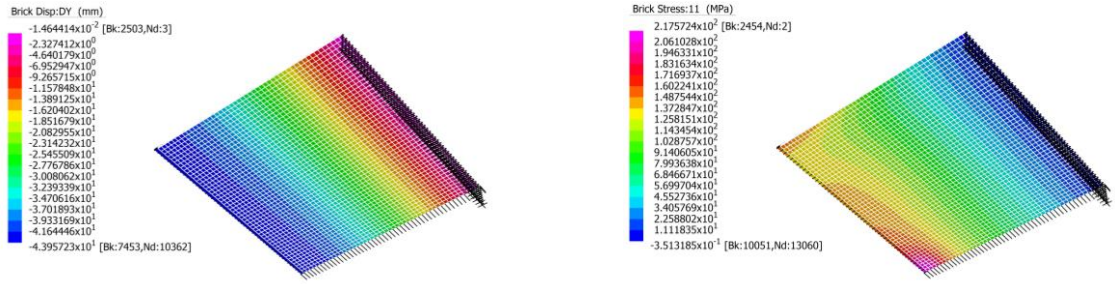

Figure E.13: Vertical displacement (DY) and principal stress (σ_{11}) at 400 N of reference panels with SG using symmetry bottom view

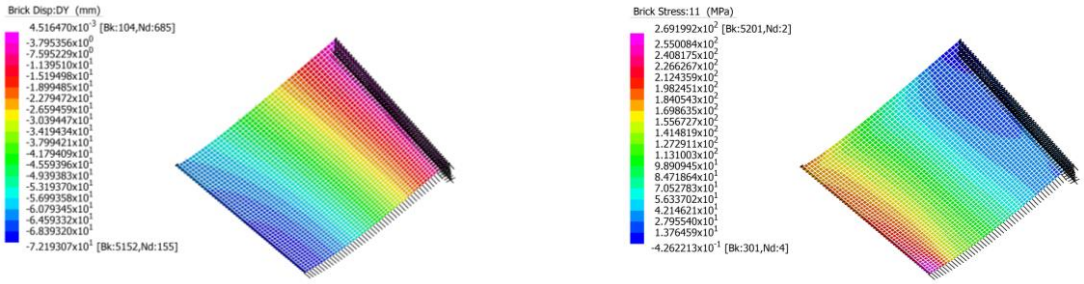

Figure E.14: Vertical displacement (DY) and principal stress (σ_{11}) at 400 N of panel 1.2 using symmetry bottom view

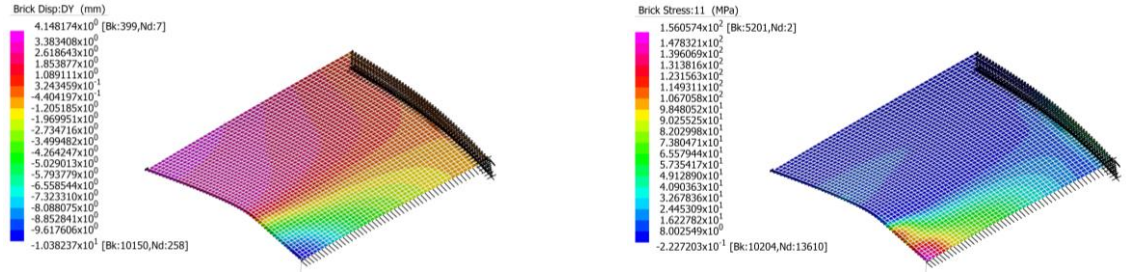

Figure E.15: Vertical displacement (DY) and principal stress (σ_{11}) at 360 N of panels 1.1 and 2.1 using symmetry bottom view

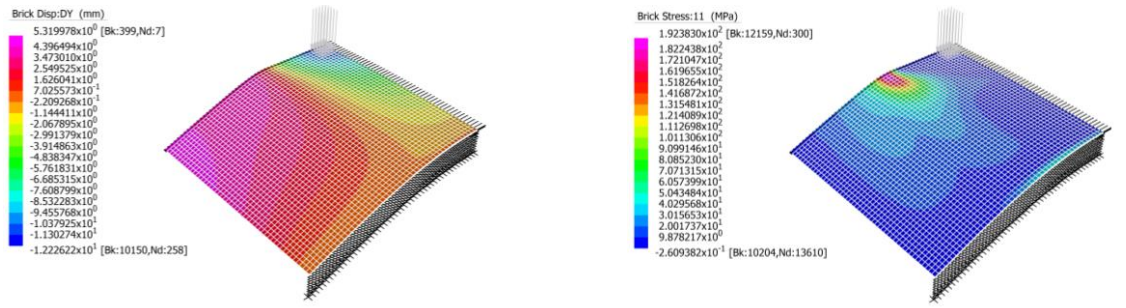

Figure E.16: Vertical displacement (DY) and principal stress (σ_{11}) at 400 N of panels 1.1 and 2.1 using symmetry top view

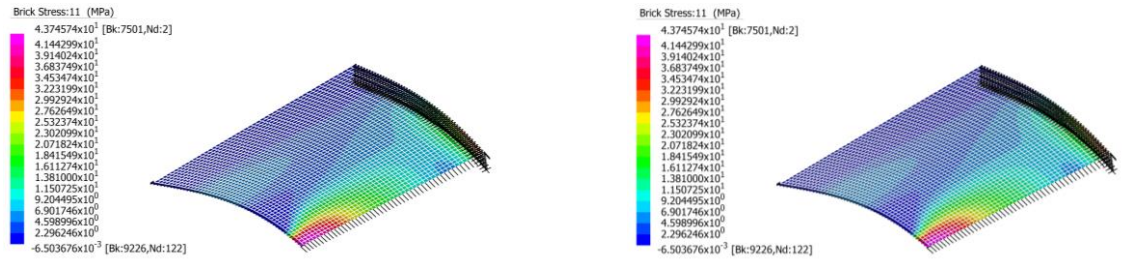

Figure E.17: Vertical displacement (DY) and principal stress (σ_{11}) at 400 N of panels 3.1 and 3.2 using symmetry bottom view

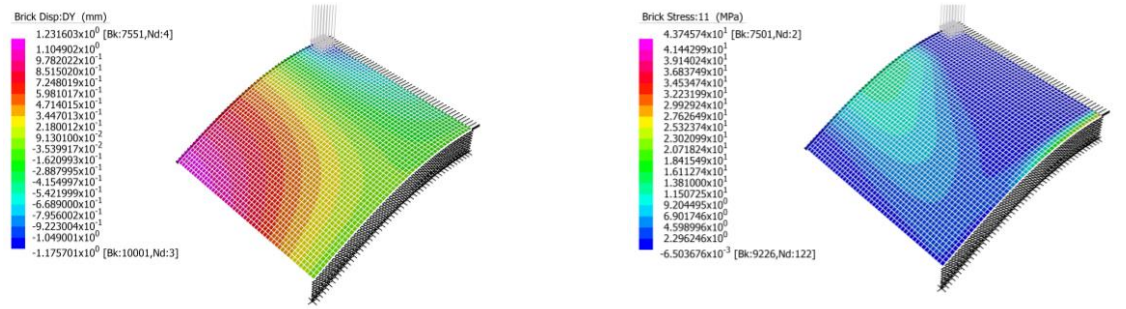

Figure E.18: Vertical displacement (DY) and principal stress (σ_{11}) at 400 N of panels 3.1 and 3.2 using symmetry top view

E.2. Experimental analysis

Several coordinates of the bent aluminium plate are roughly measured with a measuring tape and plotted in the figure below to compare the curvature of both moulds to the analytical curvature. It follows that the aluminium plates capture the analytical sinusoidal curvature quite well.

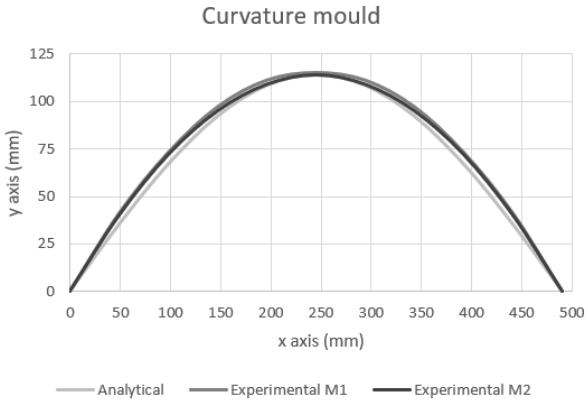

Figure E.19: Analytical and experimental geometry of the aluminium mould

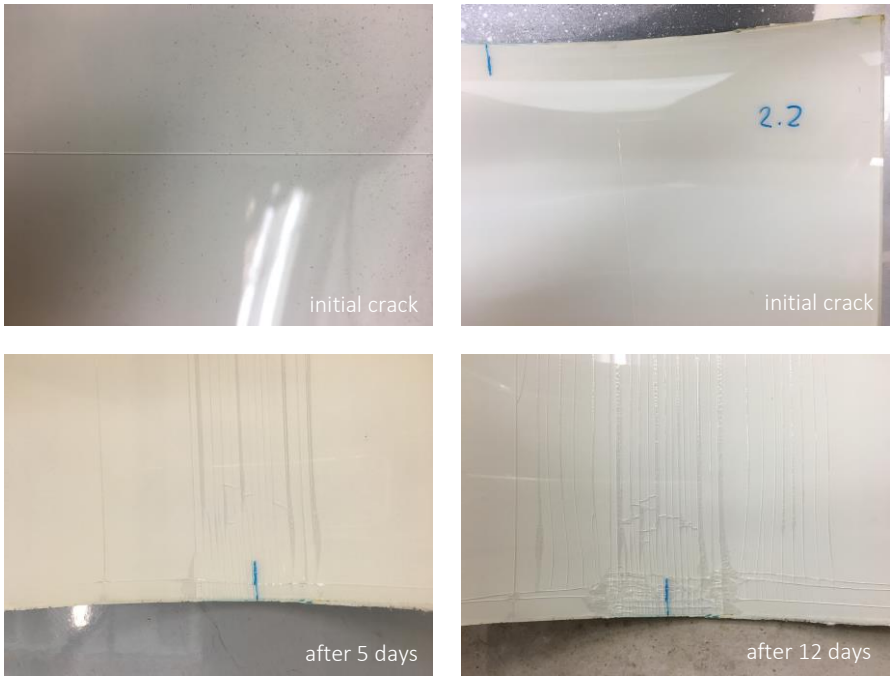

Figure E.20: Cracking pattern of panel 2.2

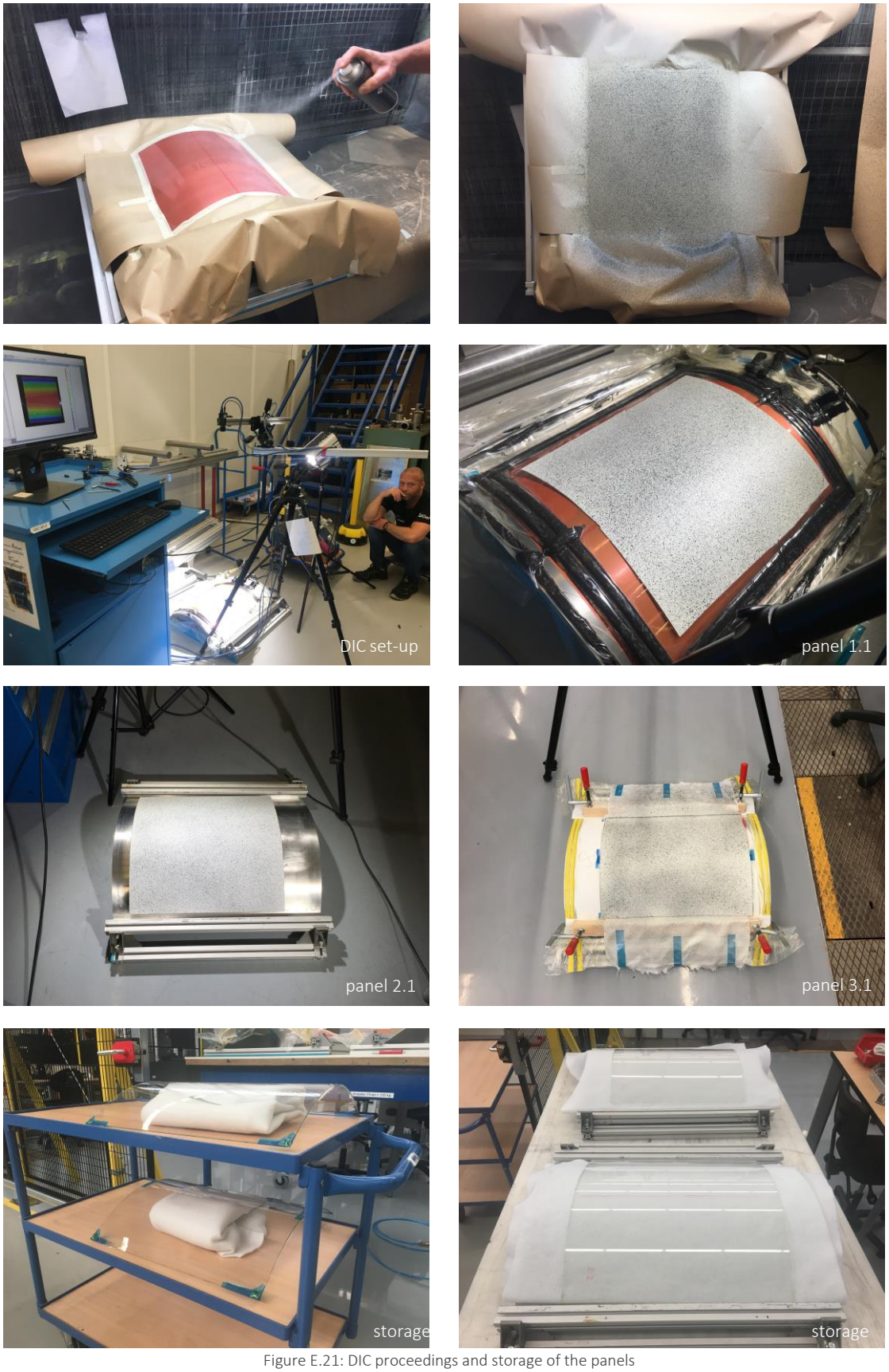

Figure E.21: DIC proceedings and storage of the panels

E.2.1. Bending

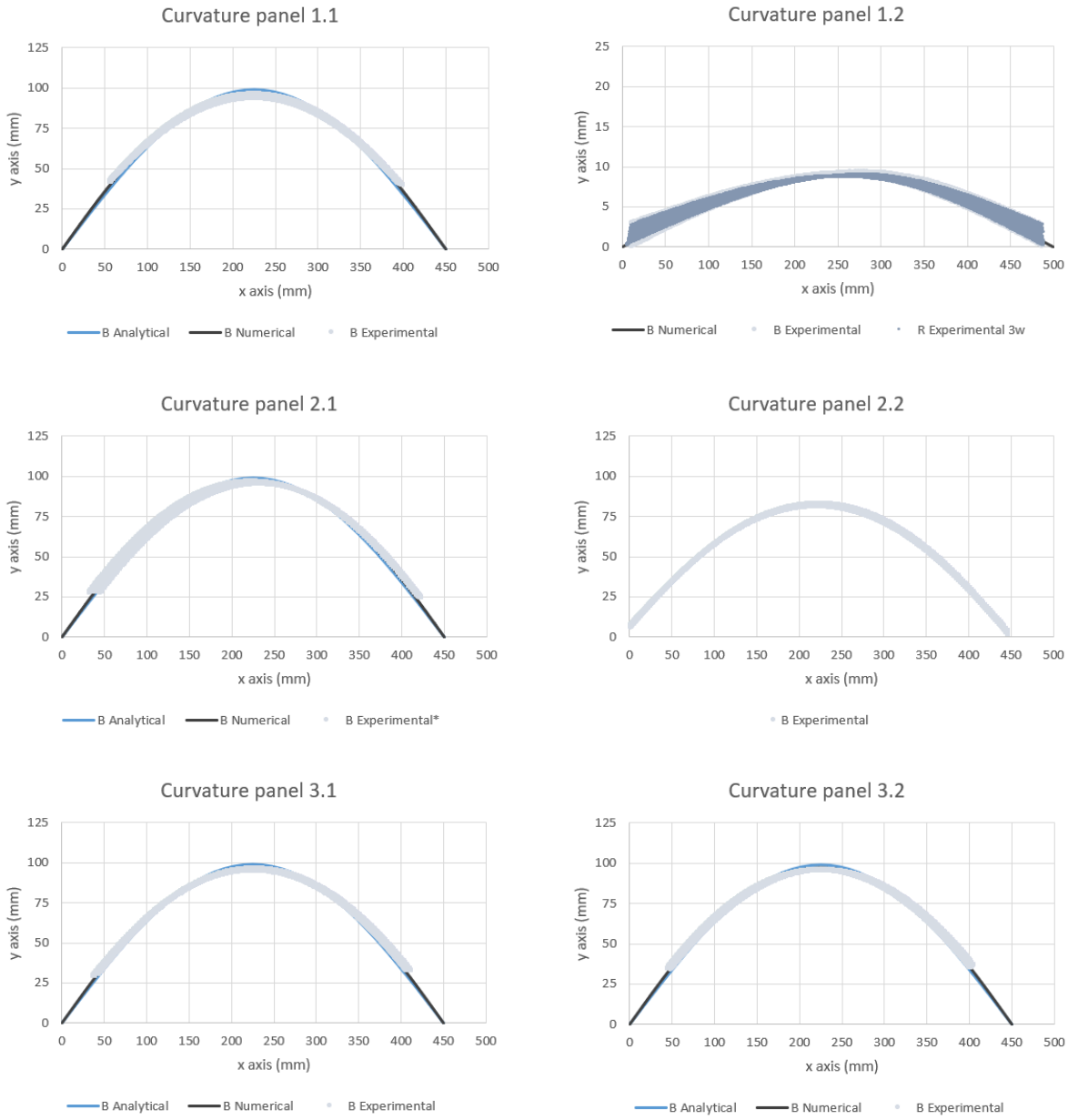

Figure E.22: Analytical, numerical and experimental geometry obtained during bending

E.2.2. Spring back

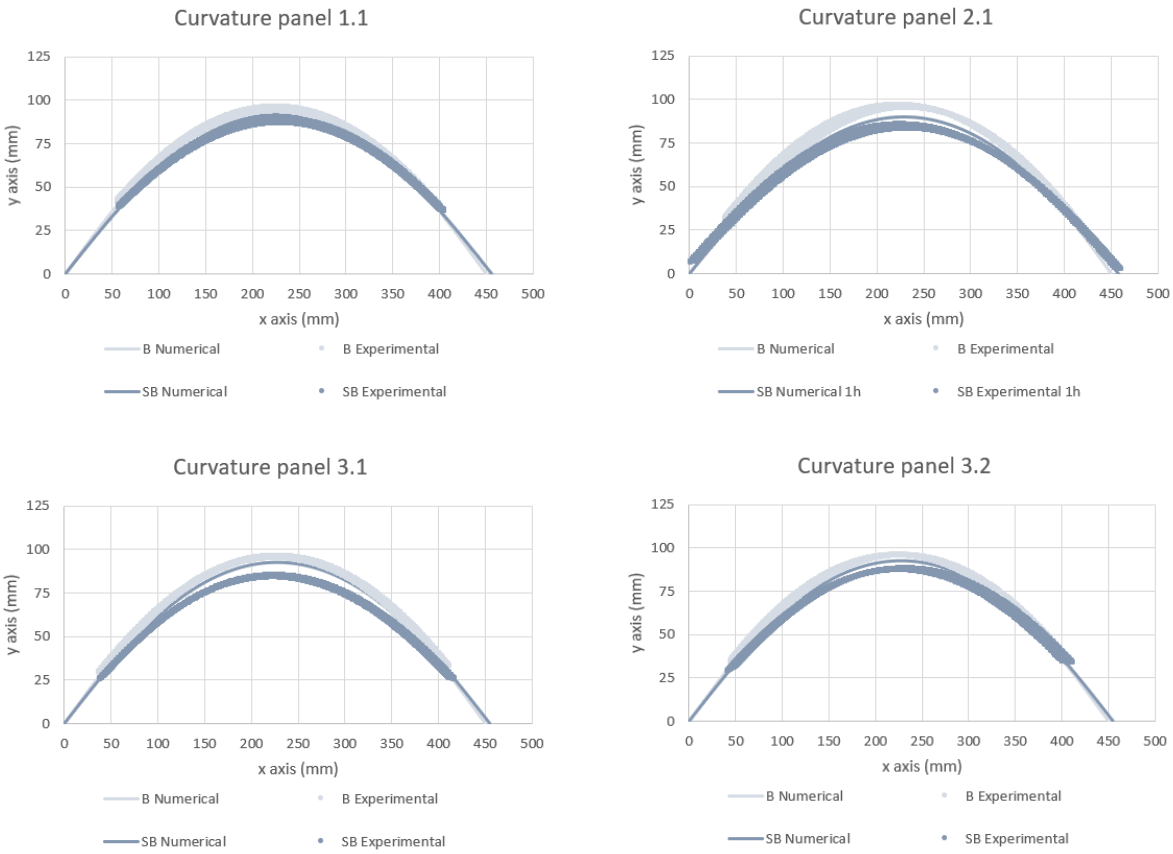

Figure E.23: Numerical and experimental geometry obtained during spring back

E.2.3. Relaxation

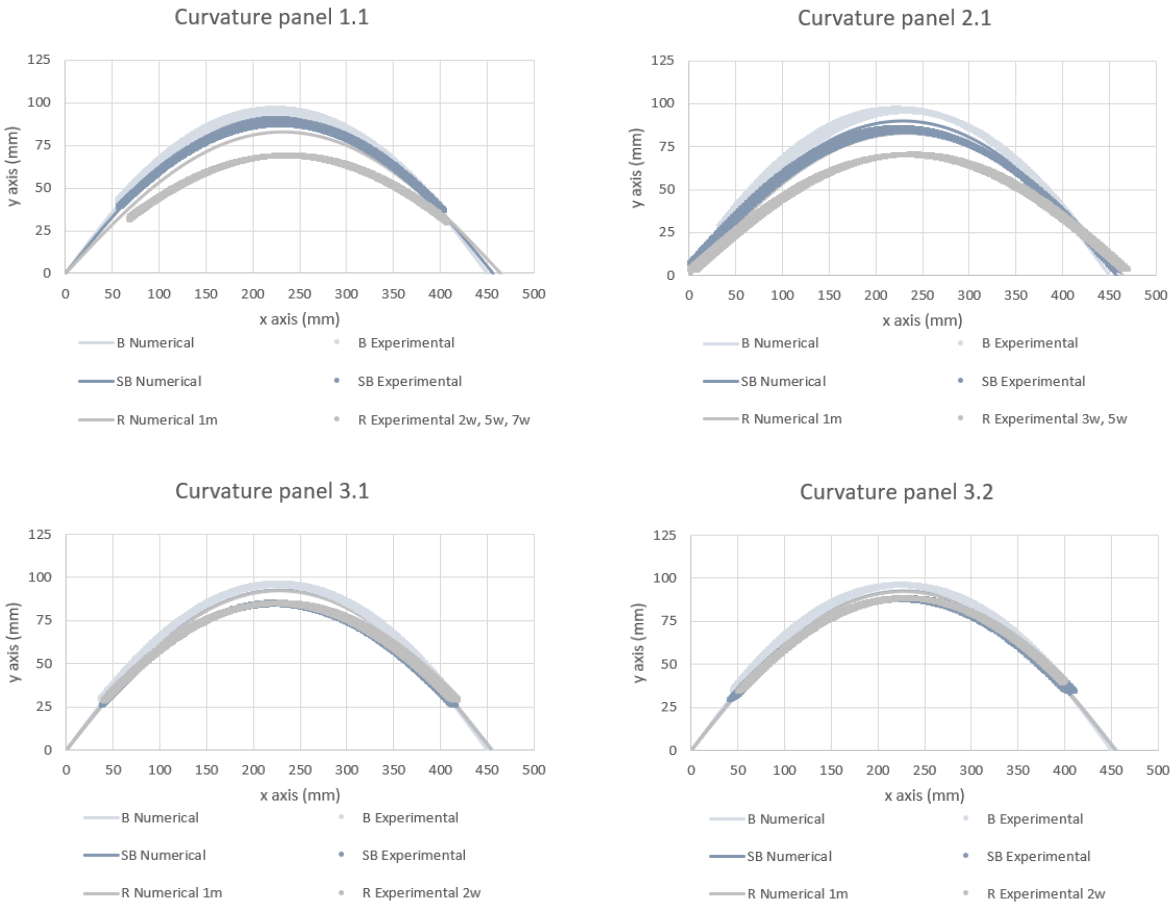

Figure E.24: Numerical and experimental geometry obtained during relaxation

E.3.4. Loading

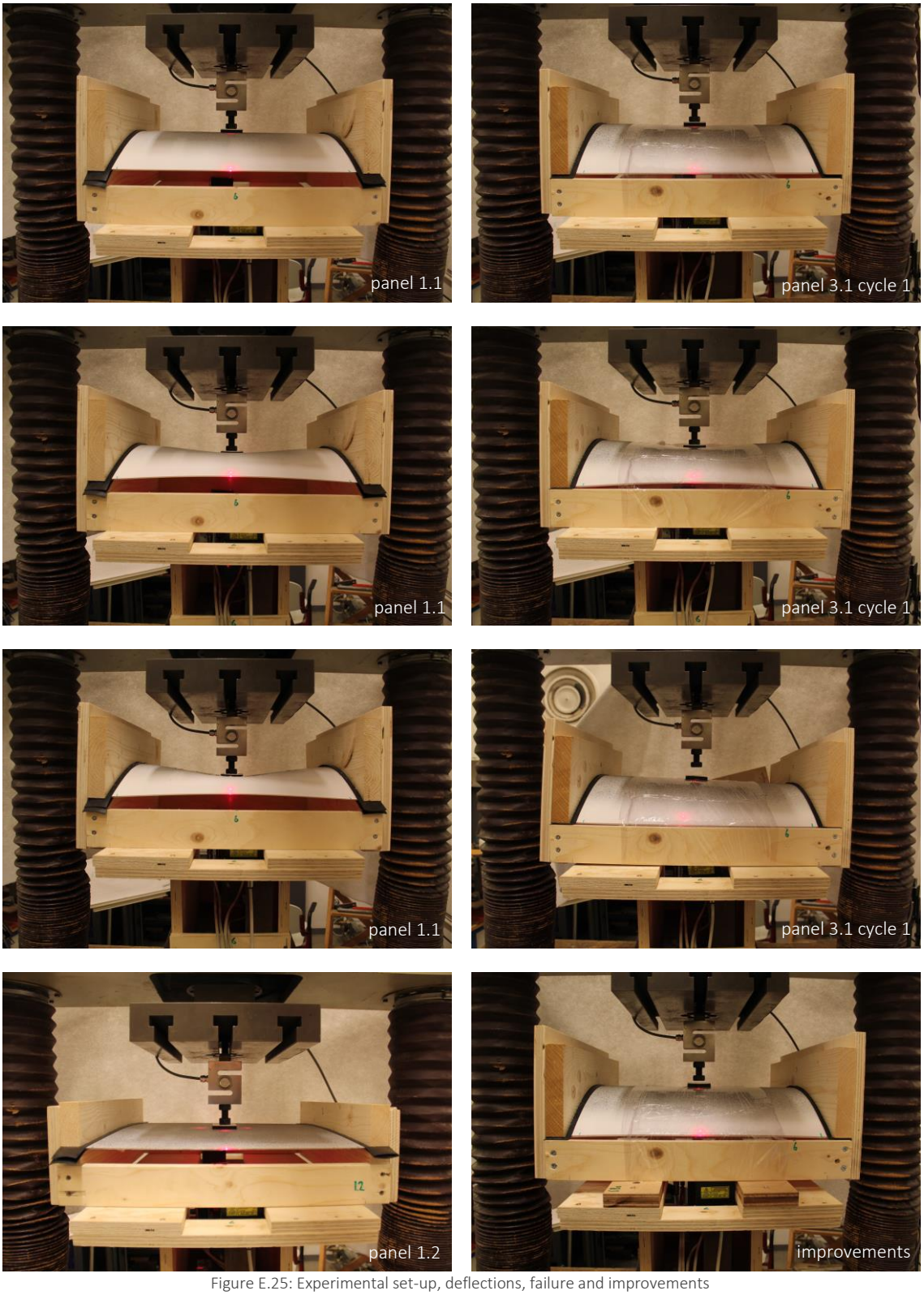

Figure E.25: Experimental set-up, deflections, failure and improvements

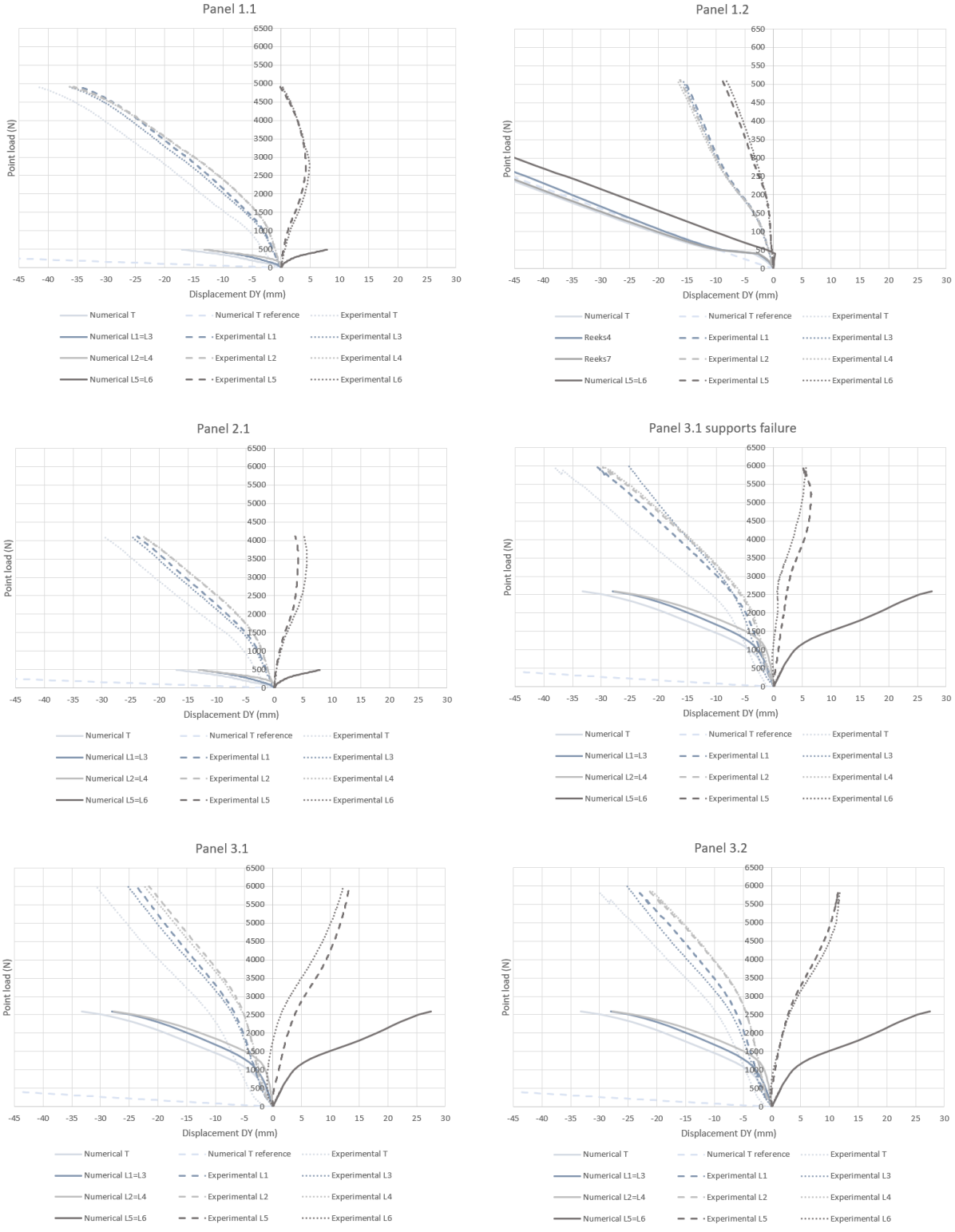

Figure E.26: Numerical and experimental point load vs displacement obtained during loading

E.3.5. Cracking

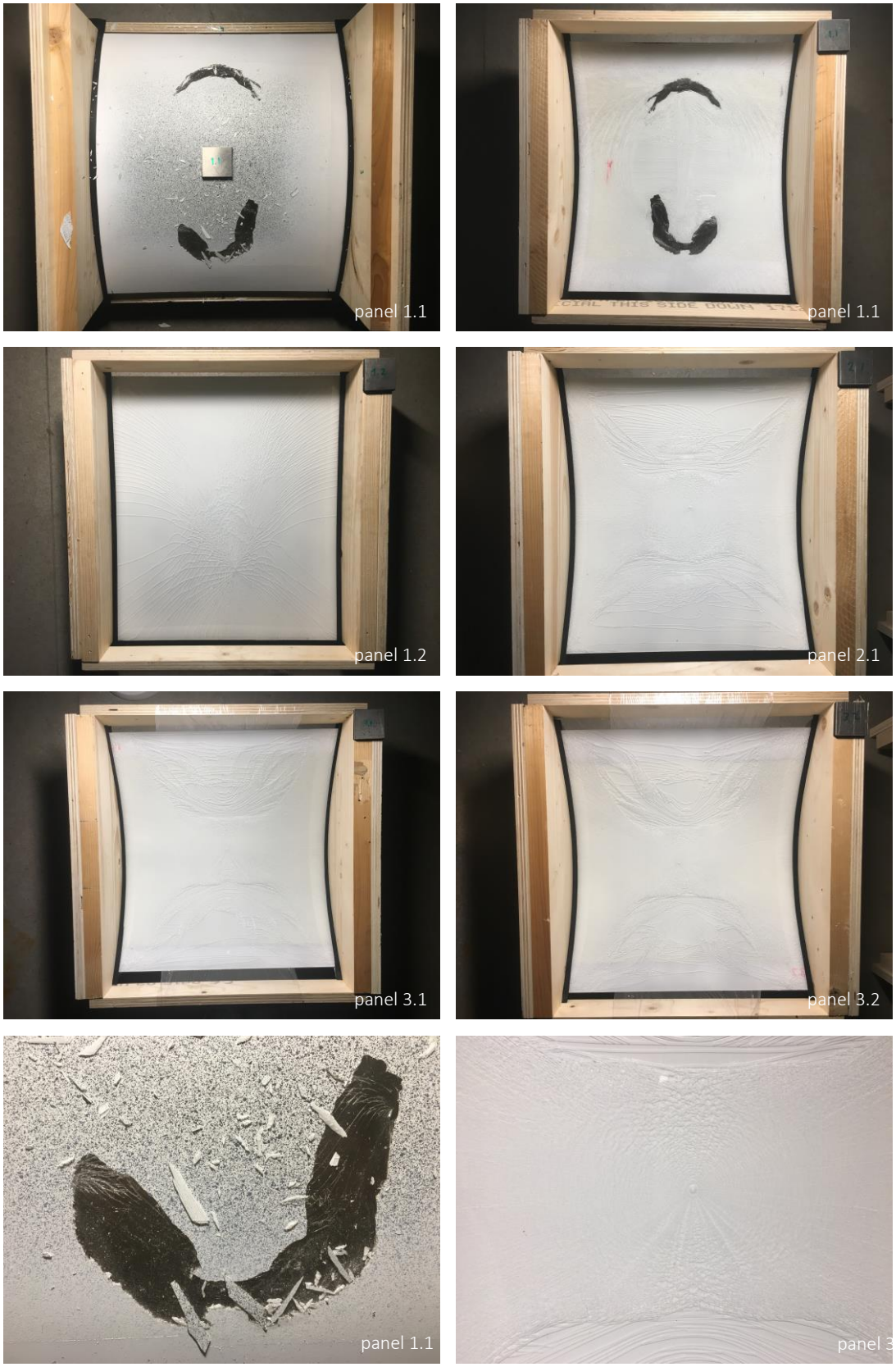

Figure E.27: Crack patterns at failure

Appendix F

Appendix D presents the wind loads acting on a chemically tempered aluminosilicate thin glass panels, as well as results from the numerical analysis for a single panel cold bent laminated thin glass panel.

F.1. Wind loads

The scope of this research is limited to the structural behaviour of free-formed thin glass panels by loading the structure using only distributed area loads representing wind loads. Assumptions are made that, if the pavilion would be build, the geographical location is an area at the Technical University of Delft in the Netherlands. The wind loads acting perpendicular to the panel are thus determined according to the general Dutch standard NEN 1991: Actions on structures - Part 1-4: General actions - Wind actions. The wind pressure on the complete structure or a structural element is determined by using the following expression:

$$Q_w = c_s c_d * c_f * q_p(z_e) \quad (F.1)$$

With $c_s c_d$ as the structural factor, c_f as the force coefficient for a structure or a structural component and $q_p(z_e)$ as the peak velocity pressure with z_e as the reference height.

The structural factor $c_s c_d$ can be taken as 1.0 for buildings with a height smaller than 15 m. To calculate the peak velocity pressure $q_p(z_e)$, the exposure factor $c_e(z)$ is covered by figure 4.2 in the NEN 1991. A building height of 3.21 m and wind area II estimate a value of 1.7 as the exposure factor $c_e(z)$. The basic pressure is calculated by the formulas below. The air density ρ is assumed to be 1.25 kg/m^3. The wind direction factor and the seasonal factor are recommended to be 1.0, therefore the fundamental value for the basic wind velocity is equal to the actual wind velocity and assumed to be 27 m/s.

$$q_b = \frac{1}{2} * \rho * v_b^2 = \frac{1}{2} * 1.25 * 27^2 = 455\ Pa = 0.455\ kN/m \quad (F.2)$$

$$q_p(z_e) = c_e(z) * q_b = 1.7 * 0.455 = 0.774\ kN/m^2 \quad (F.3)$$

The Dutch standard NEN 1991 doesn't include curved surfaces as a façade. Therefore, in order to calculate the force coefficient c_f an assumption is being made that the pavilion is designed as a rectangular box. The most unfavourable force coefficient façades is covered by Table 7.1 in the NEN 1991 and is taken as -1.2. The value corresponds to zone A as illustrated in Figure F.1 and indicates that the governing wind load is wind suction.

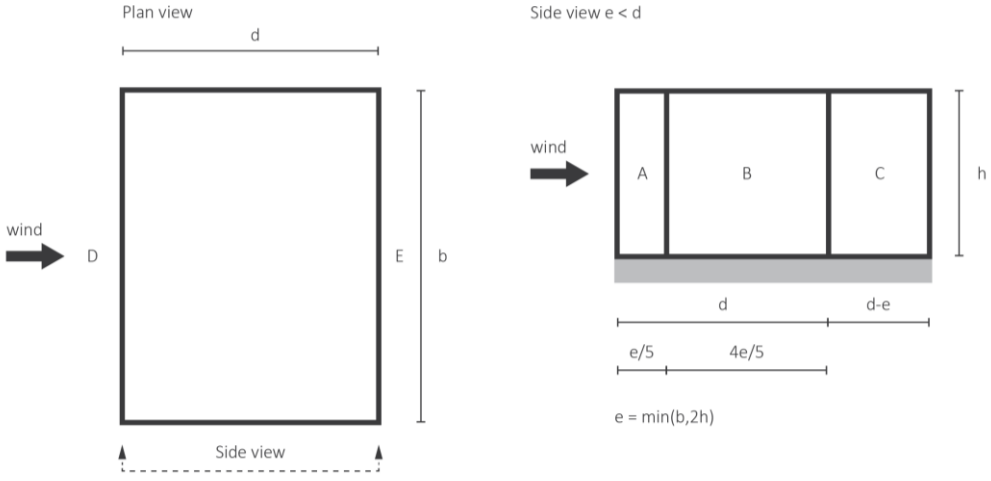

Figure F.1: Different wind zones on the façade of a building adapted from NEN 1991

The values and equations obtained above, result in a wind pressure of:

$$Q_w = 1.0 * 1.2 * 0.774 = 0.929\ kN/m^2 \quad (F.4)$$

F.2. Final design

The numerical model used for bending, spring back and relaxation is the same as for the precious analysis. The numerical model used for loading is illustrated below. The left and bottom edge make up for symmetry, while the top edge operates as a support. The right edge is unsupported.

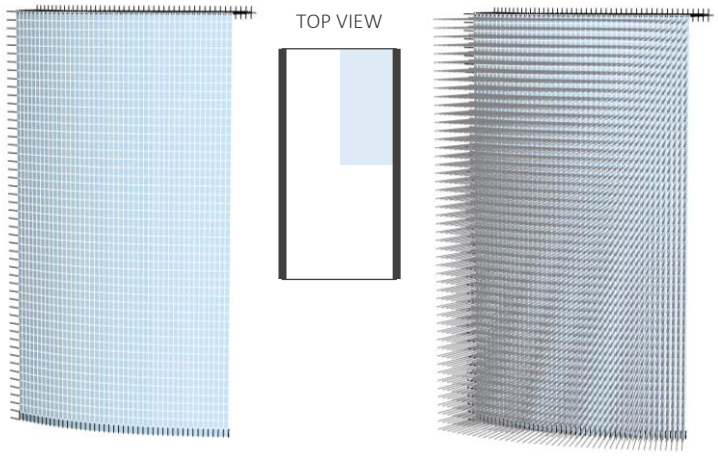

Figure F.2: Strand7 model illustrating mesh (left) during loading (right) using symmetry conditions in 3D

F.2.4. Bending

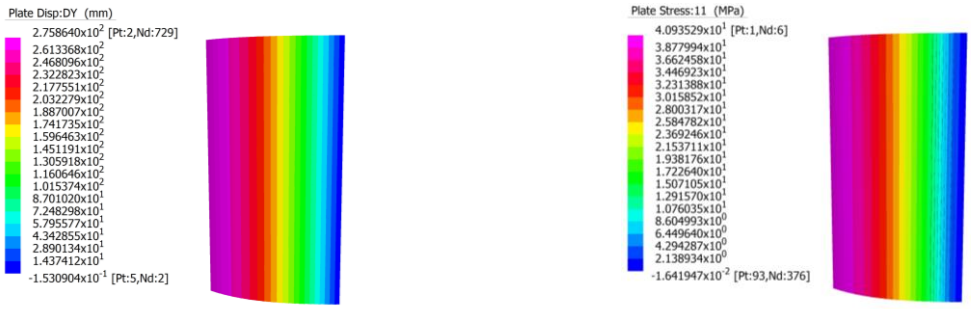

Figure F.3: Vertical displacement (DY) and principal stress (σ_{11}) during bending using symmetry

F.2.5. Spring back

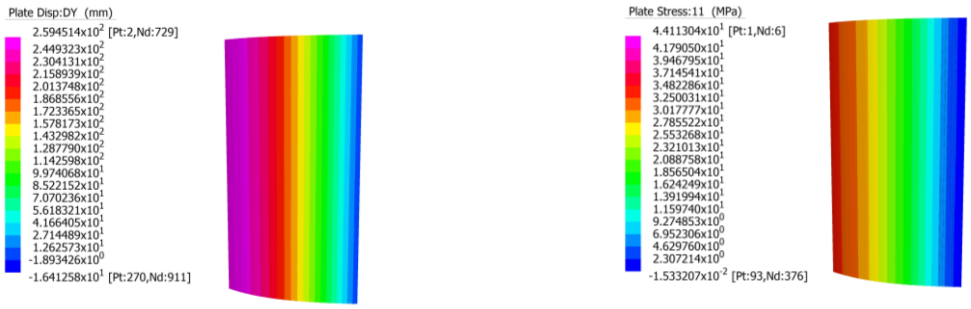

Figure F.4: Vertical displacement (DY) and principal stress (σ_{11}) during spring back using symmetry

F.2.6. Relaxation

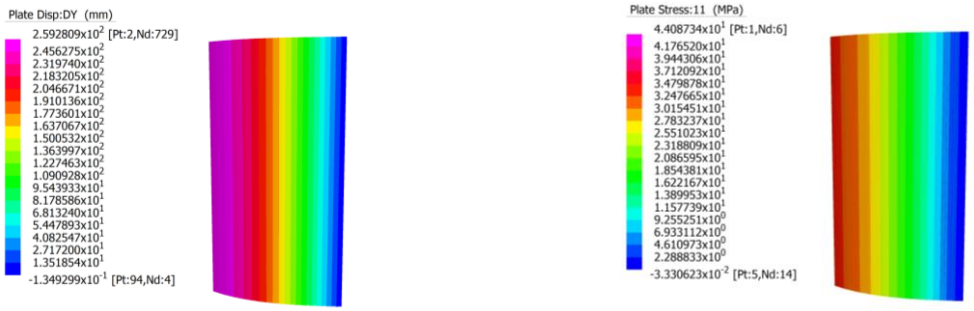

Figure F.5: Vertical displacement (DY) and principal stress (σ_{11}) at one month of relaxation using symmetry

F.2.7. Loading

Figure F.6: Vertical displacement (DY) and principal stress (σ_{11}) at 3200 N using symmetry